

**MAGNETIC ABRASIVE FINISHING (MAF)
OF NONMAGNETIC ROLLERS**

By

KISHOR AGRAWAL

Bachelor of Technology

Indian Institute of Technology


Bombay, India

1992

Submitted to the Faculty of the
Graduate College of the
Oklahoma State University
in partial fulfillment of
the requirements for
the Degree of
MASTER OF SCIENCE
December, 1994

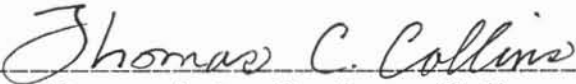
MAGNETIC ABRASIVE FINISHING (MAF)
OF NONMAGNETIC ROLLERS

Thesis Approved:


Thesis Adviser






Dean of the Graduate College

PREFACE

The magnetic abrasive finishing (MAF) technique can be used to finish both magnetic and nonmagnetic materials. In this process, a magnetic abrasive brush is formed in the magnetic field between the N and the S poles. This process enables i) the achievement of superfinishing (surface roughness $R_a \cong 5 \text{ nm}$) of ceramics with minimal crack generation and ii) more flexibility regarding the complexity of the shape of a surface to be polished.

The evolution of MAF [Krgalov, 1939] took place out of necessity, in polishing irregular shaped articles. Although, the process originated in the 30's in the U. S., it was in the former U.S.S.R. [Baron, 1975] and Bulgaria [Mekedonski and Kotshemidov, 1974] that much of the developments took place in the late 1950's and 1960's [Fox et al, 1994]. They applied the magnetic abrasive finishing technique not only for finishing of rollers and plates but also for deburring, precision chamfering, removal of scale/thin oxide layers, and texturing of industrial parts [Baron, 1975]. In the 1980's, Japanese researchers, mainly Shinmura and his associates at Utsunomia university [Shinmura et al., 1983-90], conducted extensive research on MAF in order to formulate the principles of the process, to determine the finishing and material removal characteristics of the process under various polishing conditions, and to investigate applications of the process.

However, much of the work by these researchers was concerned with polishing of ferromagnetic materials. The aim of the present investigation is to apply the

principles of magnetic abrasive finishing to nonmagnetic rollers (austenitic stainless steel and silicon nitride ceramic).

Some of the factors responsible for the surface finish and the material removal rates in a magnetic abrasive finishing process, are the magnetic field distribution and the magnetic force exerted on the workpiece by the magnetic abrasives. Finite element analysis (FEM) is used for this purpose. Magnetic pressure profiles on the surface of the rollers are calculated, using the Maxwell stress tensor approach. This work is further utilized to optimize the magnetic head design to achieve optimum magnetic pressure exerted by the magnetic abrasives on the surface of the roller, for high removal rates and/or best finish. Using FEM, complex shapes of the magnetic head can be effectively modelled and the exact nature of the magnetic field density distribution in the abrasive region can be determined. As, the magnetic field density and the magnetic pressure on the surface of the roller are greatly influenced by the length of the magnetically conducting path through the abrasive region, the included angle of the magnetic pole is given the main consideration.

In order to efficiently generate a smooth finished surface from a ground workpiece, it is necessary to investigate the effect of various process parameters on the finishing characteristics. Optimum conditions should be selected for an efficient finishing operation. For this, the nonmagnetic stainless steel rollers were polished under conditions that include duration of finishing, abrasive size, amount of lubricant, magnetic field density, workpiece rotational speed, and the combined effect of rotational speed and axial vibration.

The process principles developed for the finishing of austenitic stainless steel rollers were used in turn for the finishing of Si_3N_4 ceramic rollers. In this

investigation, several magnetic heads with different included angles were designed, fabricated, and characterized. They were evaluated in terms of their finishing efficiency and the material removal rate in the finishing of Si_3N_4 rollers.

It is found that the magnetic force in the magnetic abrasive region varies parabolically with the magnetic field density. Hence, a high magnetic field density should be achieved in the abrasive region to achieve a high magnetic pressure on the surface of the roller. This becomes an important factor in the case of finishing of ceramic rollers, which are hard and brittle. From the FEM analysis of the magnetic head design, magnetic heads with converging geometry, a sharper corner, the presence of air gap slot, and shorter magnetically conducting path in the abrasive region result in better field density concentration in this region.

From the experimental work, it is found that the surface finish of ~ 10 nm (Ra) can be achieved on rollers in about 10 minutes in case of an austenitic stainless steel roller and ~ 30 minutes in case of Si_3N_4 rollers. From the studies conducted on different process parameters, it is found that the presence of lubricant, a high magnetic field density in the abrasive region, axial vibration of the magnetic head, and a high rotational speed of the workpiece enhance the surface finishing that can be achieved on the surface of the rollers. It is also found that by controlling the magnetic pole shape, the surface finish and material removal rate in the process can be controlled.

ACKNOWLEDGEMENTS

I wish to express my sincere appreciation to my major adviser, Dr. Ranga Komanduri for his intelligent supervision, constructive guidance, inspiration and moral support. My sincere appreciation extends to my other thesis committee members Dr. C. E. Price and Dr. D. Lucca for agreeing to serve on the committee and for their suggestions. This project is supported in part by a contract from ARPA on Ceramic Bearing Technology Program (F33615-92-5933) and in part from a grant from the National Science Foundation on Design, Construction and Optimization of Equipment for Magnetic Field Assisted Polishing (DDM - 9402895). I would like to thank Dr. K. R. Mecklenburg of WPAFB, and Dr. W. Coblenz of ARPA, and Dr. B. M. Kramer and Dr. K. Srinivasan of NSF for their interest in this work. I would like to thank the sponsors for the financial support without which this work would not have been performed. I would also like to thank OCIDM and the MOST Chair for their support.

I wish to express my sincere gratitude to those who provided suggestions and assistance during this investigation namely, Dr. Ali Noori Khajavi, Dr N. Umehara, Dr. T. Shinmura, and Dr. T. R. Rama Mohan.

Further, I wish to thank my colleagues Mr Michael Fox, Ms. Hitomi Yamaguchi, Mr. Shekhar Bhagavatula, Mr. Makaram Raghunandan, and Mr. Sanjai Keshavan for their suggestions and active participation in this work. Thanks are

due to Mr. Robert Taylor and the North laboratory staff for assisting me with the using instrumentation and machining facilities.

I would also like to take this opportunity to offer my special appreciation to my parents for their support and constant encouragement.

TABLE OF CONTENTS

CHAPTER	TITLE	PAGE
1	INTRODUCTION	1
1.1	Magnetic abrasive finishing (MAF)	2
1.1.1	Process description	2
1.1.2	Process principles	5
1.1.3	Problem statement	9
2	LITERATURE REVIEW	12
2.0	Introduction	12
2.1	Evolution of the magnetic abrasive finishing process	12
2.2	Magnetic abrasive finishing devices	15
2.3	Synthesis of magnetic abrasive powder	28
2.4	Movement of magnetic abrasives in the finishing zone	30
2.5	Generation of the finishing pressure in MAF apparatus	37
2.6	Factors influencing the magnetic abrasive finishing process:	45

	2.6.1	Magnetic abrasive agglomerate	47
	2.6.2	Shape of the magnetic poles	49
	2.6.3	Vibration of the workpiece	52
	2.6.4	Magnetic field density	52
	2.6.5	Surface finishing time	54
	2.6.6	Surface speed of the workpiece	54
	2.6.7	Machining fluid and Lubricant	54
	2.6.8	Materials of workpiece	57
	2.7	Applications	61
3		ANALYTICAL MODELLING	63
	3.0	Introduction	63
	3.1	Theory	64
	3.2	A Simple Model for the MAF system	66
	3.3	Finite element analysis	69
	3.3.1	ANSYS analysis	69
	3.4	Magnetic force distribution on a nonmagnetic roller	78
	3.5	Characterization of the magnetic heads	83
	3.6	Determination of the cutting force	93
	3.7	Development of the design principles for the magnetic head used in the MAF apparatus	95
	3.8	Results and Discussion	96

4	EXPERIMENTAL APPROACH	118
4.1	Experimental apparatus	118
4.2	Experimental procedure	122
4.3	Characterization equipment	123
4.4	Results and Discussion	123
4.4.1	Finishing of nonmagnetic stainless steel roller	123
4.4.1.1	Time duration of finishing process	123
4.4.1.2	Effect of abrasive size	126
4.4.1.3	Effect of lubricant	126
4.4.1.4	Source current density	131
4.4.1.5	Workpiece rotational speed	131
4.4.1.6	Combined effect of rotational speed and axial vibration	131
4.4.2	Polishing of Si_3N_4 rollers using different head designs	134
5	DISCUSSION	146
6	CONCLUSIONS	149
	REFERENCES	152
	APPENDIX	160

LIST OF TABLES

Table	Title	Page
1	The properties of the materials used in a simple model of the MAF apparatus	68
2	Results obtained from the finite element analysis of the magnetic abrasive finishing process using various magnetic heads.	115
3	The specifications of the Magnetic Abrasive Finishing equipment and test conditions used in the investigation	121
4	The specifications of the Magnetic Abrasive Finishing equipment and test conditions used in the investigation for polishing of Si_3N_4 rollers	135

LIST OF FIGURES

Figure	Title	Page
1.1	Photograph of the magnetic abrasive finishing apparatus for polishing rollers.	3
1.2	Close-up of the magnetic abrasive finishing apparatus showing roller, flexible magnetic abrasive brush, and magnetic poles	3
1.3	ESEM photograph of a magnetic abrasive particle (KMX80)	4
1.4.	Photograph showing flexible magnetic abrasive brushes formed by linking magnetic abrasives between the magnetic poles N and with non-magnetic work materials	4
1.5	Schematic view of cylindrical magnetic abrasive finishing	6
1.6	Diagram showing two dimensional magnetic field distribution in the working zone during the finishing of magnetic rollers	7
1.7	Diagram showing two dimensional magnetic field distribution in the working zone during the finishing of nonmagnetic rollers	7
2.1	Schematic of devices for MAF in an alternating magnetic field: (A) polishing the inner surface of a tube; (B) polishing small parts with complicated shapes	13
2.2	Schematic of MAF apparatus for finishing of small parts	17
2.3	Schematic of MAF for finishing of sewing machine parts	17
2.4	Schematic of MAF for finishing of the inner surface of thin nonferromagnetic pipes	18

2.5	Schematic of MAF for finishing (A) medium and (B) large cylindrical parts	18
2.6	Schematic of MAF for finishing of sheets and plates	19
2.7	Schematic of MAF for fine ball finishing	19
2.8	Schematic of MAF for finishing of a ball valve, also shown are profiles of the surface roughness before and after finishing	20
2.9	Schematic of a magnetic abrasive tool (MAT) for polishing of a cylindrical surface	20
2.10	Schematic of MAF for finishing of a shaft with thread, annular groove, spherical, and conic surface	21
2.11	Schematic of magnetic abrasive buffing wheels (A) flat face treatment; (B) large flat surface treatment by a set of buffing wheels; (C) treatment of pipe inner surface.	21
2.12	Schematic diagram of internal finishing apparatus by the application of a linearly travelling magnetic field	23
2.13	Basic construction of finishing equipment	23
2.14	Shape and size of magnetic finishing tool used in experiments	24
2.15	Magnetic force acting on a magnetic finishing tool	24
2.16	Schematic view of new internal finishing process using rotating magnetic poles	26
2.17	Assembly view of the magnetic finishing apparatus	27
2.18	Shape and size of magnetic finishing jig	27
2.19	Schematics of Ferromagnetic abrasive powder (FAP) grain structures	29
2.20	Type of short fiber magnetic polishing materials	31

2.21	Transfer of the magnetic abrasives to the adjacent finishing zone in the direction of movement of the workpiece	31
2.22	Variation of normal component of the velocity of magnetic abrasives as function of working length of magnetic gap after polishing for (1) 10, (2) 20, and (3) 30 seconds	34
2.23	Variation of tangential component of the rate of motion of magnetic abrasives along working length of magnetic gap at workpiece speed of 2.35 m/s after polishing for (1) 30, (2) 20, and (3) 10 seconds at speed of (4) 3.14 m/s, and (5) 3.93 m/s	34
2.24	Variation of the resistance force exerted by the abrasives to the movement of the component in finishing process in relation to the length of the path travelled by the blade in the treatment zone. $B = 0.7T$, Abrasive particle diameter = $300\mu m$, speed of motion = (1) 1.57, (2) 2.355, (3) 3.14, (4) 3.915, and (5) 4.71 m/s	36
2.25	Variation of the work carried out by the component in reforming the magnetoabrasive powder in relation to the length of the path travelled by the workpiece in the treatment zones. Speed: 3.915 m/s, B : (1,2) 0.67T, (3,6) 0.67T, (4, 5) 0.7T, particle size: (1, 5, 6) $300\mu m$, (2, 4) $100\mu m$.	36
2.26	Measurement of action force F generated by magnetic-abrasives in the magnetic field	38
2.27	Magnetic pressure acting between substance I and substance II	40
2.28	Relationship between magnetic abrasive pressure and magnetic flux density using equation	40
2.29	B-H curves for 0.16% carbon steel and magnetic abrasives	43

2.30	μ_r - B_i curve for carbon steel (0.16%C) and μ_{rm} - B_j curve of magnetic abrasives	44
2.31	Calculated relationship between magnetic flux density and exciting current	46
2.32	Relationship between magnetic flux density and exciting current	46
2.33	Schematic of a magnetic abrasive particle	48
2.34	Various shapes of magnetic pole used in experiments (Width of magnetic pole: 40 mm)	48
2.35	Effects of shape of magnetic pole on finishing characteristics	51
2.36	Effect of vibration frequency of the workpiece on finishing characteristics (Shinmura et. al. 1985)	53
2.37	Effect of magnetic field density on finishing characteristics	53
2.38	Relationship between magnetic pressure and flux density for different filling densities of abrasives	55
2.39	Variation of the surface finish, and material removal rate with finishing time	56
2.40	Variation of the surface finish, and material removal rate, with finishing time at different rotational speeds	56
2.41	Variation of stock removal, and surface roughness with finishing time using different lubrication type	58
2.42	Variation of stock removal, and temperature of the workpiece with finishing time using stearic acid (5wt%) as a lubricant	59
2.43	Effects of vickers hardness number on stock removal and surface roughness	60

3.1	Simple model of the magnetic abrasive finishing system using a magnetic circuit	67
3.2	Two dimensional geometry of MAF apparatus used in the finite element analysis	70
3.3	B-H plot for the iron core (0.16% C steel)	72
3.4	B-H plot for the magnetic abrasives (KMX80)	73
3.5	The finite element model for the complete magnetic abrasive finishing cell	75
3.6	The fine element distribution of the finite element model at the nonmagnetic workpiece	76
3.7	The variations in the magnetic field density with different current densities through the current carrying coils in MAF process	77
3.8	Various head designs used in the finite element analysis the MAF process	79
3.9	Calibration curve for strain guage (350 ohm) using strain guage indicator	85
3.10	Set up for the measurement of the action force F exerted by the magnetic abrasive on the roller surface using Experiment 1	86
3.11	Set up for the measurement of the action force F exerted by the magnetic abrasive on the roller surface using Experiment 2	87
3.12	Variation of the action force F exerted by the magnetic abrasives on the roller surface using Experiment 1 for different head designs of various included angles with magnetic field density	88

3.13	Variation of the action force F exerted by the magnetic abrasives on the roller surface using Experiment 1 for head design E with magnetic field density	90
3.14	Variation of the action force F exerted by the magnetic abrasives on the roller surface using Experiment 2 for head design E with magnetic field density	91
3.15	Variation of the action force F exerted by the magnetic abrasives on the roller surface using Experiment 1 for head design I with magnetic field density	92
3.16a	Variation of the material removal rate with the cutting force exerted by the abrasives on the surface of the roller in case of head design E	94
3.16b	Variation of action force with magnetic field density for various weights of magnetic abrasives used with/without axial vibration on the surface of roller	94
3.17	Normal magnetic field density at the roller - abrasive interface for head design A (included angle 170°)	97
3.18	Tangential magnetic field density at the roller - abrasive interface for head design A (included angle 170°)	97
3.19	Normal magnetic field density at the roller - abrasive interface for head design B (included angle 90°)	98
3.20	Tangential magnetic field density at the roller - abrasive interface for head design B (included angle 90°)	98
3.21	Normal magnetic field density at the roller - abrasive interface for head design C (included angle 90°)	99
3.22	Tangential magnetic field density at the roller - abrasive interface for head design C (included angle 90°)	99
3.23	Normal magnetic field density at the roller - abrasive interface for head design D (included angle 30°)	100

3.24	Tangential magnetic field density at the roller - abrasive interface for head design D (included angle 30°)	100
3.25	Normal magnetic field density at the roller - abrasive interface for head design E (included angle 90°)	101
3.26	Tangential magnetic field density at the roller - abrasive interface for head design E (included angle 90°)	101
3.27	Normal magnetic field density at the roller - abrasive interface for head design F (included angle 90°)	102
3.28	Tangential magnetic field density at the roller - abrasive interface for head design F (included angle 90°)	102
3.29	Normal magnetic field density at the roller - abrasive interface for head design G (included angle 90°)	103
3.30	Tangential magnetic field density at the roller - abrasive interface for head design G (included angle 90°)	103
3.31	Normal magnetic field density at the roller - abrasive interface for head design H (included angle 90°)	104
3.32	Tangential magnetic field density at the roller - abrasive interface for head design H (included angle 90°)	104
3.33	Normal magnetic field density at the roller - abrasive interface for head design I (included angle 170°)	105
3.34	Tangential magnetic field density at the roller - abrasive interface for head design I (included angle 170°)	105
3.35	Normal stress distribution at the roller - abrasive interface for head design A (included angle 170°)	106
3.36	Tangential stress distribution at the roller - abrasive interface for head design A (included angle 170°)	106

3.37	Normal stress distribution at the roller - abrasive interface for head design B (included angle 90°)	107
3.38	Tangential stress distribution at the roller - abrasive interface for head design B (included angle 90°)	107
3.39	Normal stress distribution at the roller - abrasive interface for head design C (included angle 90°)	108
3.40	Tangential stress distribution at the roller - abrasive interface for head design C (included angle 90°)	108
3.41	Normal stress distribution at the roller - abrasive interface for head design D (included angle 30°)	109
3.42	Tangential stress distribution at the roller - abrasive interface for head design D (included angle 30°)	109
3.43	Normal stress distribution at the roller - abrasive interface for head design E (included angle 90°)	110
3.44	Tangential stress distribution at the roller - abrasive interface for head design E (included angle 90°)	110
3.45	Normal stress distribution at the roller - abrasive interface for head design F (included angle 90°)	111
3.46	Tangential stress distribution at the roller - abrasive interface for head design F (included angle 90°)	111
3.47	Normal stress distribution at the roller - abrasive interface for head design G (included angle 90°)	112
3.48	Tangential stress distribution at the roller - abrasive interface for head design G (included angle 90°)	112
3.49	Normal stress distribution at the roller - abrasive interface for head design H (included angle 90°)	113

3.50	Tangential stress distribution at the roller - abrasive interface for head design H (included angle 90°)	113
3.51	Normal stress distribution at the roller - abrasive interface for head design I (included angle 170°)	114
3.52	Tangential stress distribution at the roller - abrasive interface for head design I (included angle 170°)	114
4.1	Photograph of the magnetic abrasive finishing apparatus used for polishing of rollers.	119
4.2	Close-up of the magnetic abrasive finishing apparatus showing roller, flexible magnetic abrasive brush, magnetic poles	119
4.3a	SEM micrograph of magnetic abrasive (400/5 μm)	121
4.3b	SEM micrograph of magnetic abrasive (KMX 80)	121
4.4a	Talysurf traces of the as-received, ground stainless steel rod and the same finished by magnetic field assisted polishing surfaces showing improvement in the finish between the ground and polished surfaces.	124
4.4b	Photograph of the as-received, ground stainless steel rod and the same finished by magnetic field assisted polishing	125
4.5	Figures showing the Talysurf traces of the stainless steel roller depicting the surface finish obtained in the magnetic abrasive finishing process at varying polishing time (a) 0 minute (b) 1/2 minute (c) 1 minute (d) 2 minute (e) 3 minute (f) 5 minute	127
4.6	Variation of surface roundness (O) with finishing time	129
4.7	Variation of the surface finish (Ra) with finishing time for KMX80 and 400/5 μm abrasives	130
4.8	Variation of surface finish (Ra) with 0 w/o, 2W/o, 5 w/o and 8 w/o of zinc stearate.	130
4.9	Variation in the magnetic field density within the magnetic abrasives with the source current density in the copper coil	132

4.10	Variation of surface finish (Ra) with finishing time for various magnetic flux densities.	132
4.11	Variation of surface finish (Ra) with finishing time for various rotational speed of the workpiece	133
4.12	Variation of removal rate and surface finish after finishing for 5 min. with half included angle.	133
4.13	SEM micrograph of unused magnetic abrasives (Fe (40#, 75%) + Cr ₂ O ₃ (4μm, 25%)) at 200X, and 165X magnifications	137
4.14	SEM micrograph of used magnetic abrasives (Fe (40#, 75%) + Cr ₂ O ₃ (4μm, 25%)) at 270X, and 1000X magnifications	138
4.15	Effect of revolution speed of the workpiece on the material removal rate for head design C with included angle of 90°.	139
4.16	Effect of revolution speed of the workpiece on the material removal rate for head design D with included angle of 30°.	140
4.17	Effect of revolution speed of the workpiece on the material removal rate for head design J with included angle of 120°.	140
4.18	Effect of revolution speed of the workpiece on the surface roughness achieved for different head designs	142
4.19	Effect of different head designs for different included angles on surface roughness achieved for Si ₃ N ₄ rollers.	143
4.20	SEM micrograph of unpolished Si ₃ N ₄ roller at 100X, and 2000X magnifications	144
4.21	SEM micrograph of unpolished Si ₃ N ₄ roller at 2000X, and 5000X magnifications	145
A1	Figure showing a typical Talysurf trace of the stainless steel roller and the various parameters measured by the Talysurf series	161
A2	Figure showing a typical Talyrond trace of the stainless steel roller and the various parameters measured by the Talyrond series	163

CHAPTER 1

INTRODUCTION

Structural ceramics, such as silicon nitride, aluminium oxide, and zirconia are increasingly being considered for many advanced applications due to their high strength at elevated temperatures, high modulus, greater resistance to chemical degradation, high wear resistance, and lower density than ferrous alloys. These intrinsic properties of ceramics make them prime candidates for many applications ranging from ball bearings to engine components. However, the strength and reliability of components that are subject to rolling-contact fatigue, such as in bearings, can be significantly affected by surface or subsurface defects. Mechanical removal of material by conventional grinding of ceramics has long been an art, the progress of which has almost entirely been based on experience. True scientific knowledge in this area has been meager. This is surprising since a major factor in the manufacture or fabrication of ceramic products is detailed knowledge of the variables and their interrelation in the processing and finishing cycles. Conventional grinding of ceramics, with diamond wheels, involves large forces and results in cracks due to brittle fracture, which can lead to failure when the material is under a tensile stress. Also, with these processes, it is difficult to finish complex parts, especially when used for internal finishing. As the reliability and performance of the components made of these materials are largely affected by the surface defects, it is necessary to achieve superfinishing of the ceramic with minimal or no surface defects such as microcracks, pits etc. This can be accomplished by applying controlled, low level forces during finishing.

Magnetic field assisted polishing has been introduced to achieve surface finishing by means of a magnetic abrasive brush that is formed in the magnetic field between the N and the S poles. This process permits more flexibility regarding the surface shape, which is applicable for the finishing of a complex part.

1.1 MAGNETIC ABRASIVE FINISHING

1.1.1 PROCESS DESCRIPTION:

Figure 1.1 shows the magnetic abrasive finishing apparatus mounted on a Hardinge precision lathe. The workpiece (roller) is clamped on the chuck of the lathe and is introduced in the magnetic field. Rotating motion between the magnetic field and the workpiece can be achieved either by a static magnetic field or a rotating magnetic field. In the magnetic abrasive finishing using a static magnetic field, a cylindrical workpiece is rotated around its axis (1000-3000 rpm). In finishing using a rotating magnetic field, a rotating magnetic field is obtained by supplying current to the three coils arranged at intervals of 120° with a three phase current. A pneumatic air vibrator is used for supplying the axial motion to the magnetic head. This is necessary to prevent the formation of a circumferential groove on the surface of the roller.

Figure 1.2 is a close-up of the apparatus showing key elements. Either an electromagnet or permanent magnet can be used for the generation of the magnetic field. The magnetic field generated in the cell passes through the gap between the N and the S poles. The magnetic heads have to be so designed that the magnetic field can be concentrated, with minimal leakage of the field taking place surrounding the air gap between the magnetic heads. As pointed out earlier, axial vibration of the the magnetic poles relative to the workpiece is introduced to prevent the formation of circumferential grooves on the workpiece and to increase the finishing efficiency. Magnetic abrasive comprising of a magnetic material (e.g. iron particles) and an abrasive (either as a sintered body or a mechanical mixture) is introduced in the head gap. Due to the presence of the magnetic field the abrasive is aligned in the direction of the field as shown in Figure 1.3.

The magnetic abrasives used in this investigation consist of a sintered product of iron particles (size of 80-400 μm), and fine aluminium oxide abrasive particles (grain size 1-10 μm). A SEM photograph of a typical magnetic abrasive used in the present study is shown in Figure 1.4. The white particles are aluminium oxide abrasives and the darker matrix is iron.

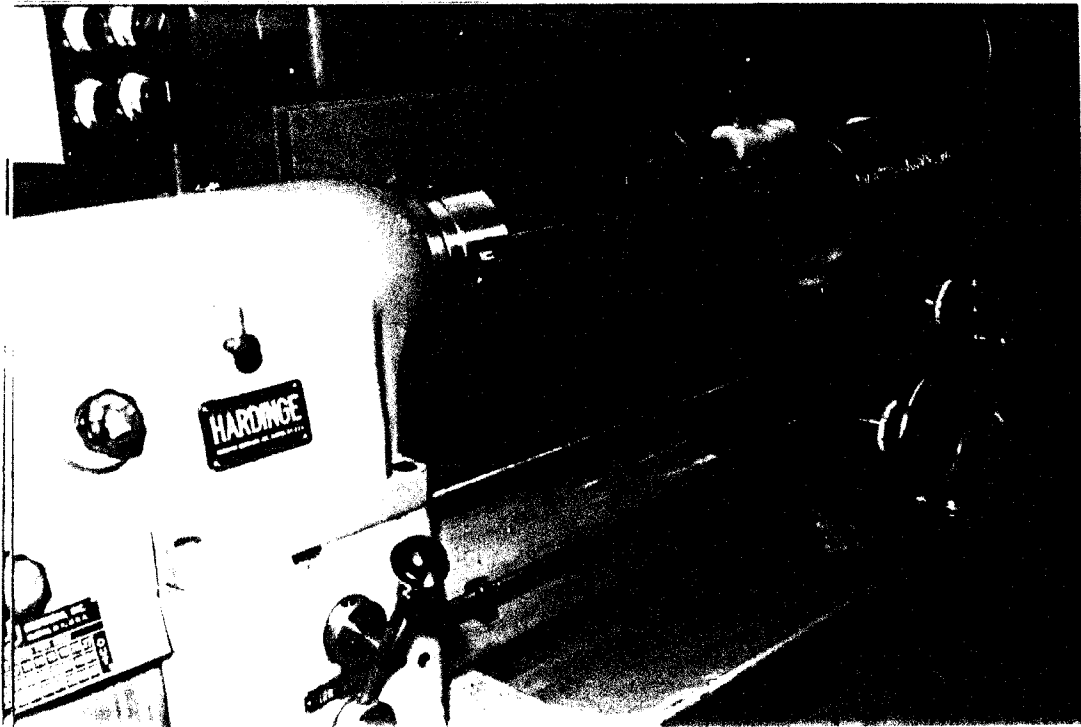


Figure 1.1 Photograph of the magnetic abrasive finishing apparatus used for polishing of rollers.

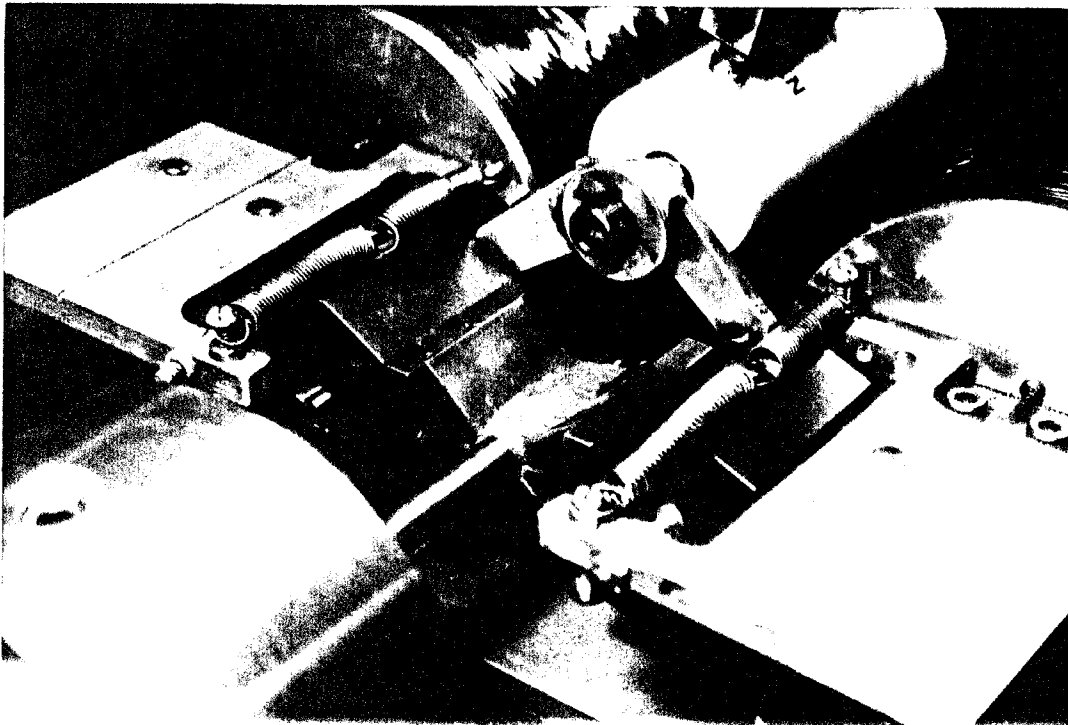


Figure 1.2 Close-up of the magnetic abrasive finishing apparatus showing roller, flexible magnetic abrasive brush, magnetic poles

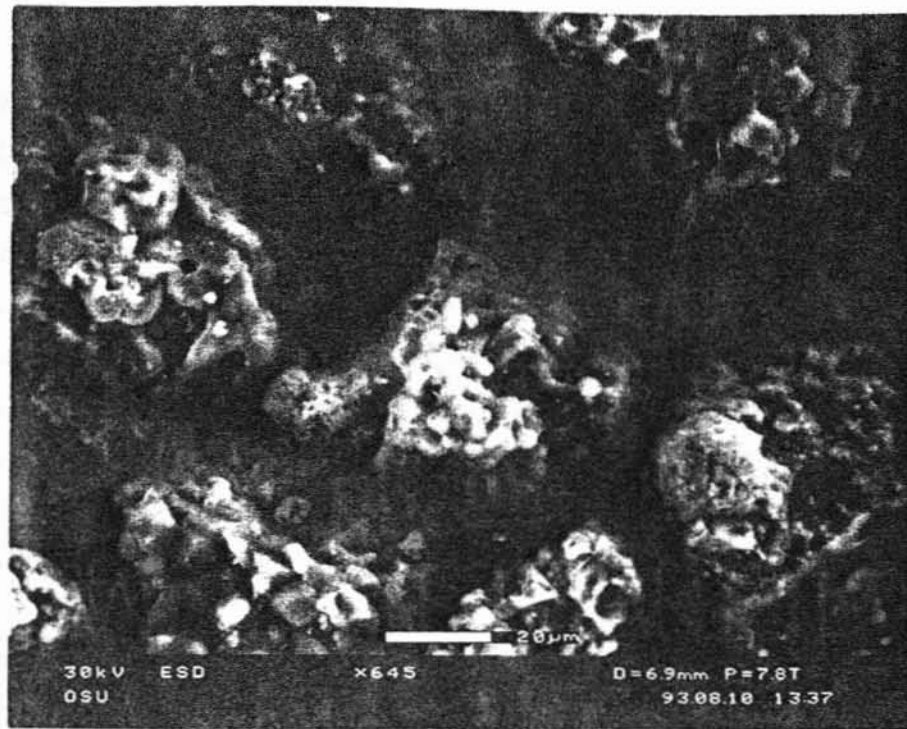


Figure 1.3: ESEM photograph of a magnetic abrasive particle (KMX80)

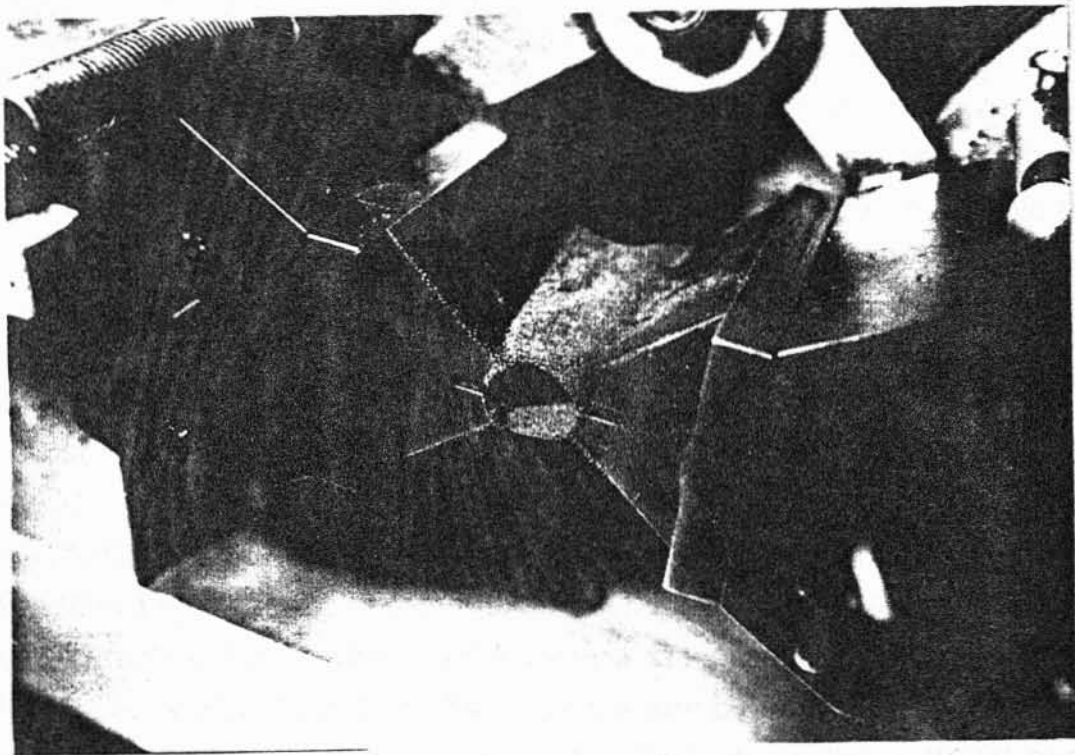


Figure 1.4. Photograph showing flexible magnetic abrasive brushes formed by linking magnetic abrasives between the magnetic poles N and S with non-magnetic work materials

The magnetic abrasive finishing process is considered very efficient for finishing of difficult to machine materials. The removal rate and finish obtainable depend on the workpiece circumferential speed, magnetic flux density, working clearance between the magnetic heads and the workpiece, workpiece material, and the type of magnetic abrasive conglomerate (including the type of abrasive used, the grain size of the abrasive, and volume fraction in the conglomerate). Typical conditions used by Shinmura (Shinmura, 1984) for finishing of steel rollers are the following: roller speed: 1.3 m/s, magnetic flux density: 1.2 T, working clearance: 2 mm, vibrational frequency: 20 Hz, vibrational amplitude: 3.5 mm, and mean diameter of magnetic abrasive particles: 100 μm .

1.1.2 Process Principles

In the magnetic abrasive finishing (MAF) process, a magnetic abrasive conglomerate is introduced between the N and the S poles. Due to the generation of magnetic field, the magnetic abrasives are linked to each other magnetically between the poles along the lines of magnetic force, forming flexible magnetic abrasive brushes as shown in Figure 1.5. When a vibrating and rotating roller is introduced in this abrasive brush, surface finishing is achieved with the help of the finishing pressure exerted by the magnetic brush in the magnetic field on the roller. The generation of the finishing pressure and its role in polishing is described in the following.

As mentioned earlier, the rollers to be finished can be either magnetic (e.g. magnetic steel) or non-magnetic (e.g. ceramic roller). Figure 1.6 shows the two-dimensional magnetic field distribution in the working zone during the finishing of a ferromagnetic material [Shinmura et al., 1990]. The workpiece is magnetized in the presence of the magnetic field and the magnetic force acts on the top of brush between the workpiece and the abrasive grain. As a result, abrasive grains are pressed on to the work surface by an extremely small force, F_x , and perform cutting. In the initial period of polishing, the material removal rate is highest and as polishing progresses the micro irregularities are smoothed out.

Figure 1.7 shows the two-dimensional magnetic field distribution in the working zone during the finishing of nonmagnetic materials. In this case, the magnetic

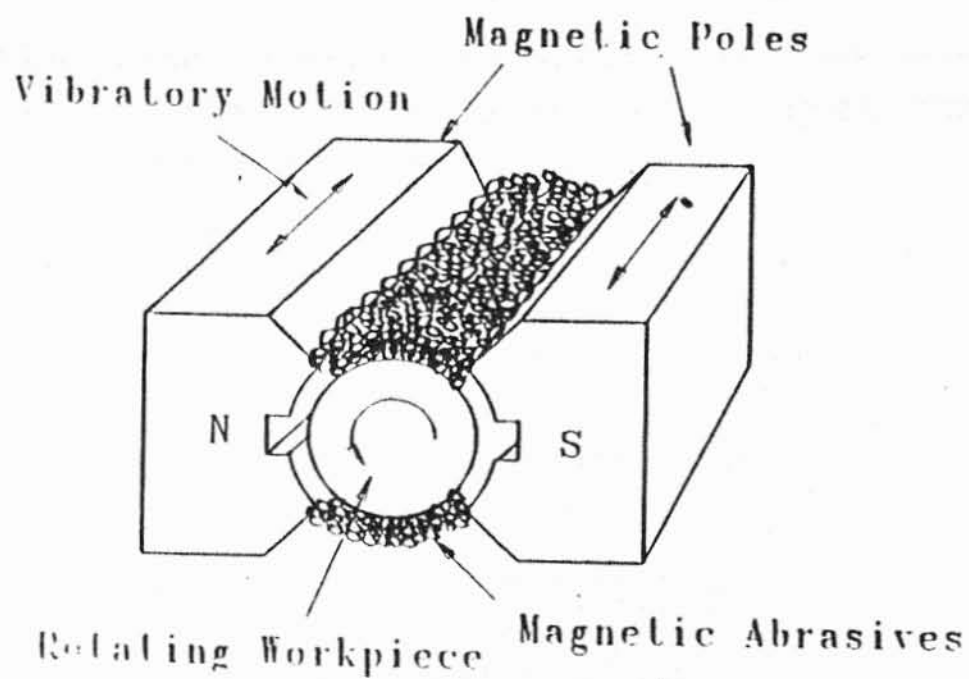


Figure 1.5: Schematic view of cylindrical magnetic abrasive finishing

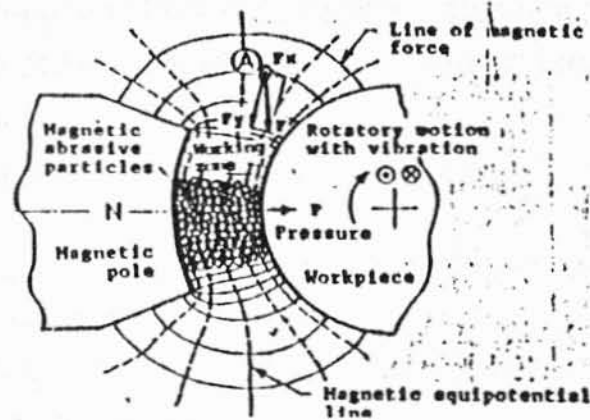


Figure 1.6: Diagram showing two dimensional magnetic field distribution in the working zone during the finishing of magnetic rollers (Shinmura et al, 1990)

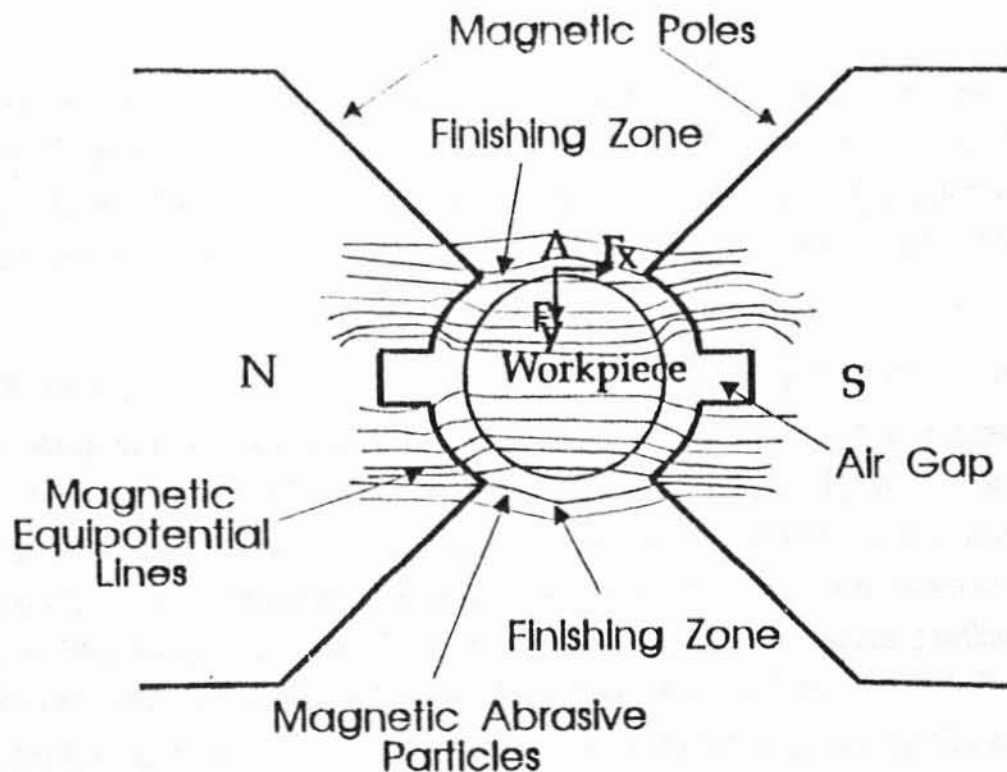


Figure 1.7: Diagram showing two dimensional magnetic field distribution in the working zone during the finishing of nonmagnetic rollers

field lines go around the periphery of the cylindrical workpiece by linking the N and S poles of the magnetic heads. A magnetic abrasive particle at position "A", far from the working zone, is affected by the magnetic forces represented by the following equations:

$$F_r = V \times H \frac{\partial H}{\partial r} \quad F_\theta = V \times H \frac{\partial H}{\partial \theta} \quad (1.1)$$

where, F_r = The magnetic force acting on the magnetic abrasive particle in the radial direction

F_θ = The magnetic force acting on the abrasive grain in the tangential direction of the work surface

V = volume of the magnetic abrasive particle

x = susceptibility of the particle,

H = magnetic field strength at point A,

θ = direction of the magnetic equipotential lines, and

$\partial H/\partial r$, $\partial H/\partial \theta$ are gradients of the magnetic field strengths in the r and θ directions

From equation 1.1, it is evident that, even if x is nonzero, the magnetic force will not act, if $\partial H/\partial r$ and $\partial H/\partial \theta$ are equal to zero. The larger values of magnetic strength gradients force the abrasive grains to move towards the working zone, thus preventing separation and splashing of the abrasives from the working zone.

Also from equation 1.1 it is evident that the magnetic forces F_r and F_θ are proportional to the volume of the magnetic abrasive particle, the susceptibility of the particle, the magnetic field strength, and its gradient. If there is any change of magnetic field strength in the direction of the line of magnetic force near the work surface, the magnetic abrasive particles are pushed toward the work surface. The magnetic force F_r actuates the magnetic abrasive particles to take part in the finishing of the workpiece. In addition, the force F_θ on the abrasive grain (in the tangential direction of the work surface) is given by the cutting and frictional action. The runoff of the abrasive grains from the working zone is prevented in the balance of the force F_θ to magnetic force F_m due to the gradient of the magnetic field strength.

Salient features of magnetic field assisted polishing techniques are (Shinmura et al, 1990) the following:

1. Both the finishing pressure and the magnetic field density in the magnetic abrasive region can be controlled by varying the exciting current in the coil and shape of the magnetic pole. This, also, enables adjustment of the binding force of magnetic abrasives and controls the supply, discharge, and recycle of magnetic abrasives automatically.
2. Due to allowance of clearance between the magnetic poles and the workpiece (working clearance), it is possible to finish both the interior and the exterior surfaces of complex shaped parts besides simple cylindrical and plane surfaces. In addition to the improvement of the surface finish, this process can also enhance surface integrity by applying residual compressive stresses.
3. Finishing efficiency (i.e. $(R_t - R_0)/t$, where R_t is the surface finish at time t and R_0 is the initial surface finish) is excellent. Surface finish R_a of ~20-30 nm can be achieved in short finishing time of 6-8 minutes. Further, it has the ability to improve the form accuracy.
- 4 The finishing operation is carried out without generating much heat which minimizes thermal distortions, localized microstructural changes and thermally induced oxidation especially to metals and their alloys. This may not be a serious limitation with ceramics.
5. There is no scattering of abrasives due to the absorption of dust by the magnetic field.
6. Magnetic abrasives can be replaced.
7. Consumption of magnetic abrasives is less and their recycling is possible.
- 8 Since there is no heat build up, fire hazards are minimized.
- 9 The process can be easily integrated into a computer control system.

1.1.3 Problem Statement

The magnetic abrasive finishing (MAF) process has been investigated by many researchers [Baron 1987, Shinmura et al 1984-94]. They studied the effect of various parameters on the material removal rate and surface finish. The process was applied for a range of finishing applications, including finishing of rollers, plates, deburring, precision chamfering, removal of scale/thin oxide layers, and

texturing of industrial parts [Baron, 1975]. However, most of their work was concentrated on the finishing of magnetic materials. The possibility of finishing nonmagnetic work materials, including nonmagnetic ceramics, has not been studied in detail, yet. Polishing nonmagnetic materials, especially hard ceramic materials, requires higher polishing pressures. This has been a difficult task since to generate a higher polishing pressure requires an understanding of the magnetic head design principles, capable of providing higher magnetic field density in the magnetic abrasive region and higher magnetic forces on the surface of the rollers. They affect the surface finish and the material removal rate obtainable by the process.

This study will optimize the magnetic head design, to achieve optimum magnetic pressure exerted by the magnetic abrasives on the surface of the roller. For this purpose, an ANSYS FEM package was used.

In order to efficiently generate a smooth finished surface from a ground workpiece, it is necessary to understand the effect of various process parameters on finishing characteristics. Optimum conditions should be selected for efficient finishing operation. Initially, a detailed study of magnetic abrasive finishing of austenitic stainless steel roller was conducted to evaluate the performance of the finishing operation under various processing conditions. The nonmagnetic stainless steel rollers were polished under various conditions. The variables included duration of finishing, abrasive size, amount of lubricant, magnetic field density, workpiece rotational speed, combined effect of rotational speed and axial vibration. The process principles used in the finishing of austenitic stainless steel rollers were used in turn for the finishing of Si_3N_4 ceramic rollers. In this investigation, various magnetic heads with different included angles were designed, fabricated and characterized. They were evaluated in terms of their finishing efficiency and material removal rate in the finishing of Si_3N_4 rollers.

The present investigation focuses on the following aspects of MAF:

- To determine the magnetic field distribution and the magnetic forces exerted on the workpiece using finite element analysis. A commercial ANSYS package developed for magnetic field analysis is used for this study. The magnetic field distribution and the magnetic forces exerted

on the workpiece are factors that govern the surface finish and the removal rates obtainable in the process.

- To optimize the magnetic head design in order to achieve desirable magnetic pressure, exerted by the magnetic abrasives on the surface of the roller, for maximum material removal and /or best finish.
- To investigate the effect of different parameters on the finishing characteristics and the material removal rate.
- To investigate the mechanism of material removal in MAF.

This thesis is divided into the following six chapters.

Chapter 1 introduces MAF and describes the process in brief.

Chapter 2 reviews the literature on MAF of rollers. It describes the various steps used in the development of the theory starting from the magnetics used for the prediction of the magnetic pressure on the surface of the workpiece. It also discusses the effect of various parameters used on the capabilities of the process in terms of finishing characteristics and the removal rates.

Chapter 3 presents various steps taken in the finite element analysis of the process using ANSYS program. This analysis facilitates the determination of the magnetic field density near the magnetic head region. It also assists in the determination of the maxwell forces exerted on the surface of the workpiece which governs the material removal mechanism occurring in this process. The results obtained by the finite element analysis of the process are then discussed.

Chapter 4 describes the experimental setup and the test procedure used in MAF of nonmagnetic stainless steel rollers. The effect of various parameters of this process on removal rate and finish are discussed.

Chapter 5 discusses the results obtained both by finite element analysis and by the experimental investigation. Chapter 6 presents conclusions of this investigation.

CHAPTER 2

LITERATURE REVIEW

2.0 INTRODUCTION

This section reviews the literature on the magnetic abrasive finishing (MAF) process. It describes the U. S. patents reported since the 1940s. It further describes the steps used in the development of theory, from the magnetics used to the prediction of the magnetic pressure on the surface of the workpiece. It discusses the effect of parameters used to evaluate the capabilities of the process in terms of the finishing characteristics and the removal obtained. The parameters covered under this heading includes magnetic abrasive (size and shape), magnetic pole shape, magnetic field density, vibration of the magnetic head, rotational speed of the workpiece.

2.1 Evolution of the magnetic abrasive finishing process:

The evolution of magnetic abrasive finishing took place out of the necessity in polishing irregular shaped articles. The first invention to fully realize the concept of magnetic abrasive finishing was conceived by a Soviet engineer, Kargalov, in 1939 (Figure 2.1a) [Kargalov, 1939]. He attempted to polish the inner circumference of a rotating tube with an alternating magnetic field. The earlier work on magnetic abrasive finishing was mostly done in United States [Coats, 1940]. In 1940, Coats demonstrated the polishing of the inner surface of a circumferential weld, in a container using the magnetic abrasives under the action of a magnetic field [Coats, 1940]. The main principle used in this method was that the magnetic abrasives under the influence of the magnetic field are aligned in the direction of the magnetic field. If the rotating workpiece is introduced in this magnetic abrasive, the magnetic pressure exerted by the magnetic abrasive on the workpiece causes the polishing action.

In the 1950s, finishing of materials by this process was carried out with a mixture of SiC and iron fillings as the magnetic abrasive. The emphasis was on

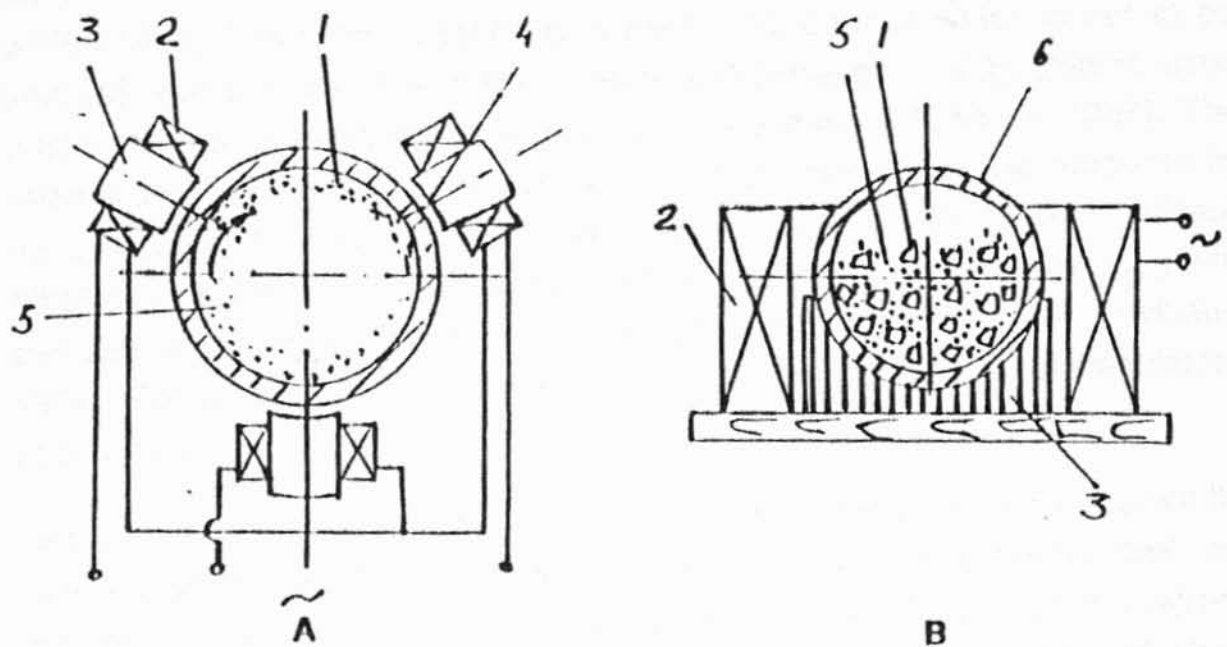


Figure 2.1: Schematic of devices for MAF in an alternating magnetic field: (A) polishing the inner surface of a tube; (B) polishing small parts with complicated shapes
 1. workpiece, 2. coil, 3. yoke, 4. magnetic poles, 5. ferromagnetic abrasive powder, 6. nonferrous tank [Kargalov 1939, Hershler, 1969].

polishing of irregular shaped objects. Using the same principle, Simjian developed polishing apparatuses in which magnetic abrasives were imparted random motion, under the influence of a polyphase alternating magnetic field [Simjian, 1956a, 1956b, 1957]. A similar technique was also used to preferentially finish the surface, by masking the surface which is not to be finished with a resinoid or rubber compound [Simjian, 1959]. Bodine used packed abrasive mass to achieve a high field density [Bodine, 1957]. The relative oscillation between the abrasive mass and workpiece was produced by transmitting sonic waves through the abrasive mass. Loveness and Feldhaus emphasized the chemical inertness of the carrier fluid with the magnetic particles in the abrasive bath in the finishing action [Loveness and Feldhaus, 1974]. The carrier fluid contains additional components such as pH regulators, softeners, surfactants etc.

Research on MAF, including potential applications, has been ongoing since the 1960s in the former USSR (e.g. Konovalov and Shulev, 1967, Baron, 1986, and Sakulevich, 1977) and in Germany [Dehoff A. et al., 1984]. In Bulgaria, magnetic abrasive finishing has been under development since the middle of 1970s [Makedonsky et al., 1974, 1977], and in Japan since the beginning of 1980s [Shinmura et al., 1985a]. In the former USSR, magnetic abrasive finishing was applied to the finishing of rollers, plates, deburring, precision chamfering, removal of scale/thin oxide layers, texturing of industrial parts [Baron, 1975].

Major emphasis of the work in the 1970s was on the finishing of sheet materials, rollers and spherical parts. The relative motion between the magnetic field and the workpiece was achieved by moving the workpiece relative to the magnetic field. Shikhirev developed a device for the finishing of sheet materials which utilized a pair of cylindrical rolls with opposing polarities rotating in opposite directions [Shikhirev et al., 1977, 1980a, 1980b]. The abrasive powder is fed in the gap between the rolls through helical grooves formed on the surface of the rolls. The sheet material is fed along the axis of the rolls in the gap between the rolls.

Sakulevich developed a method for finishing nonmagnetic articles in which the workpiece was moved along the working gap relative to magnetic abrasive brush [Sakulevich et al., 1979a, 1981]. He, also, used ferromagnetic particles with an aerodynamic profile between the nonmagnetic articles, so as to restore

the density of the magnetic abrasives in the working zone. In the case of polishing of ferromagnetic materials, initially, both ferromagnetic abrasive powder and ferromagnetic workpiece are magnetized to the saturation induction, before their introduction into the magnetic field [Sakulevich et al., 1979b]. Yascheritsyn developed a method for finishing spherical surfaces of the parts [Yascheritsyn et. al., 1980]. In this device, one of the magnet carries the workpiece while the shape of the other magnet corresponds to the spherical surface of the workpiece.

The research on MAF was initiated in Japan in the early 1980s. Watanabe used the method to crush the granular ferromagnetic working substances using the travelling magnetic field [Watanabe et al., 1986]. Knuieda used the method in which magnetic attraction force was generated between cast iron metallic powders, bonded grindstone, and the surface of the workpiece, thereby providing the grinding pressure [Knuieda et al., 1986]. Sugawara developed a method to polish the inner surface of a barrel by filling the magnetic abrasives in the barrel, and attaching the work to a spindle with rotating motion [Sugawara et. al., 1988].

Shinmura, and his associates at Utsunomia University, conducted systematic research on the magnetic abrasive finishing of rollers and tubes [Shinmura et al., 1983-94]. They studied the principles of operation, finishing characteristics under different conditions, and various applications of magnetic abrasive finishing. They extended these studies and designed various equipment for internal finishing of tubes, external finishing of rods, finishing of flat surfaces etc [Shinmura et al, 1989b, 1993a, 1993b, 1994a, 1994b].

In the following, a detailed review of the work carried out by the Japanese and the Russian researchers in the field of magnetic abrasive finishing of rollers, is given.

2.2 Magnetic abrasive finishing devices

Krymsky classified all devices used in MAF into two main groups depending on the type of the magnetic field used [Krymsky, 1993].

In the first group, a permanent magnetic field is used for forming a magnetic abrasive tool (MAT), with the cutting motion provided by the relative motion

between MAT and the workpiece (Figures 2.1-2.10). Sometimes, axial vibration of the magnetic pole is also introduced to enhance the finishing process. This group of devices uses ferromagnetic abrasive powders (FAP) that are easy to magnetize and demagnetize, and have a high saturation magnetic flux. The devices in this group contain an electric coil or permanent magnet as the source of the magnetic field, a yoke with magnetic poles and a working gap (or gaps) between the magnetic pole surfaces and the workpiece filled with FAP. The schematic version of MAT is shown in Figures 2.2 and 2.3 [Baron, 1986, Sakulevich et al, 1977, Shinmura et al, 1985]. The rotation and displacement (feed) of the workpiece ensure its finishing by the MAT. Cutting forces in such a tool are only magnetostatic in nature, and are not very large. Shinmura et al found that the magnetostatic pressure of MAT on the worksurface can reach a pressure of 77 kPa (0.7 kg/m^2) [Shinmura et al, 1985d]. In general, this pressure is barely sufficient for polishing. However, low finishing forces in MATs are compensated by the ability to treat workpieces with complicated shapes and, at times, inaccessible work surfaces (Figure 2.4).

Devices with poles equidistant from the surface being machined are most common. These devices can be used for machining cylindrical (Figure 2.4) [Konavalov et al., 1967, Baron, 1986], plane (Figure 2.6) [Baron, 1986], spherical (Figures 2.7 and 2.8) [Sakulevich et al., 1977], and conical surfaces (Figure 2.10). The self packing of the MAT in the magnetic field makes it possible to polish shafts and axles with annular grooves or threads, to depths of 2-3 mm (Figure 2.11) [Baron, 1986].

In the second group, an alternating or travelling magnetic field is used for magnetic abrasives movement. It is used for ferromagnetic abrasive powder (FAP) movement (Figures 2.1a, and 2.1b) [Kargalov, 1939, Hershler, 1969]. The FAP used in these devices must have strong magnetic properties, such as a high coercive force ($>200 \text{ kA/m}$), because with a low coercive force, reversal of magnetization takes place in FAP, and the FAP stays practically immobile.

Shinmura and Yamaguchi [Shinmura and Yamaguchi, 1994] designed equipment for the internal finishing of a slender tube, which used a linearly travelling magnetic field [Figure 2.12]. In this apparatus, the yoke, the electromagnetic coils, and the magnetic poles, are set up linearly and a three phase AC current with 120° phase shift is used to excite the coils. The magnetic

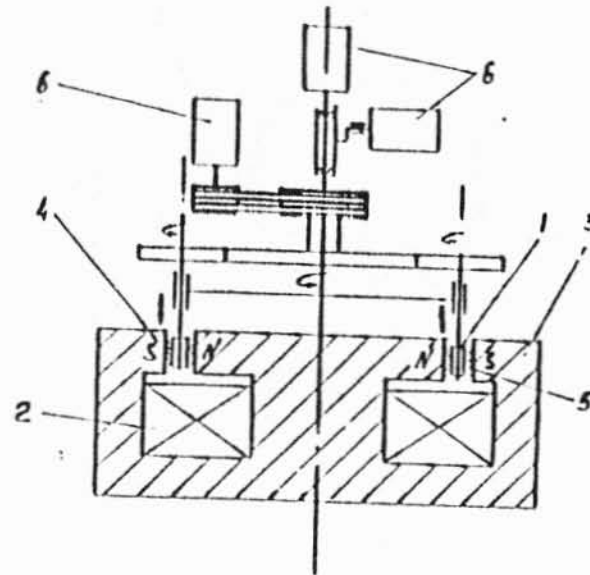


Figure 2.2: Schematic of magnetic abrasive finishing apparatus for finishing of small parts:

1. workpiece, 2. exciting coil, 3. yoke, 4. magnetic poles, 5. gaps with ferromagnetic abrasive powder, 6. electric motor, N= North, S= South [Baron 1986].

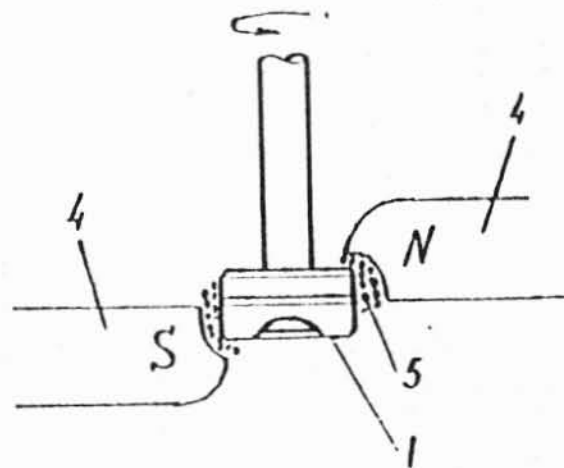


Figure 2.3: Schematic of MAF for finishing of sewing machine parts

1. workpiece, 2. exciting coil, 3. yoke, 4. magnetic poles, 5. gaps with ferromagnetic abrasive powder, 6. electric motor, N= North, S= South [Sakulevich et al., 1977]

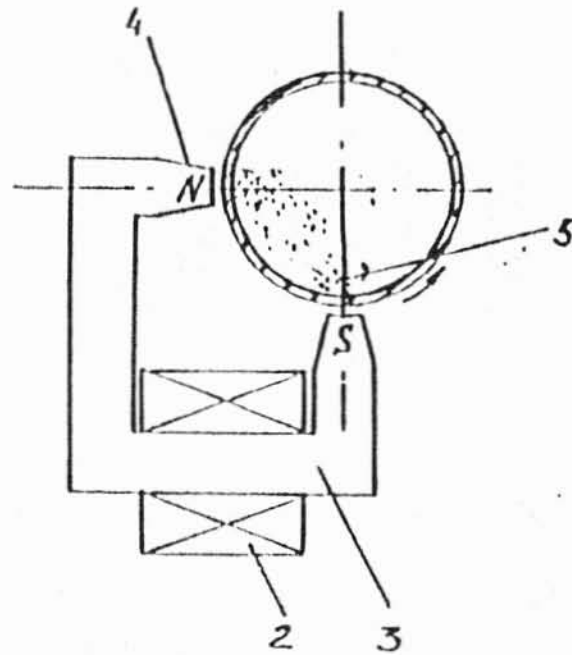


Figure 2.4: Schematic of MAF for the finishing of inner surface of thin nonferromagnetic pipes [Krymsky, 1993].

1. workpiece, 2. exciting coil, 3. yoke, 4. magnetic poles, 5. gaps with ferromagnetic abrasive powder, 6. electric motor, N= North, S= South

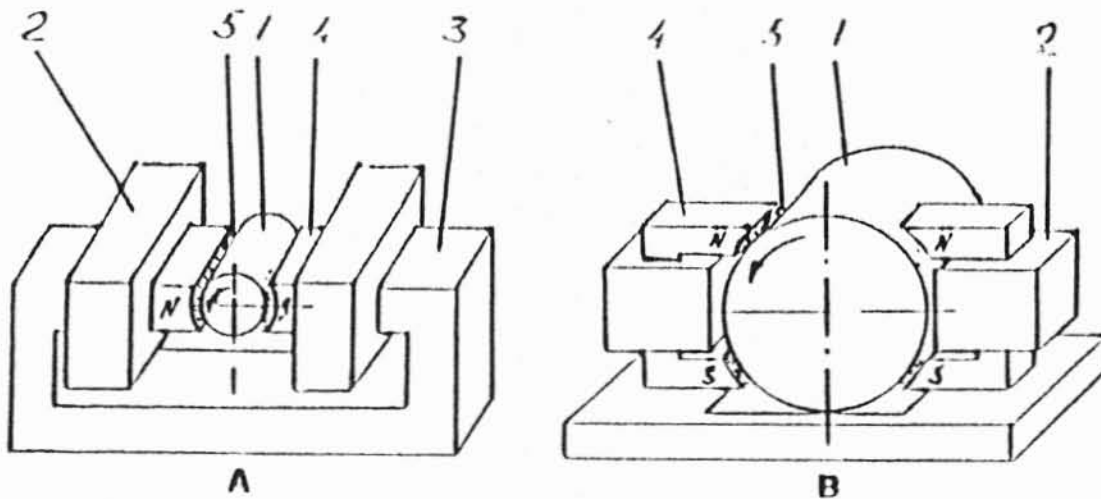


Figure 2.5: Schematic of MAF for (A) medium size and (B) large cylindrical parts [Konavalov et al, 1967]

1. workpiece, 2. exciting coil, 3. yoke, 4. magnetic poles, 5. gaps with ferromagnetic abrasive powder, 6. electric motor, N= North, S= South

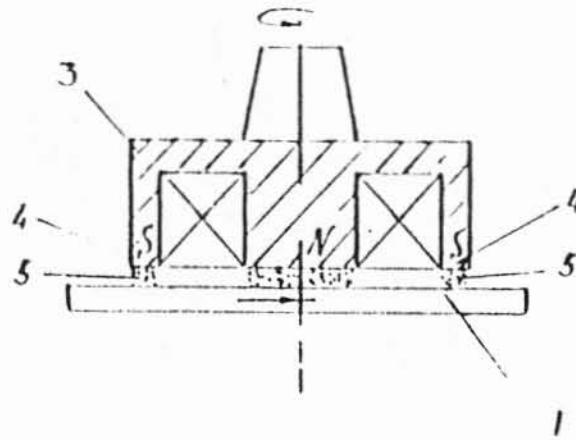


Figure 2.6: Schematic of MAF for sheets and plates [Baron 1986].

1. workpiece, 2. exciting coil, 3. yoke, 4. magnetic poles, 5. gaps with ferromagnetic abrasive powder, 6. electric motor, N= North, S= South

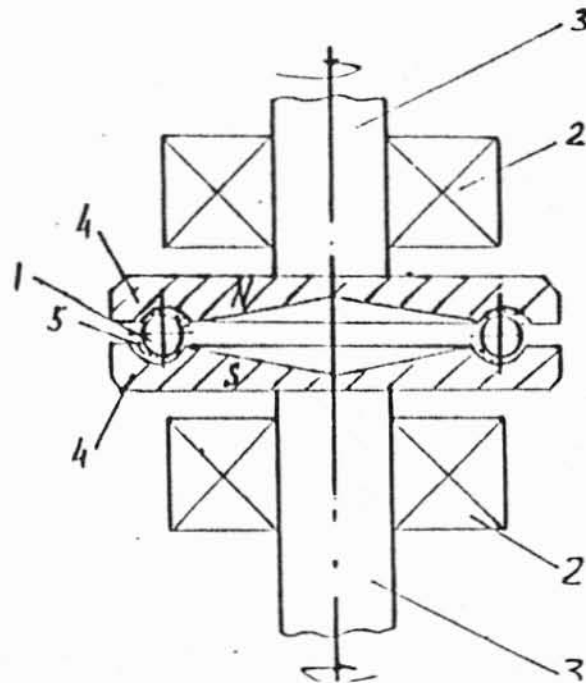


Figure 2.7: Schematic of MAF for fine ball finishing [Sakulevich et al, 1977].

1. workpiece, 2. exciting coil, 3. yoke, 4. magnetic poles, 5. gaps with ferromagnetic abrasive powder, 6. electric motor, N= North, S= South

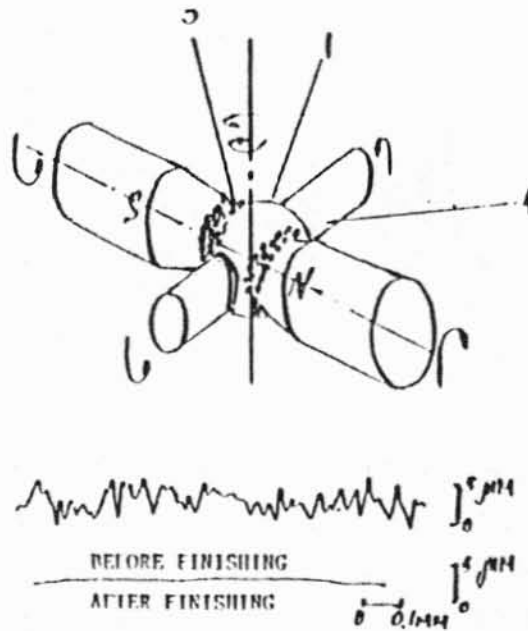


Figure 2.8: Schematic of MAF for finishing of a ball valve, showing profile of surface roughness before and after finishing [Salulevich et al, 1977].

1. workpiece, 2. exciting coil, 3. yoke, 4. magnetic poles, 5. gaps with ferromagnetic abrasive powder, 6. electric motor, N= North, S= South

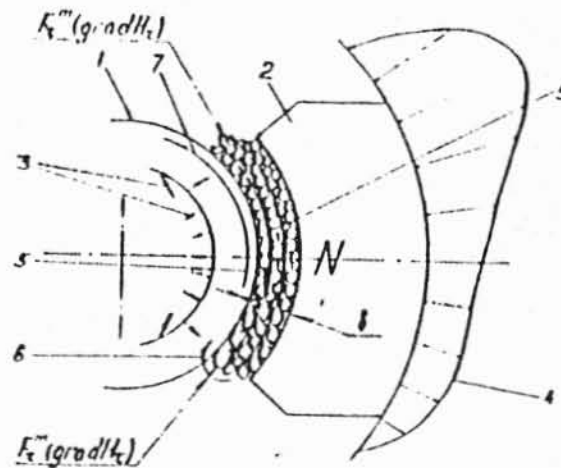


Figure 2.9: Schematic example of a magnetic abrasive tool (MAT) for polishing of a cylindrical surface [Krymsky, 1993]

1. workpiece, 2. magnetic pole, 3. direction of magnetostatic force acting on magnetic abrasive particles in the working gap, 4. normal pressure on work surface pattern 5. trajectory of slow grain reorientation in the MAT, 7 finishing direction

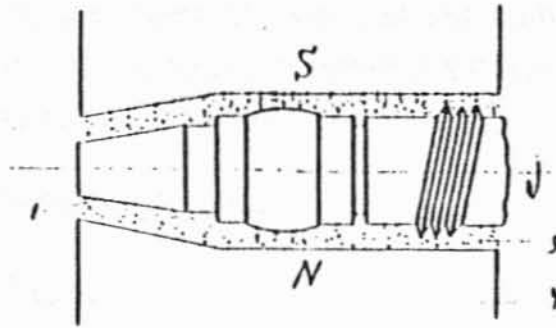


Figure 2.10: Schematic of MAF for finishing of a shaft with thread, annular groove, spherical and conic surface [Krymsky, 1993].
 1. workpiece, 2. exciting coil, 3. yoke, 4. magnetic poles, 5. gaps with ferromagnetic abrasive powder, 6. electric motor, N= North, S= South

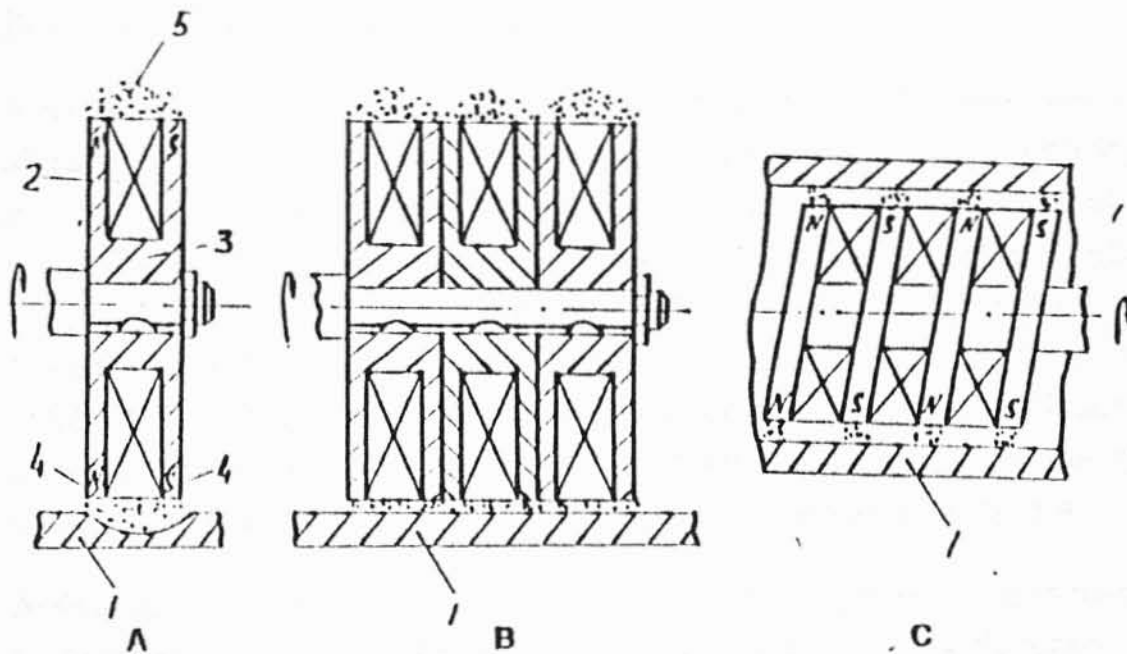


Figure 2.11: Schematic of magnetic abrasive buffing wheels (A) flat face treatment; (B) large flat surface treatment by a set of buffing wheels; (C) treatment of pipe inner surface [Baron 1986].
 1. workpiece, 2. exciting coil, 3. yoke, 4. magnetic poles, 5. gaps with ferromagnetic abrasive powder, 6. electric motor, N= North, S= South

abrasive finishing tool comprising of an abrasive cloth is introduced inside the tube and is driven by the magnetic force at the same speed as that of the rotating magnetic field along with the internal surface of the tube. Thus, the internal surface of the tube is finished.

2.2 a: Internal finishing of tubes

Using electromagnet coils:

A rotating magnetic field is generated by six electromagnetic coils installed on a circular yoke and powered by a three phase AC current (Figure 2.13)[Shinmura et al, 1993b]. The finishing tool comprises a permanent magnet made of rubber sheets with N-S poles that is driven by the magnetic force, so as to rotate along with the internal surface of the tubing at high speed (Figure 2.14 and 2.15).

Process Principle:

Rotating mechanism of the finishing tool

A sinusoidal three phase current with a 120° phase shift excites each coil as shown in Figure 2.15. Consequently, the magnetic field also changes in a sinusoidal mode. When pole 1 is magnetized as N to its maximum at time a, poles 2 and 3 are magnetized as S. Pole S of the finishing tool receives a magnetic attractive force from magnetic pole 1 and repulsive force from pole 3. N pole of the finishing tool, on the other hand, receives a magnetic attractive force from magnetic poles 2 and 3. The attractive force of pole 2 is less than the attractive force of pole 1. Thus, the finishing tool advances in the direction shown by the arrow, along the internal surface of the tubing, at time a.

At time b, the magnetic pole 2 is changed from S to N, and pole 3 is magnetized to its maximum value S. The magnetic pole 2, which is now N, repulses the N pole of the finishing tool, while pole 3 provides attractive force to the tool. S pole of the tool rotates in the direction of the arrow, under the attractive force from pole 1 and repulsive force from pole 3.

At time c, the magnetic pole 1 changes from N to S, while pole 2 becomes N. The initial situation is reproduced if pole 2 is considered instead of pole 1, pole 3 instead of pole 2, and pole 1 instead of pole 3.

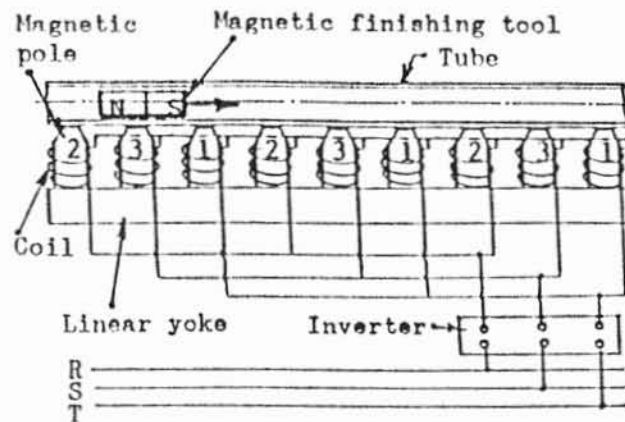


Figure 2.12: Schematic diagram of internal finishing apparatus by the application of a linearly travelling magnetic field [Shinmura and Yamaguchi, 1994]

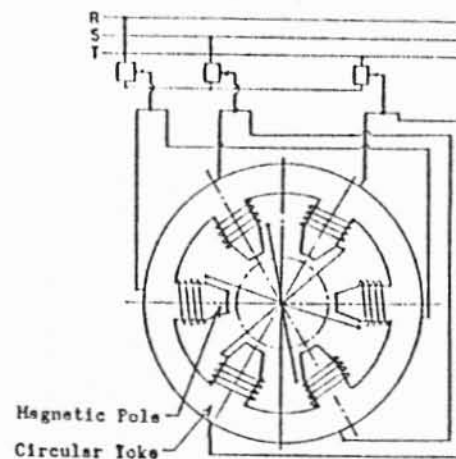


Figure 2.13: Basic construction of finishing equipment [Shinmura et al, 1994].

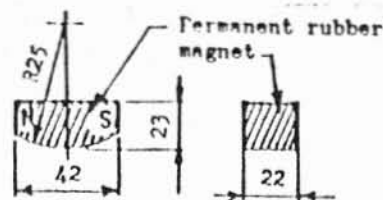


Figure 2.14: Shape and size of magnetic finishing tool used in experiments [Shinmura et al, 1994].

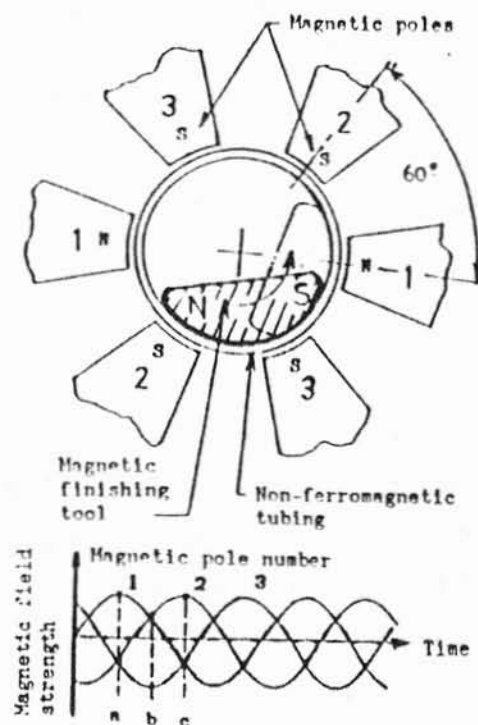


Figure 2.15: Magnetic force acting on a magnetic finishing tool. [Shinmura et al, 1994].

Thus, rotating action is repeated. In this way, the magnetic finishing tool is driven smoothly along the internal surface of a tube by the magnetic force, synchronous with the external rotating magnetic field. The precision internal finishing of tubing is performed by the abrasive materials attached to the tool surface.

In the internal finishing of a bent tubing, where the conventional machining processes are inaccessible, the internal surface can be uniformly finished using this process to $0.4\text{ }\mu\text{m Rmax}$ [Shinmura et al, 1993b]. It is also found that this process is feasible for internal finishing of tubes with thickness up to 20 mm.

Using permanent magnets:

Using rotating permanent magnets:

In this process, four magnetic poles (N-S poles), with rare earth permanent magnets installed on a circular yoke, are rotated at high speed around a stationary circular tubing, as shown in Figure 2.16 [Shinmura et al, 1994]. A mixing type magnetic abrasive, in which small size magnetic abrasives ($44\text{ }\mu\text{m}$ diameter) are mixed with large size iron particles ($330\text{ }\mu\text{m}$ in diameter), is supplied to the working area of the tubing and rotated by the magnetic force, together with the external rotating magnetic poles. This results in an extremely smooth finish on the internal surface of the tubing.

Using vibratory permanent magnets:

Figure 2.17 shows an internal finishing apparatus consisting of a small unit type which incorporates ferrite permanent magnets, installed on the carriage of the lathe assembly [Shinmura et al, 1993]. A magnetic finishing jig comprising rare earth permanent magnets and a ferromagnetic material, is used in this finishing apparatus (Figure 2.18). The shape and size of the magnetic finishing jig and magnetic poles are shown in Figure 2.18. This configuration makes a non-uniform magnetic field distribution between the magnetic finishing jig and the magnetic poles. The rare earth permanent magnets are fixed on the finishing parts of the magnetic finishing jig. When polishing cloth is stuck on this jig, it becomes a magnetic finishing tool. It is found that both magnetic flux density and the magnetic finishing pressure by the magnetic finishing jig are much

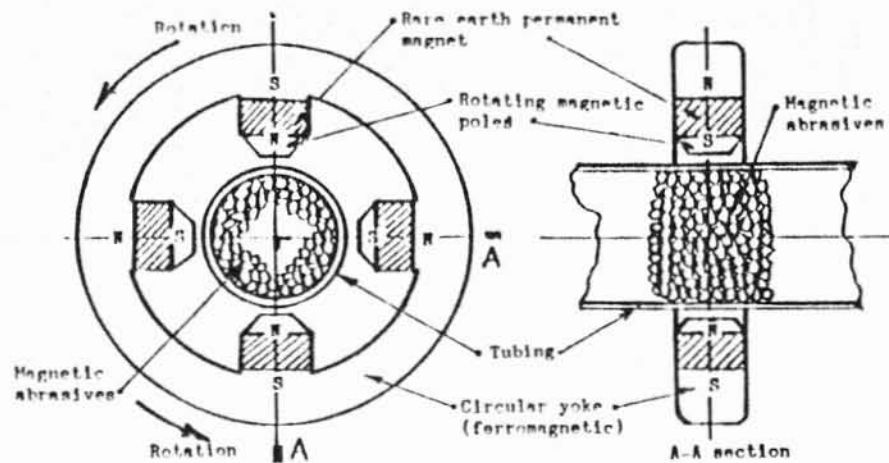


Figure 2.16: Schematic view of new internal finishing process using rotating magnetic poles [Shinmura et al, 1994]

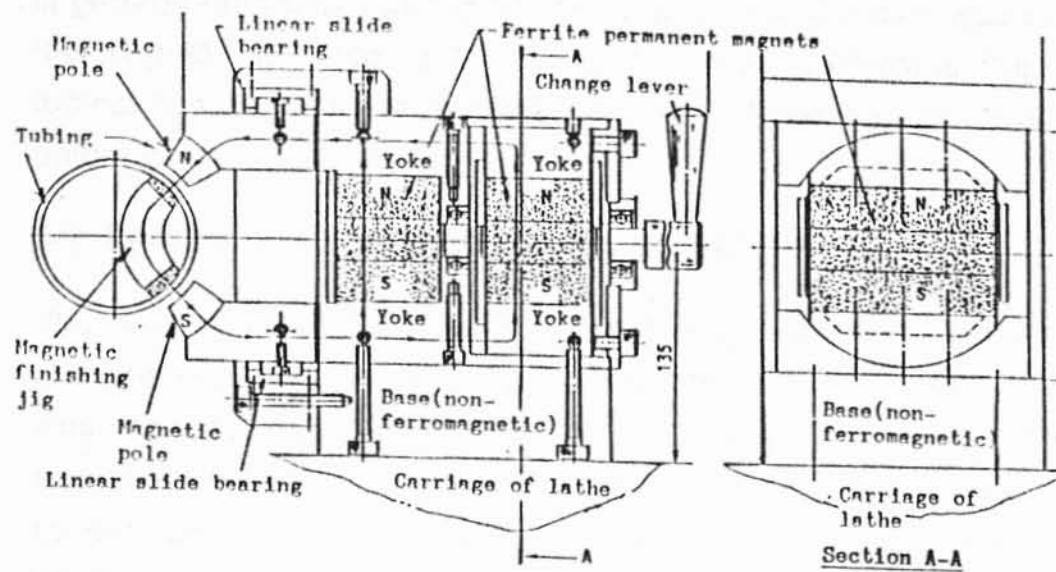


Figure 2.17: Assembly view of the magnetic finishing apparatus [Shinmura et al, 1993]

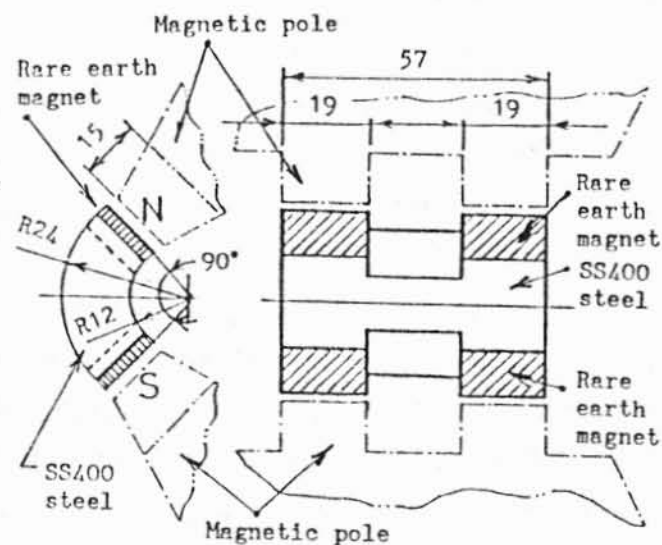


Figure 2.18: Shape and size of magnetic finishing jig [Shinmura et al, 1993]

higher than those by the magnetic abrasives. A vibration generator is installed to vibrate the magnetic poles. The magnetic force used as the finishing pressure is generated in between the magnetic poles and the magnetic finishing jig. As the magnetic finishing jig generates the finishing pressure from inside of the tubing, this can make a reciprocating action following motion of the magnetic poles.

2.3 Synthesis of magnetic abrasive powder

The development of the MAF process requires the development of special abrasive materials with ferromagnetic properties. The simplest of these are the well know powders of hard alloys of iron (iron-carbon, iron-aluminium-carbon, iron-titanium, etc.), which are generally used for finishing soft alloys or nonferrous metals, steel, wood and plastic [Baron, 1975]. They can be used to remove soft oxide films or scale. But, harder materials can not be finished by iron powder. So, bonded magnetic abrasives of ferromagnetic powder and hard abrasive were developed. In the former USSR [Nalivka et al., 1991, Liashchenko et al., 1983, Dyad'ko and Krymsky, 1992, and Oliker et al, 1983] and later in Bulgaria [Bradvarov et al., 1987]) and in Japan [Hori and Watanbe, 1987] special composite FAPs were developed with different structures (Figure 2.19). For the ferromagnetic component, these materials generally contain iron and its alloys, and for the abrasive component hard, refractory compounds such as titanium carbide, Al_2O_3 etc. are used. Several techniques such as internal nitriding [Liaschenko, 1982], solid-phase combustion synthesis [Kiparisov, 1979], melt spray have been used for the production of such bonded magnetic abrasives [Baron, 1975]. As the iron content in the abrasive material is important from the point of view of magnetic properties of the magnetic abrasive, studies have been conducted to optimize the composition of the magnetic abrasives to achieve better removal rate, using an abrasive agglomerate with better magnetic properties [Krymsky, 1984]. These studies indicate that the quantity of the magnetic component should be in the range of 35-70% (by volume). The optimum composition depends on the device field strength and its configuration in the working gap. The average grain size of the magnetic component is in the range of 100-300 μm and the abrasive component is in the range of 1-10 μm . Dyad'ko and Krymsky showed that the polishing ability of MAPs depends not

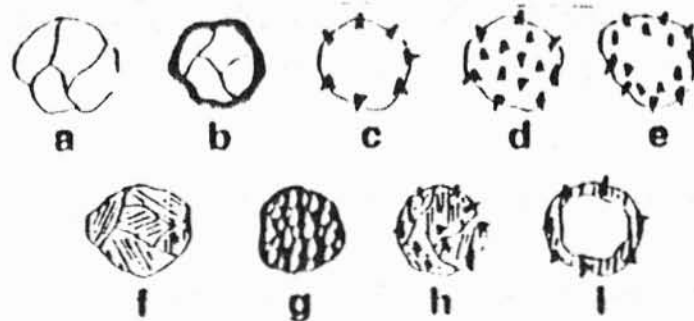


Figure 2.19 :

Schematics of FAP grain structures [Krymsky, 1993]

white, ferromagnetic phase; black abrasive phase; a: pure ferromagnetic metal or its solid solution with other metals (e.g. iron-aluminium-silicon) or its chemical compound (e.g. iron oxide); b: FAP with entire abrasive coating; c: FAP with abrasive particles located only on the grain surface; d, FAP with uniform distribution of abrasive particles; e: FAP with abrasive particle layer; f: FAP on the base of eutectic alloys of iron (e.g. iron-iron carbide); g: FAP with abrasive matrix; h: FAP with matrix of eutectic alloy i: FAP with core of pure magnetic alloy and coating of eutectic alloy with inclusions of abrasive particles

only on the microstructure of the grains but also on their macrostructure [Dyad'ko and Krymsky, 1992].

Suzuki et al showed that the polishing capacity of the magnetic polishing of free curved surfaces in moulds was greatly improved using short fiber magnetic polishing material [Suzuki et al, 1991]. The use of short fibers shown in Figure 2.20 in conjunction with magnetic abrasives increased the finishing efficiency and useful life of the magnetic abrasives. This was due to the reduced friction between the polishing grains. Anzai et al showed the possibility of magnetic abrasive finishing of curved surfaces of a WC-Co alloy, using iron bonded diamond magnetic abrasives developed by a sintering process [Anzai et al, 1992].

2.4 Movement of magnetic abrasives in the finishing zone:

All MAF devices depend on the properties of the magnetoabrasive tool (MAT) [Krymsky, 1993]. Compared with traditional abrasive tools with hard mechanical bonding (e.g. grinding wheels), or free abrasives (lapping), MAT has the following advantages [Krymsky, 1993]:

- Magnetic abrasive grains are not fixed rigidly in space. Investigation of the MAF process using high-speed photography showed that grains in the MAT slowly migrate in the finishing zone under the action of tangential friction force exerted by the rotating workpiece. Periodically, the grains rotate around their axes. This complete motion of the grains ensures self-sharpening of the MAT and a complete trajectory of finishing motion which is necessary for polishing.
- Automatic leveling of the grains relative to the work surface, due to attraction of the grains to the ferromagnetic work surface in the magnetic field.

The levelling of the grains and the presence of several grain layers between the poles and the workpiece allows the use of FAPs that are significantly coarser, with a wider range of sizes. These FAPs are cheaper than those used for common finishing. The finishing efficiency of the MAF depends to a large degree on the method of forming the abrasive brush and its movement during the finishing process.

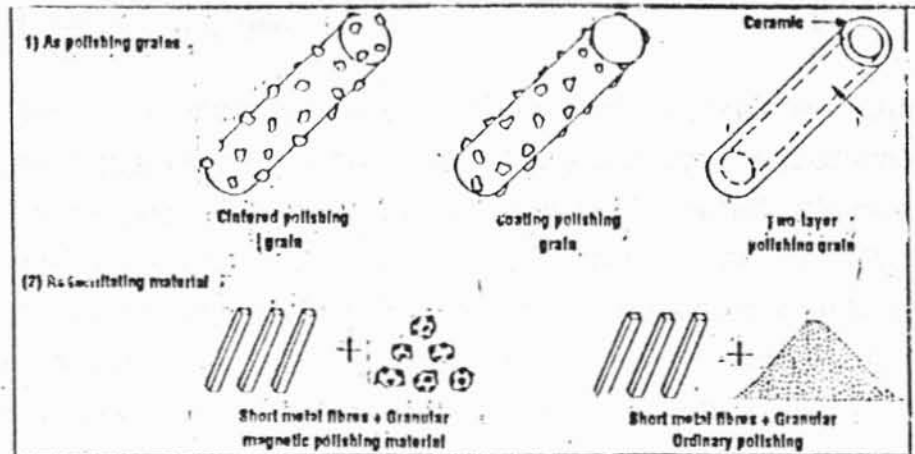


Figure 2.20: Type of short fiber Magnetic polishing materials [Suzuki et al, 1991]

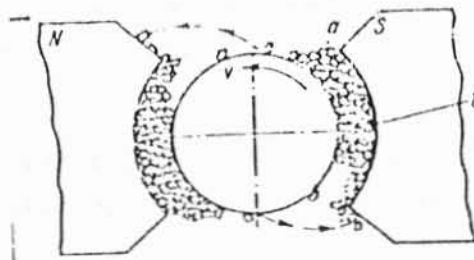


Figure 2.21: Transfer of the magnetic abrasives to the adjacent finishing zone in the direction of movement of the workpiece [Maiboroda et al., 1989]

When a rotating workpiece is introduced into the magnetic abrasive region, the abrasive brush is displaced in the direction of the movement of the workpiece towards the outlet of the finishing zone (Figure 2.21). This displacement occurs because of the following two factors:

1. The disturbance introduced by the rotating workpiece to the abrasive brush results in pushing apart of the abrasives [Maiboroda et al, 1989]. The magnetic abrasive brushes consist of tapered columns, the base of which is located on the working surfaces of the magnetic pole tips [Shlyuko et al, 1985]. In the direction of movement of the rotating workpiece, the disturbances propagate only within the tapered columns. The columns themselves possess increased elasticity in the direction approaching the direction of the magnetic force lines, and may not deflect under the action of disturbances introduced by an amount sufficient for contact with the adjoining columns. In any case, the rate of propagation of these disturbances may not be comparable with the rotational speed of the workpiece.
2. The ferromagnetic abrasive powder (FAP) is held in the working gap by the tangential component of the magnetostatic force F , which occurs only along the edges of the magnetic poles. But the tangential cutting force and the frictional force F_f combine to carry the magnetic abrasive particles (MAPs) from the working gap. To retain the MAPs in the working gap, F_t must be greater than F_f . As there is no tangential magnetostatic force inside the working gap, the MAPs can be moved by F_f toward the exit of the working gap, which causes an increase in the packing density of the powder and its wedging near the exit.

As a result of the small displacement in the magnetic abrasive brush, a group of abrasive grain positioned at the exit of working zone is separated from the main abrasive brush during rotational movement of the workpiece. As shown in Figure 2.21, part of this separated powder settles on the nonworking surfaces of the magnetic poles. The rest of the abrasive mass is transferred to the region of the adjacent finishing zone and takes part in further polishing. After a certain period of polishing, stabilization is reached when the amount of abrasive carried into the finishing zone is equal to that carried away from it. The relative

stabilization of the magnetic brush in the magnetic gaps starts approximately 20-30 seconds after the start of polishing.

Maiboroda conducted a mathematical analysis of the motion of magnetic abrasives in transverse and longitudinal directions through the finishing zone [Maiboroda et. al., 1987]. Figure 2.22 shows the variation of the normal component of the direction of motion of abrasives in the finishing zone with distance from the entry zone. It shows that after a 10 second period, the normal speed of the magnetic abrasives falls near the region of entry into the working zone, and subsequently grows linearly. After 20-30 seconds the normal speed increases almost linearly. The reason for this is that, at the initial instant of time, the magnetic abrasives experience intense transformation into a state characterized by maximum agitation of the abrasives which are being displaced by the workpiece. A stable state is attained in about 30 seconds after the beginning of the abrasive finishing process. The figure also shows that at the entry of the working zone, the normal rate of motion of the powder is negative after 20 and 30 seconds of polishing, i.e. the powder has a tendency to move away from the workpiece towards the magnetic poles. An explanation of this phenomena is found by the formation of fan-shaped condensed regions at the entry of the workpiece, during the latter's movement through the finishing zone [Shlyuko et al., 1985]. Such condensed regions, under the action of a rotating workpiece, tend to split the magnetic abrasive brush, imparting to the abrasives, at the same time, a normal velocity component in a direction away from the workpiece towards the magnetic poles. Another characteristic feature is the distribution of the magnetic abrasive brush in the finishing zones towards the end of the polishing cycle. In the entry region, where the normal velocity component has large absolute value, the distance between the tips of the powder columns resting on their bases on the working surfaces of the pieces is a maximum. As the normal component tend to zero, this distance decreases, resulting in the formation of a continuous, dense magnetic abrasive brush. Figure 2.23 shows the variation of the speed of magnetic abrasive in the tangential direction along the length of finishing zone. During the motion of the workpiece, at velocities of 3.14 and 3.93 m/s, the tangential component of the speed of the particles in a batch of powder was found to be independent of the position of the abrasive grain in the finishing zone and is determined by the rotation speed of the workpiece. This was assumed to be due to the integration

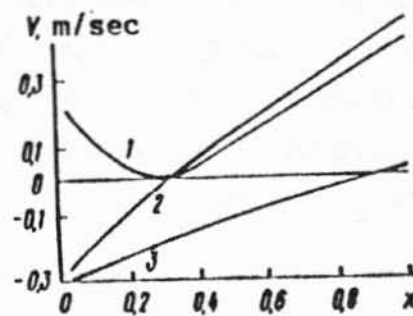


Figure 2.22: Variation of normal component of the velocity of magnetic abrasives as function of along working length of magnetic gap after polishing for (1) 10, (2) 20, (3) 30 seconds [Maiboroda et. al., 1987]

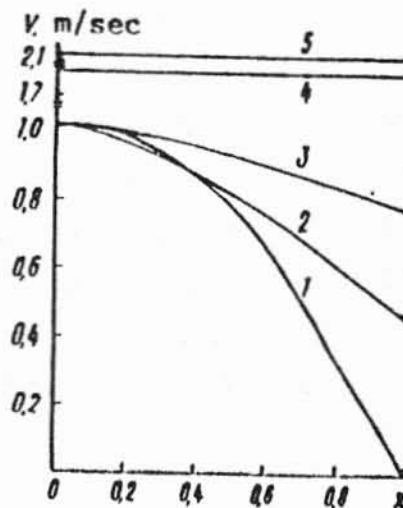


Figure 2.23: Variation of tangential component of the rate of motion of magnetic abrasives along working length of magnetic gap at workpiece speed of 2.35 m/s after polishing for (1) 30, (2) 20, (3) 10 seconds at speed of (4) 3.14 m/s and (5) 3.93 m/s [Maiboroda et. al., 1987]

of the fan-shaped condensed regions of magnetic abrasive brushes at certain speeds and workpiece-to- magnetic abrasive size ratios. This analysis shows that the most effective mixing of magnetic abrasive takes place near the entry point of the finishing zone.

The movement of the abrasives during polishing is analyzed by evaluating the resistance exerted by the abrasive grains to the movement of the rotating workpiece [Maiboroda et al., 1985]. The method is based on measuring the current of the electric motor that rotates the workpiece. The authors observed that with increasing speed, the frictional resistance exerted by the magnetic abrasives to the movement of the workpiece increases with the length of path travelled by the workpiece.

The work performed during the reforming of magnetic abrasive material from a uniformly distributed state into the working stable state, is calculated by measuring the area of the curve in Figure 2.24 for different rotational speeds. When the work done is plotted against the path travelled by the magnetic abrasives, four regions are observed (Figure 2.25). In region I, the linear increase of the work, carried out by the workpiece, is significant and the typical process is the reforming of magnetic abrasives from the initial state to a comparatively stable state, and the transferring of the powder from one finishing zone to other. Region II is a transition region between regions I and II. In region III, the rate of increase of the work is linear, with a smaller slope of the curve than in region I. In this region, the position of the magnetic abrasive brush is comparatively stable, and the transfer of the abrasives from one finishing zone to the other is of a steady nature. Region IV is identical to III but the intensity of carried out work decreases, since a certain part of the magnetic abrasives settles on the nonworking surfaces of the magnetic poles without taking part in the finishing process. This, in turn, decreases the total mass of the abrasives and, consequently, the amount of work required for its displacement also decreases.

From Figure 2.25, it appears that the resistance exerted by the abrasives to the movement of the workpiece decreases with increasing speed of travel of the components. This is associated with the reduction of the size of fan-shaped seals formed at the entry stages of the workpiece and their partial or complete failure.

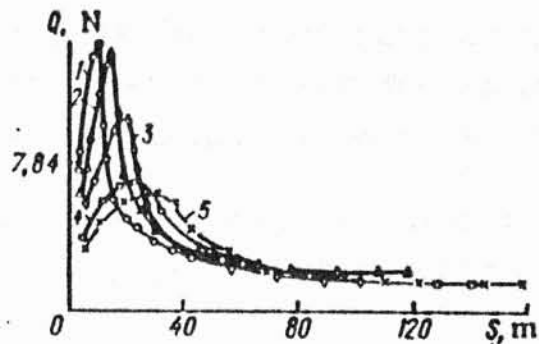


Figure 2.24: Variation of the resistance force exerted by the abrasives to the movement of the component in finishing process in relation to the length of the path travelled by the blade in the treatment zone. $B = 0.7T$, Abrasive particle diameter = $300\mu m$, speed of motion = (1) 1.57, (2) 2.355, (3) 3.14, (4) 3.915, and (5) 4.71 m/s [Maiboroda et al., 1985].

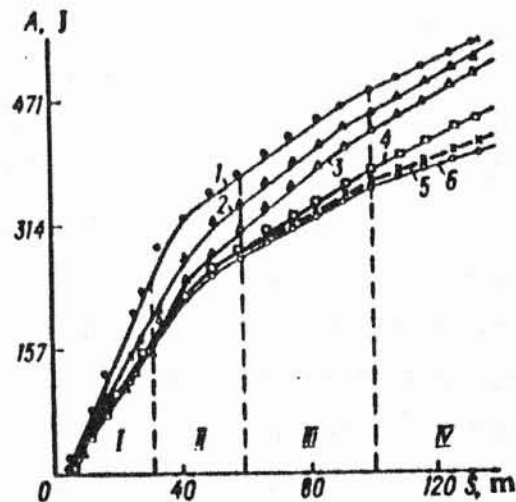


Figure 2.25: Variation of the work carried out by the component in reforming the magnetoabrasive powder in relation to the length of the path travelled by the workpiece in the treatment zones. Speed: 3.915 m/s, B : (1,2) 0.67T, (3,6) 0.67T, (4, 5) 0.7T, particle size: (1, 5, 6) $300\mu m$, (2, 4) $100\mu m$ [Maiboroda et al., 1985].

It is important to obtain a sufficiently dense abrasive brush using the maximum possible volume and cutting capabilities of the abrasive powder. As explained in the above paragraphs, due to redistribution of the magnetic abrasives in the finishing zone, the density of the abrasive brush is less at the entry into the working zone and more at the exit. The dynamics of movement of the abrasive brush, in the working zones, depend both upon the rotational velocity of the workpiece and the magnetic field distribution in the abrasive region.

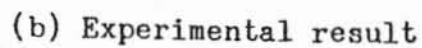
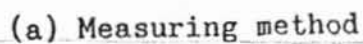
In order to study the movement of magnetic abrasive grains in relation to the magnetic pole configuration, Maiboroda et al designed three different magnetic poles [Maiboroda et al, 1985]:

- I) with a smooth working surface
- II) with four vertical rectangular concentrators equal in width and uniformly applied
- III) with rectangular concentrators nonuniformly applied, with increasing width from the entry zone.

The ability of the magnetic pole was judged from its capacity to hold and trap the magnetic abrasives and to prevent the transfer of the magnetic abrasive into the region of adjacent finishing zone. To investigate this characteristic, Maiboroda et al performed a set of experiments with different rotational speeds of the magnetic workpiece [Maiboroda et al, 1985] with each of the above three magnetic poles, and the quantity of the magnetic abrasives retained in the finishing zone was measured in each case. The rotational velocity in which the steady state condition of the abrasives is attained is termed the threshold rotational velocity. Magnetic poles with type III appeared to result in the most stable condition of the magnetic abrasive brush. This was attributed to the gradual increase with width of the rectangular barriers, in the direction of movement of the abrasives in the working zone.

2.5. Generation of the finishing pressure in MAF

Shinmura conducted experiments to examine whether the magnetic pressure generated in the finishing apparatus is capable of finishing the workpiece [Shinmura et. al., 1985d]. For this purpose, he set up a simple experiment as shown in Figure 2.26a. He measured, the action force, F , as the magnetic flux



38

density was changed, by putting strain gauges on an aluminium bar of 30 mm diameter. The bar itself is not affected by the magnetic force, because aluminium is a nonmagnetic substance. Magnetic abrasives were filled into the working clearance on one side only. Shinmura found that as the magnetic flux density increases, the action force also increases. Shinmura also observed that as more magnetic abrasives are filled, the more action force is obtained (Figure 2.26b).

In general, when magnetism acts on the boundary plane of two materials with different permeabilities, a magnetic stress is generated on its boundary plane [Shinmura et al., 1987b]. Figure 2.27 shows the magnetic pressure acting at the boundaries between substance [I] and [II]. The magnetic pressure at the boundary can be described by the equation

$$P = \frac{B^2}{2} \left(\frac{1}{\mu_1} - \frac{1}{\mu_2} \right)$$

where B is the magnetic field in mediums [I] and [II] and μ_1, μ_2 are the magnetic permeabilities of the substance [I] and [II] respectively.

If μ_{rm} is the specific permeability of the magnetic abrasives then the equation becomes

$$P = \frac{B^2}{2\mu_0} \left(1 - \frac{1}{\mu_{rm}} \right)$$

In the above equation, the magnetic abrasive is considered as a solid block of material. As the magnetic abrasive consist of ferromagnetic substance (Fe) and nonmagnetic substance (Al_2O_3 etc.), μ_{rm} is strongly dependent on the permeabilities of both of its constituents. The equation for the μ_{rm} is given as,

$$\mu_{rm} = \frac{\mu_a}{\mu_0} \frac{1 - \left[V_g \frac{\mu_a - \mu_g}{2\mu_a + \mu_g} + V_i \frac{\mu_a - \mu}{2\mu_a + \mu} \right]}{1 + \left[V_g \frac{\mu_a - \mu_g}{2\mu_a + \mu_g} + V_i \frac{\mu_a - \mu}{2\mu_a + \mu} \right]}$$

where μ_a, μ_g , and μ are the magnetic permeabilities of air, Al_2O_3 (abrasive), and iron respectively,

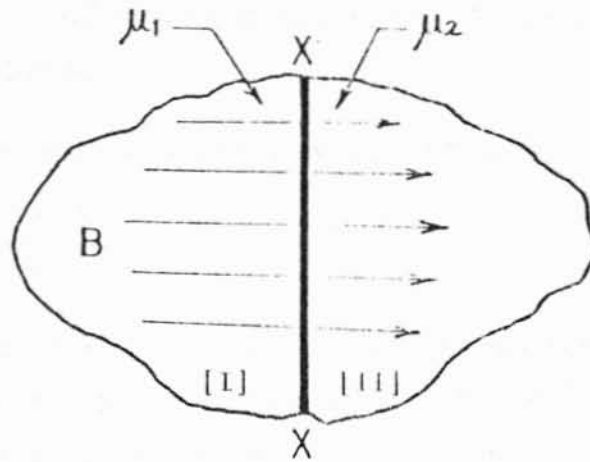


Figure 2.27: Magnetic pressure acting between substance [I] and substance [II] [Shinmura et al., 1987b]

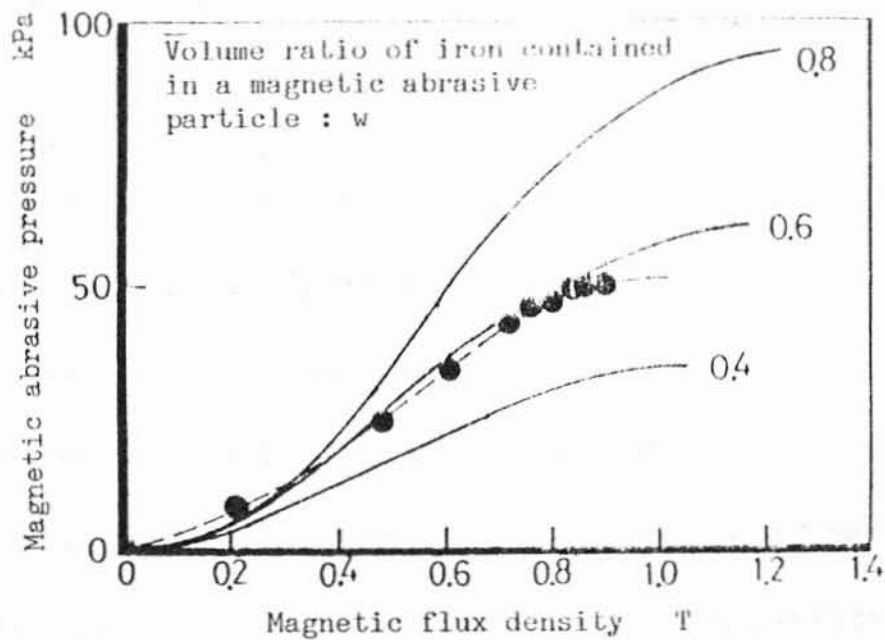


Figure 2.28: Relationship between magnetic abrasive pressure and magnetic flux density using equation [Shinmura et al., 1987b]

V_i and V_g are the volume ratio of iron and Al_2O_3 abrasive in the magnetic abrasive respectively.

If we assume, $\mu_a = \mu_g = \mu_0$ and $\mu_r = \mu/\mu_0$, we get,

$$\mu_{rm} = \frac{2 + \mu_r - 2(1 - \mu_r) V_i}{2 + \mu_r + (1 - \mu_r) V_i}$$

Assuming that the shape of the magnetic abrasive particles is spherical, and the filled state of particles is a tetragonal arrangement, and also that a group of magnetic abrasives in the working zone is composed of three elements (i.e. pure iron, abrasive grains and pores), we can assume, $V_i = \pi w/6$.

Hence,

$$\mu_{rm} = \frac{6(2 + \mu_r) - 2\pi(1 - \mu_r)w}{6(2 + \mu_r) + \pi(1 - \mu_r)w}$$

Using the equations, the theoretical formula for the finishing pressure "P" is given by:

$$P = \frac{B^2}{4\mu_0} \frac{3\pi(\mu_g - 1)w}{3(2 + \mu_g) + \pi(\mu_g - 1)w} \quad (2.1)$$

where B = magnetic flux density in the working zone

μ_0 = magnetic permeability in vacuum

μ_g = relative magnetic permeability of pure iron

w = volume percentage of pure iron contained in one particle

From equation (2), it is evident that finishing pressure generated by a group of magnetic abrasives in the working zone has no relation to the magnetic abrasive particle diameter. The calculated results are shown in Figure 2.28 which agree well with the experimental values.

If B_i is the magnetic field through the iron, then the magnetic field through the abrasive (B_j) can be given by the relation,

$$B_j = \left\{ \frac{\pi w}{6} \left(1 - \frac{1}{\mu_r} \right) + \frac{1}{\mu_r} \right\} B_i$$

Figure 2.29 shows the B-H curves for the magnetic abrasive and 0.16%C steel. From the B-H curve for iron, $B_i - \mu_r$ curve for iron is calculated, as shown in Figure 2.30. Knowing $B_i - \mu_r$ curve for iron, one can obtain the $B_j - \mu_{rm}$ curve for the magnetic abrasives. The calculated $B_j - \mu_{rm}$ curve for the magnetic abrasives matches closely with that of the measured curve, as shown by the dotted line in Figure 2.30.

Modification of finishing pressure

Real finishing pressure, P_d , during polishing can be smaller than the static finishing pressure, P , by factor of ξ , given by equation (2.2), because of a change of structure of the magnetic abrasive brush [Shinmura et al, 1987b].

$$P_d = \xi P \quad (2.2)$$

The magnetic abrasive brush can be deformed, due to a tangential resistance acting on it during polishing. If some amount of magnetic abrasive is thrown away, the concentrations of magnetic abrasive and finishing pressure were decreased. The value of ξ can be a function of the binding force ΔF_m of magnetic abrasives. F_m can be shown to be

$$\Delta F_m = \frac{3 \pi D^2 \chi_r^2 B}{8 \mu_0 (3 + \chi_r)^2} \quad (2.3)$$

where D is the average diameter of the magnetic abrasive particle.

χ_r is the relative magnetic susceptibility of the magnetic abrasive particles

B is the magnetic field density in the abrasive region.

Estimation of removal amount by magnetic abrasive finishing

The removal mechanism can be assumed as cutting by abrasive grains, whose tip shape is conical or spherical. The removal amount, M , can be estimated by the following equation.

$$M \propto L_0 (H_v)^{-(1 \sim 1.5)} (\xi)^{1 \sim 1.5} D^{0 \sim 1} \quad (2.4)$$

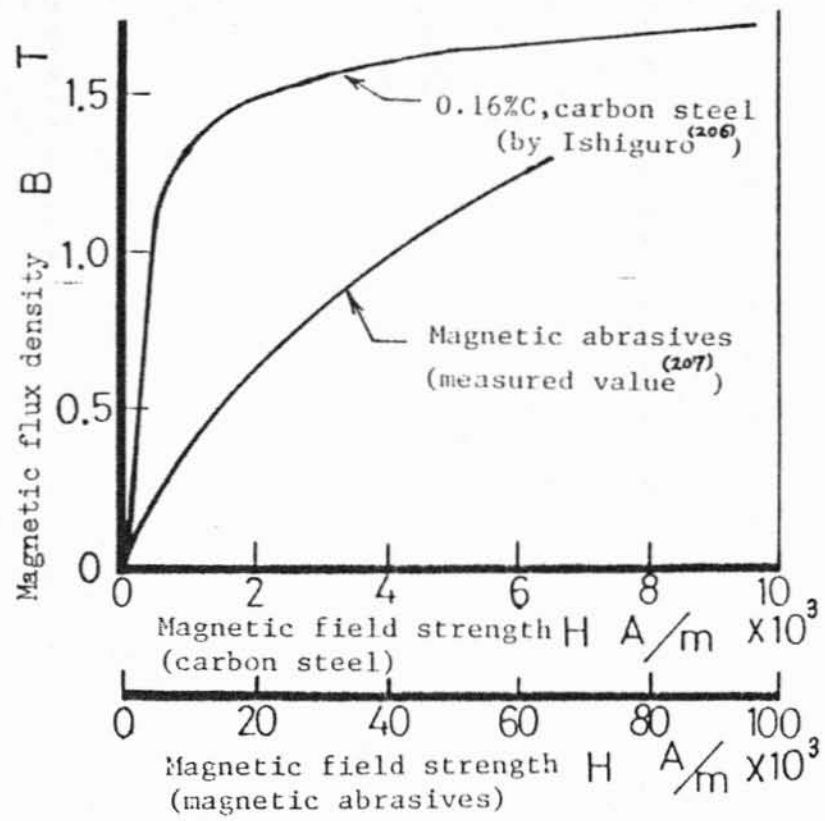


Figure 2.29: B-H curve for 0.16% carbon steel and magnetic abrasives [Shinmura et al., 1987b]

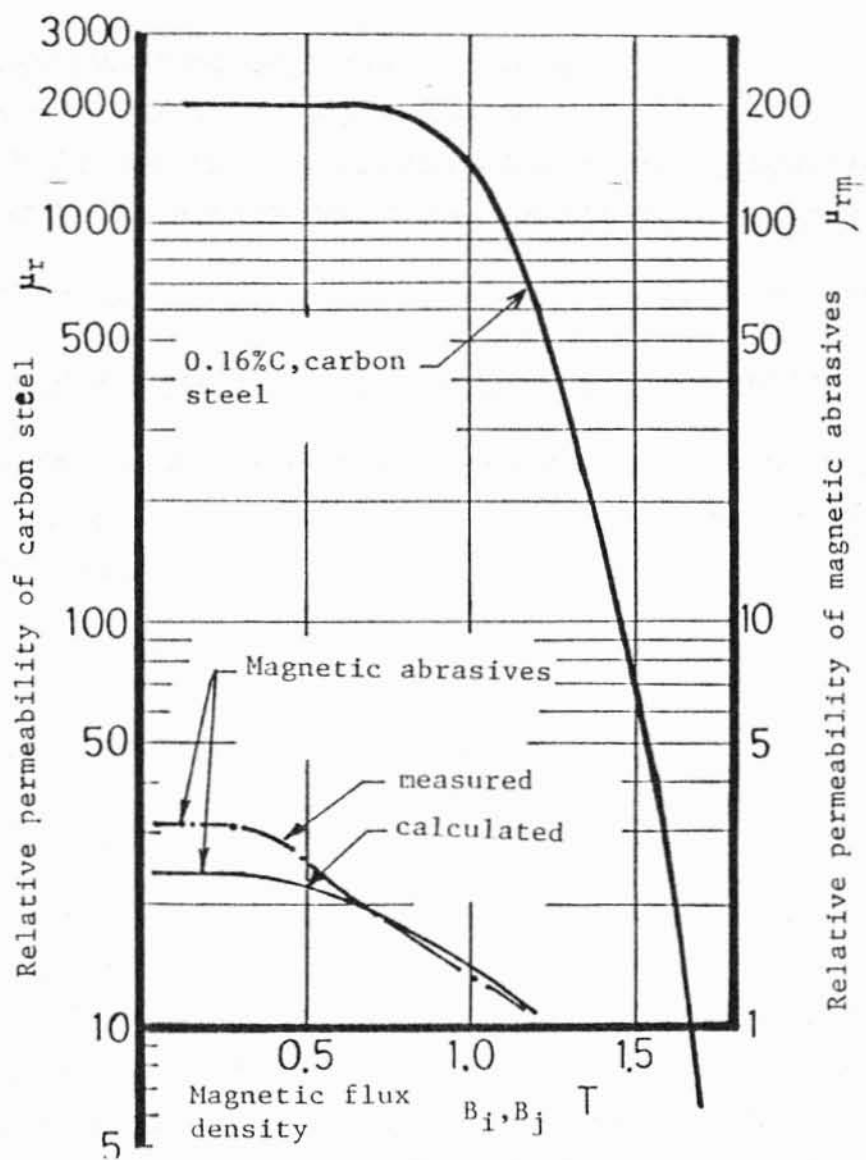


Figure 2.30: μ_r - B_i curve for carbon steel (0.16%C) and μ_{rm} - B_j curve of magnetic abrasives [Shinmura et al., 1987b]

Where, L_0 is the cutting length of one abrasive

H_v is the hardness of the workpiece

χ_r is the relative magnetic susceptibility of the magnetic abrasive particles

D is the average diameter of the magnetic abrasive particle.

But the effects of cutting fluid and vibration on M does not enter in this equation.

Estimation of surface roughness by magnetic abrasive finishing

If the finished surface was generated by the accumulation of cutting by each abrasive, surface roughness R_{max} can be estimated from the following equation [Shinmura et al., 1987b],

$$h \propto d D^{1-2} (H_v)^{-(0.5 \sim 1)} (\xi)^{(0.5 \sim 1)} \quad (2.5)$$

where d is the diameter of the abrasive grain (Figure 2.33).

Design of magnetic circuits:

Magnetic field produced by the permanent magnets is analyzed by the permanence method. The relationship between exciting current I and magnetic flux density B , both theoretically and experimentally, are shown in Figure 2.31 and 2.32 [Shinmura et al, 1987b]. From Figures 2.31 and 2.32, when I is relatively small, the theoretical values agree well with the experimental values. On the other hand, when I is relatively large, experimental values attain saturation, and theoretical values are larger than experimental. In order to predict magnetic flux density and magnetic pressure in the magnetic abrasive finishing apparatus, the simulation of the process using finite element analysis is necessary.

2.6. Factors influencing the magnetic abrasive finishing process:

In the magnetic abrasive finishing process, finishing capabilities depends on the various parameters and their mutual interaction. For efficient performance of magnetic abrasive finishing, these parameters have to be properly selected. In the following sections, the effect of above mentioned parameters on the magnetic abrasive finishing will be reviewed. This study is further utilized to investigate the process's finishing performance.

Where, L_0 is the cutting length of one abrasive

H_v is the hardness of the workpiece

χ_r is the relative magnetic susceptibility of the magnetic abrasive particles

D is the average diameter of the magnetic abrasive particle.

But the effects of cutting fluid and vibration on M does not enter in this equation.

Estimation of surface roughness by magnetic abrasive finishing

If the finished surface was generated by the accumulation of cutting by each abrasive, surface roughness R_{max} can be estimated from the following equation [Shinmura et al., 1987b],

$$h \propto d D^{1-2} (H_v)^{-(0.5 \sim 1)} (\xi)^{(0.5 \sim 1)} \quad (2.5)$$

where d is the diameter of the abrasive grain (Figure 2.33).

Design of magnetic circuits:

Magnetic field produced by the permanent magnets is analyzed by the permanence method. The relationship between exciting current I and magnetic flux density B , both theoretically and experimentally, are shown in Figure 2.31 and 2.32 [Shinmura et al, 1987b]. From Figures 2.31 and 2.32, when I is relatively small, the theoretical values agree well with the experimental values. On the other hand, when I is relatively large, experimental values attain saturation, and theoretical values are larger than experimental. In order to predict magnetic flux density and magnetic pressure in the magnetic abrasive finishing apparatus, the simulation of the process using finite element analysis is necessary.

2.6. Factors influencing the magnetic abrasive finishing process:

In the magnetic abrasive finishing process, finishing capabilities depends on the various parameters and their mutual interaction. For efficient performance of magnetic abrasive finishing, these parameters have to be properly selected. In the following sections, the effect of above mentioned parameters on the magnetic abrasive finishing will be reviewed. This study is further utilized to investigate the process's finishing performance.

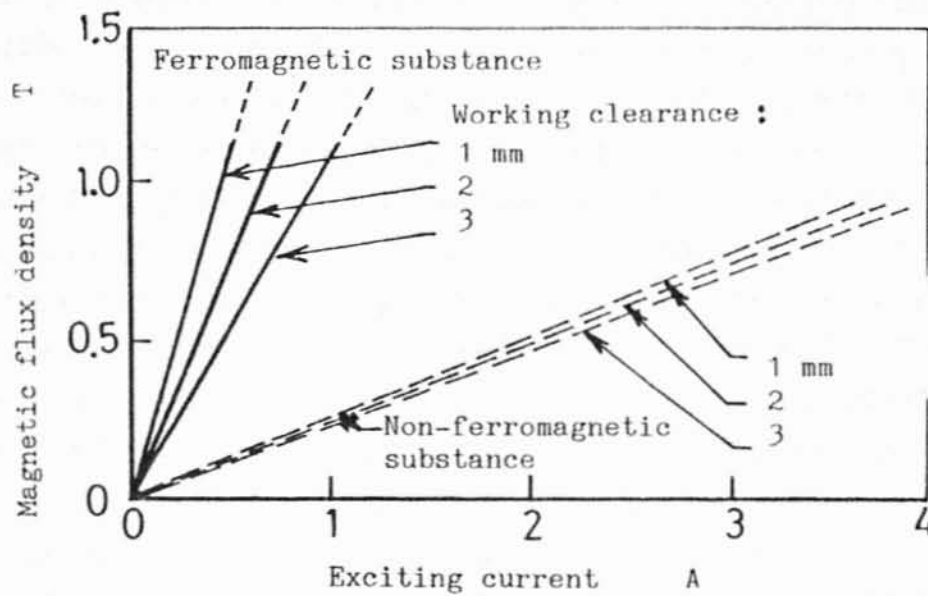
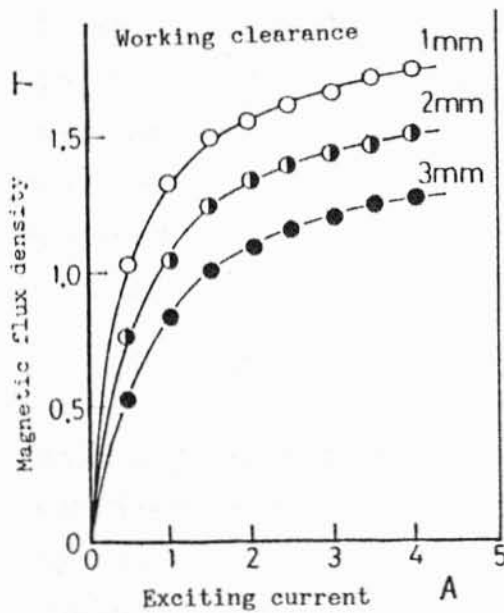
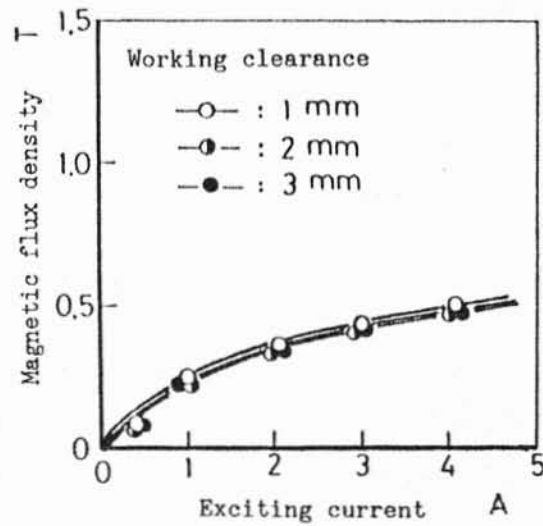


Figure 2.31: Calculated relationship between magnetic flux density and exciting current [Shinmura et al., 1987b]



(a) In the case of ferromagnetic substance (dia. = 30mm)



(b) In the case of non-ferromagnetic substance (dia. = 20mm)

Figure 2.32: Relationship between magnetic flux density and exciting current [Shinmura et al., 1987b]

2.6.1 Magnetic Abrasive Agglomerate:

The finishing capability, of the magnetic abrasive finishing process, depends considerably on the type of magnetic abrasives agglomerate, its shape [Krymsky, 1991a] and size [Shinmura et al., 1987a]. Knowing the influence of particle size, it is not only possible to select the suitable particle size, but also guide in the development of future magnetic abrasives. Use of coarse abrasive particles with sharp protuberances results in a high removal rate but also a large surface roughness [Krymsky, 1991a]. Conversely, finer abrasive diameter improve the finish on the surface at the expense of the material removal rates [Shinmura et al., 1987a]. Hence, optimum choice of abrasive (material and size) is required for removal rates and/or surface finish. As the main advantage of the magnetic abrasive finishing process is its ability to finish irregular surfaces, the magnetic abrasive brush should possess not only ready deformability but also elasticity which will insure that its shape is restored after its deformation by the part being machined [Krymsky, 1987b].

As shown in Figure 2.33, magnetic abrasives can be characterized by the particle diameter "D" and the diameter "d" of abrasive cutting grain.

Shinmura conducted experiments to study the influence of the difference of the diameters D (diameter of abrasive particle) and d (diameter of abrasive grain) on stock removal and surface roughness [Shinmura et al., 1987a]. He showed that the magnetic force acting on the magnetic abrasive particle is proportional to the particle volume (i.e. D^3) in the case of equation 1 and D^2 in the case of equation 2. These forces are expressed summarily as follows.

$$f = k_1 D^a \quad (a= 2 \text{ or } 3, k_1=\text{constant}) \quad (2.6)$$

Assuming that a number of abrasive grains, n, contained in one magnetic abrasive particle, act on the work surface at the same time, the force Δf exerted by one abrasive grain on the work surface is expressed by the following equation.

$$\Delta f = f/n = k_1 D^a/n \quad (2.7)$$

Assuming that the stock removal obtained by the magnetic abrasive particle is equal to the product of the stock removal "m" of the abrasive grain and number,

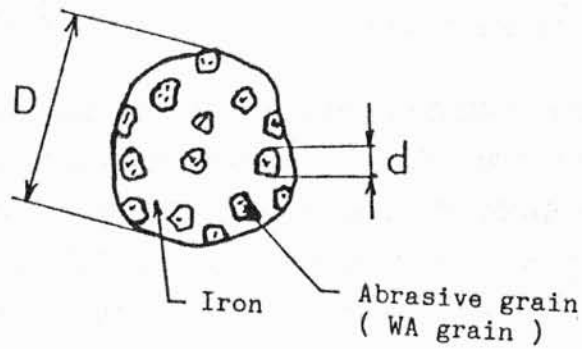


Figure 2.33: Schematic of a magnetic abrasive particle [Shinmura et al, 1987a]

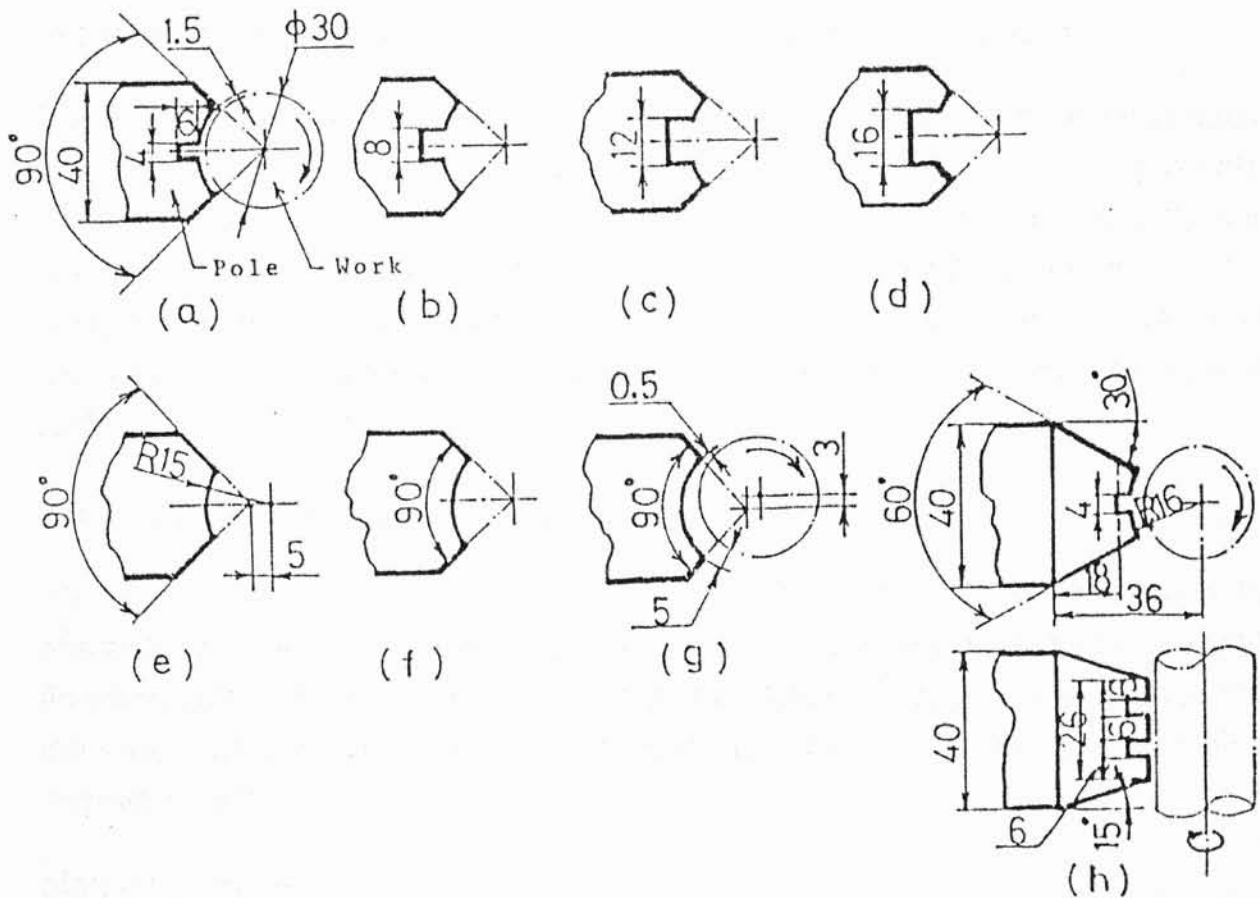


Figure 2.34: Various shapes of magnetic pole used in experiments (Width of magnetic pole: 40 mm) [Takazawa et. al., 1983]

n, of simultaneous acting abrasive grains, and that this m is proportional to the bth power of Δf , the stock removal per unit area "M" is written as follows:

$$M = k_2 D^{(ab-2)} n^{(1-b)} \quad (k_2=\text{constant}) \quad (2.8)$$

The value b is affected by the shape of the abrasive grain cutting edge. When the edge shape is a cone or sphere, the value is 1.0 or 1.5 respectively. From equation (2.8), for a conical edge shape, stock removal M is not affected by a change in d. However, for a spherical cutting edge, the stock removal M increases as D increases and as n decreases (i.e. as d increases).

In general, abrasive grain cutting edges are considered to be a combination of conical and spherical shapes. Accordingly, the bigger both the particle diameter (D) and the abrasive grain diameter (d) become, the higher the stock removal. The surface roughness also increases, as these diameters increase.

The magnetic abrasive particle is a compound substance of ferromagnetic material and minute abrasive grains, integrally mixed. The minimum possible volume of ferromagnetic material is limited by that required to obtain sufficient magnetic strength. For this reason, firstly D should be selected, then d. In order to obtain smooth surfaces, a small d should be chosen. Because stock removal decreases as d decreases, a suitable compromise between removal rate and surface roughness is required.

2.6.2. The shape of the magnetic pole:

Takazawa et al carried out experiments with different magnetic poles to characterize the magnetic pole shape, in terms of material removal rate and finishing efficiency (Fig. 2.34) [Takazawa et al, 1983]. They also investigated the influence of the variation of the magnetic pole area on the finishing characteristics.

Magnetic pole (a)-(d):

In these designs, notches with various dimensions were made on the magnetic pole in the axial direction of the work. It helps in preventing the flow of abrasive grains off the workpiece. It, however, results in an uneven magnetic field. They

observed that the removal rate is increased and surface roughness decreases, as the magnetic pole area increases (Figure 2.35a).

Magnetic poles (b) and (e):

Takazawa et al also investigated the effect of notches on the finishing characteristics. They found that the pole with notch (b) showed a high removal rate compared to one with no notch (Figure 2.35b).

Magnetic pole (f) and (g):

In the case of magnetic pole (g), the position of the magnetic pole is deviated from the work, in order to investigate the dynamic squeeze effect of the abrasive grains, by rotation of the work on the finishing characteristics compared with magnetic pole (f). The magnetic pole (g) showed larger removal and a smaller surface roughness, as compared to the pole (f) due to squeeze effect. However scratches were found in the case of (g).

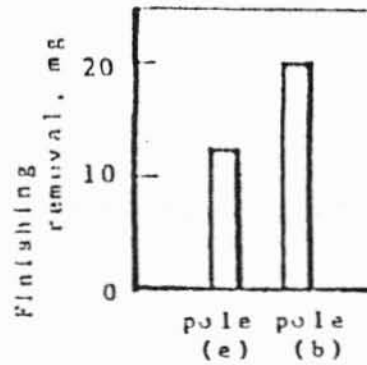
Magnetic pole (h):

This magnetic pole aims to form an uneven magnetic field and prevents a runoff of abrasive grains by setting many notches in the axial and rotary directions on the workpiece on the pole. In this case, the removal rate is large and the surface roughness is small, despite a small magnetic pole area.

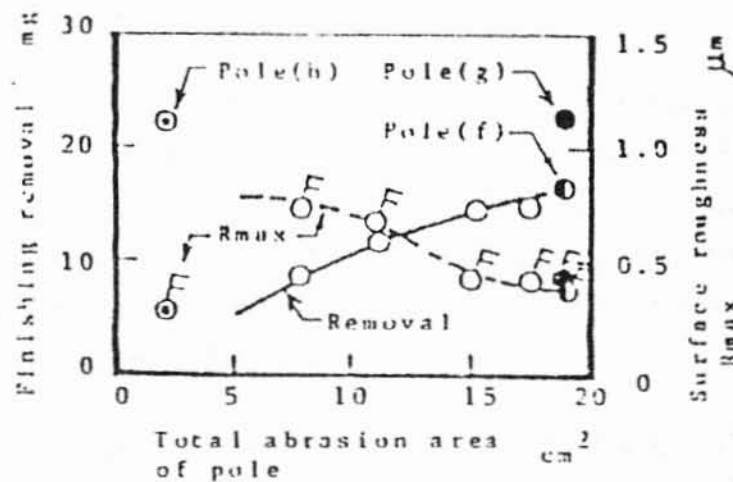
If the work is non-ferromagnetic, leakage of the magnetic flux is large, thus it is difficult to obtain the magnetic flux density effective for finishing. The design of the magnetic pole should therefore be considered so that magnetic flux leakage is held down to a minimum and abrasive grains do not escape.

Effect of clearance between the work and magnetic pole:

Krymsky analyzed the effect of clearance between the work and the magnetic poles on the wedging of the magnetic abrasives [Krymsky, 1986]. He found wedging of abrasives plays a considerable role in the material removal rate obtainable by this process. The studies were also conducted to evaluate the effect of amount of abrasive material, magnetic field density and the angle of attack of the abrasives on the normal force exerted by the abrasives on the rod and sheet material [Krymsky, 1991b].



(a): Effect of magnetic pole area on finishing removal and surface roughness of ferromagnetic substance



(b): Effect of notch in the magnetic pole on finishing removal of ferromagnetic substance

Figure 2.35: Effects of shape of magnetic pole on finishing characteristics
[Takazawa et. al., 1983]

2.6.3. Vibration of the workpiece:

With only rotation of the workpiece and absence of axial vibration, formation of circumferential grooves would be a problem. Axial vibration results in multi-directional finishing, thus improving the surface finish (Figure 2.36) [Shinmura et al, 1984a].

2.6.4. Magnetic field density:

Relative motion between the magnetic field and workpiece can be achieved in the following two ways:

a) **Static Magnetic field:**

A cylindrical workpiece, such as a ceramic bearing roller, is clamped to the chuck of the spindle providing a rotary motion. A working clearance of roughly 5 times the abrasive particle size is provided between the work surface and the magnetic pole. Axial vibratory motion is introduced in the magnetic field by the oscillating motion of the magnetic poles. The surface and edge finishing are carried out by the flexible magnetic abrasive brushes.

b) **Rotating magnetic field:**

Shinmura et al devised a finishing apparatus utilizing a rotating magnetic field [Shinmura et. al., 1986a]. They obtained a rotating magnetic field by using three current carrying coils arranged at intervals of 120° with the three phase AC current as shown in Figure 2.13. As a result of the dynamic behavior of abrasives, the rotating magnetic field component increased the stock removal compared to a static magnetic field.

Shinmura et al found the material removal rate to increase with the magnetic flux density upto a certain point, beyond which it attains saturation showing a reducing tendency thereafter (Figure 2.37) [Shinmura et al., 1984]. They explained this effect thus:

Magnetic pressure P is related to the magnetic flux density in the following way [Takazawa et al., 1983]:

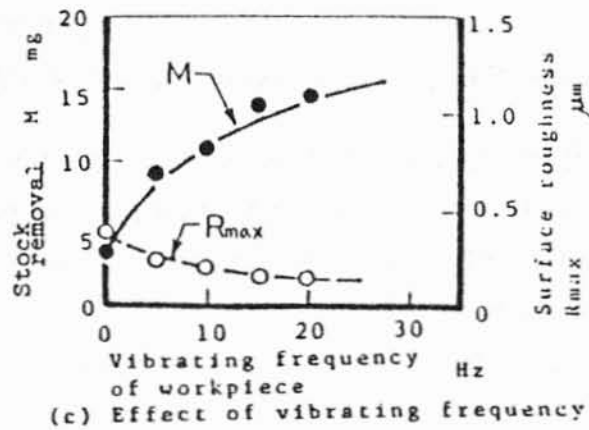


Figure 2.36: Effect of vibration frequency of the workpiece on finishing characteristics (Shinmura et. al. 1985)

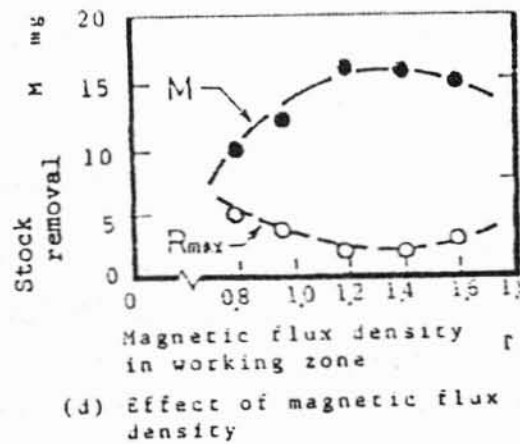


Figure 2.37: Effect of magnetic field density on finishing characteristics (Shinmura et. al. 1985)

$$P = \frac{B^2}{2\mu_0} \left(1 - \frac{1}{\mu_r}\right) \quad (2.9)$$

Where μ_0 is the permeability in air

and μ_r is the relative permeability of the magnetic abrasive grains.

μ_r decreases as B increases and with further decrease in B, μ_r becomes 1. In accordance with the above equation, the effect of B on P (Figure 2.38) can be explained. In the range of small B, $\mu_r \gg 1$ and P varies proportionally to B^2 . However as μ_r approaches unity at large values of B, magnetic pressure attains a steady value. Thus, material removal increases initially with increase in B. However, once a critical value of B is reached, the material removal attains saturation.

2.6.5 Surface finishing time:

Shinmura found the removal volume and removal rate to increase with finishing time, again reaching saturation after certain time. Also, the surface finish improves with time till it reaches saturation after a certain duration of polishing [Figure 2.39] [Shinmura et al., 1984].

2.6.6 Surface speed of the workpiece:

Shinmura found the removal rate to increase gradually with increase in rotational speed of the workpiece, due to an increase in the finishing distance per unit time [Figure 2.40] [Shinmura et al., 1984].

2.6.7 Machining fluid and lubricant

Lubricant has been found to enhance the surface finishing efficiency of the process [Shinmura et al., 1986c]. The lubricant makes the abrasive brush more flexible and enhances its capability for cutting peaks on the surface. They observed that the finishing characteristics are influenced considerably by the addition of machining fluid to magnetic-abrasives.

They carried out experiments with different machining fluids, such as emulsion type grinding fluid, straight oil type grinding fluid, light oil and stearic acid in different concentration (from 0 to 10%) [Shinmura et al., 1986c]. The effect of

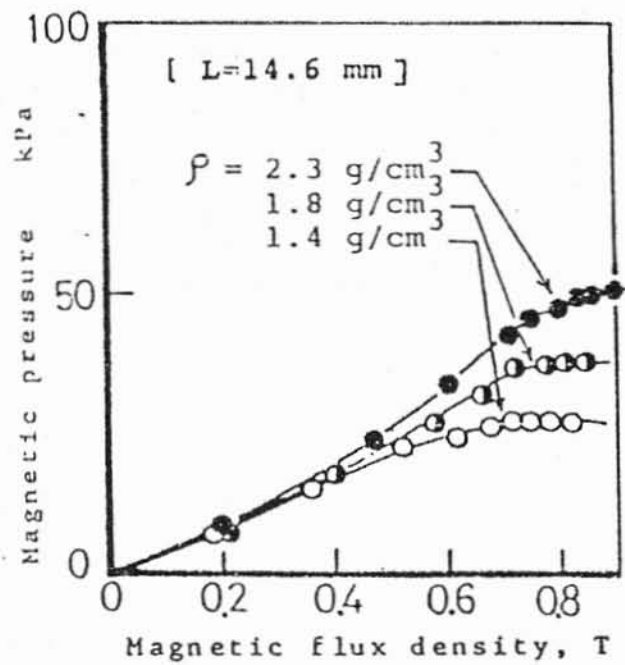


Figure 2.38: Relationship between magnetic pressure and flux density for different filling densities of abrasives [Shinmura et al, 1984]

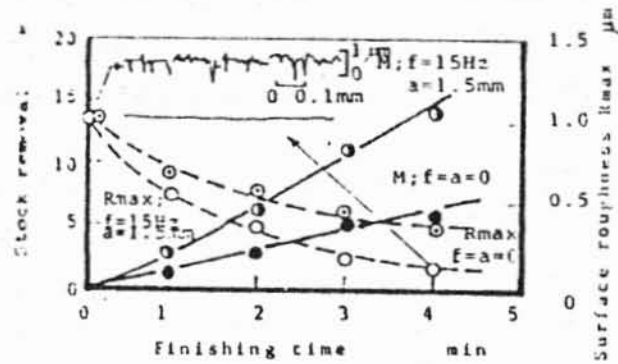


Figure 2.39: Variation of the surface finish, and material removal rate with finishing time [Shinmura et al., 1984].

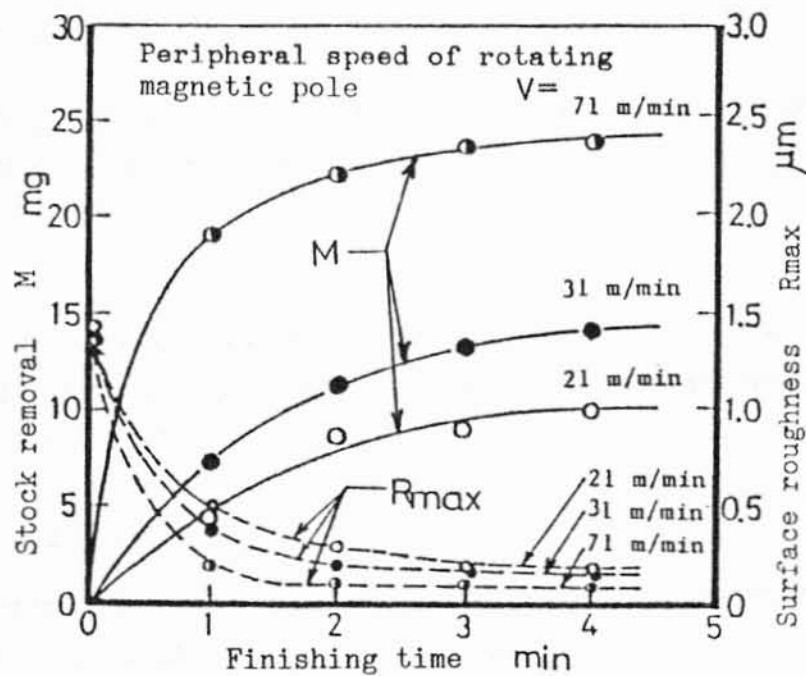


Figure 2.40: Variation of the surface finish, and material removal rate with finishing time at different rotational speed [Shinmura et al., 1984]

various machining fluids on the stock removal and the surface roughness are shown in Figure 2.41. It can be seen from this figure that the stock removal increases almost linearly against finishing time. When the amount of machining fluid exceeds 5 wt%, the magnetic-abrasive brush, which has been in stationary state in the absence of fluid, is stirred up and vibrated by the rotational and oscillational motions of the workpiece. Since, with the addition of the machining fluid, abrasives cut deeper into the surface, the surface roughness of the workpiece could not be improved beyond $0.5 \mu\text{m } R_{\text{max}}$.

The temperature in the polishing region is low within a short finishing time. Stearic acid (melting point: 71.5°C) does not become a liquid. Consequently, the stock removal rate is low. However, with increase in finishing time, stearic acid becomes a liquid due to a large increase in temperature. Consequently, the agitating action of magnetic-abrasives starts suddenly and simultaneously, the stock removal increases rapidly (Figure 2.42). However, excessive lubricant causes difficulty in recycling the magnetic abrasives.

2.6.8 Materials of workpiece [Shinmura, 1987b]:

Magnetic and nonmagnetic materials

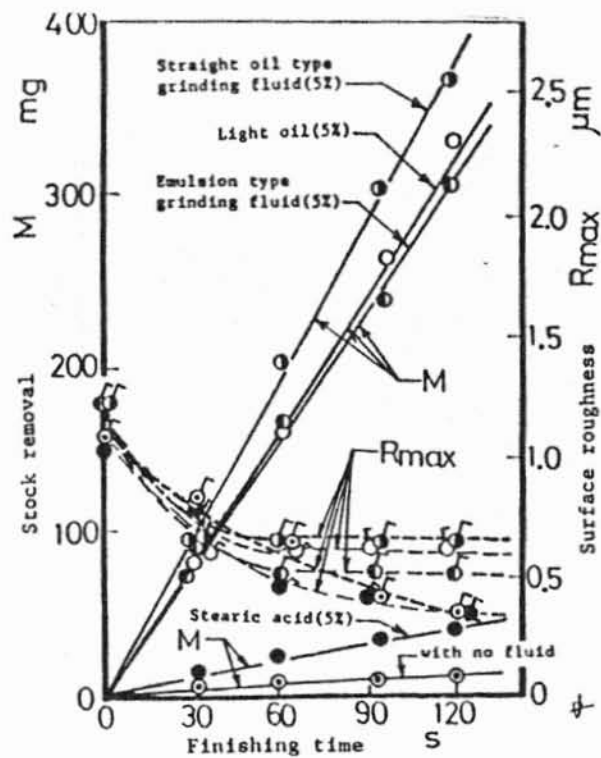
For nonmagnetic materials, a long polishing time (30 minutes) is needed because of the smaller magnetic polishing pressure.

Hardness

Shinmura found the removal volume to be proportional to $H_v^{0.6}$, in the case of stainless steel, as shown in Figure 2.43, where H_v is the hardness of the work material [Shinmura, 1987b].

Finishing of Si_3N_4 bar

Diamond abrasive with iron particles can finish a Si_3N_4 bar from $0.45 \mu\text{m } R_a$ to $0.05 \mu\text{m } R_a$ in 30 minutes [Shinmura, 1987b].



[Experimental conditions]

Work; SS41 $\phi 31 \times 45$ mm, circumferential speed of work; 30 m/min, Magnetic flux density; 1.3 T, Working interval; 1 mm, Magnetic pole shape; see Fig. 2(h) in 5th report, Magnetic abrasives; ($5 \mu\text{m Al}_2\text{O}_3$ in diameter) + Fe; 8 g supplied, Work vibration; $f = 15 \text{ Hz}$, $a = 1.5$ mm.

Figure 2.41: Variation of stock removal, and surface roughness with finishing time using different lubrication type [Shinmura et al 1986]

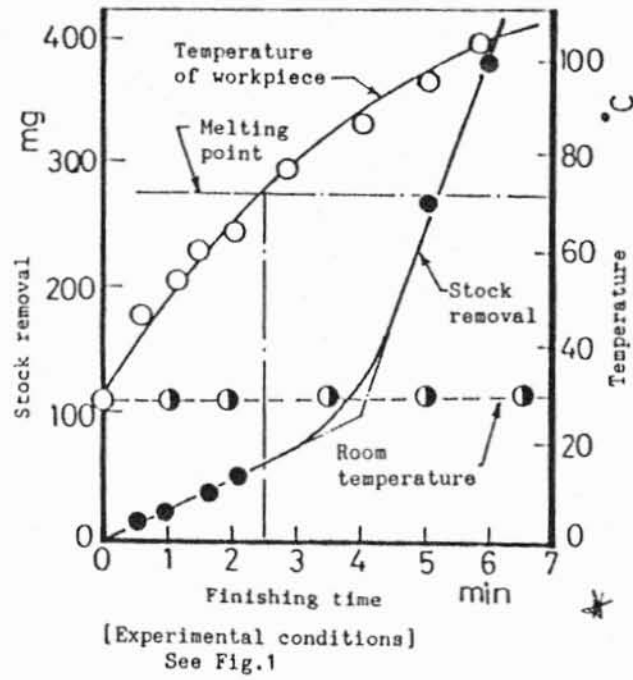
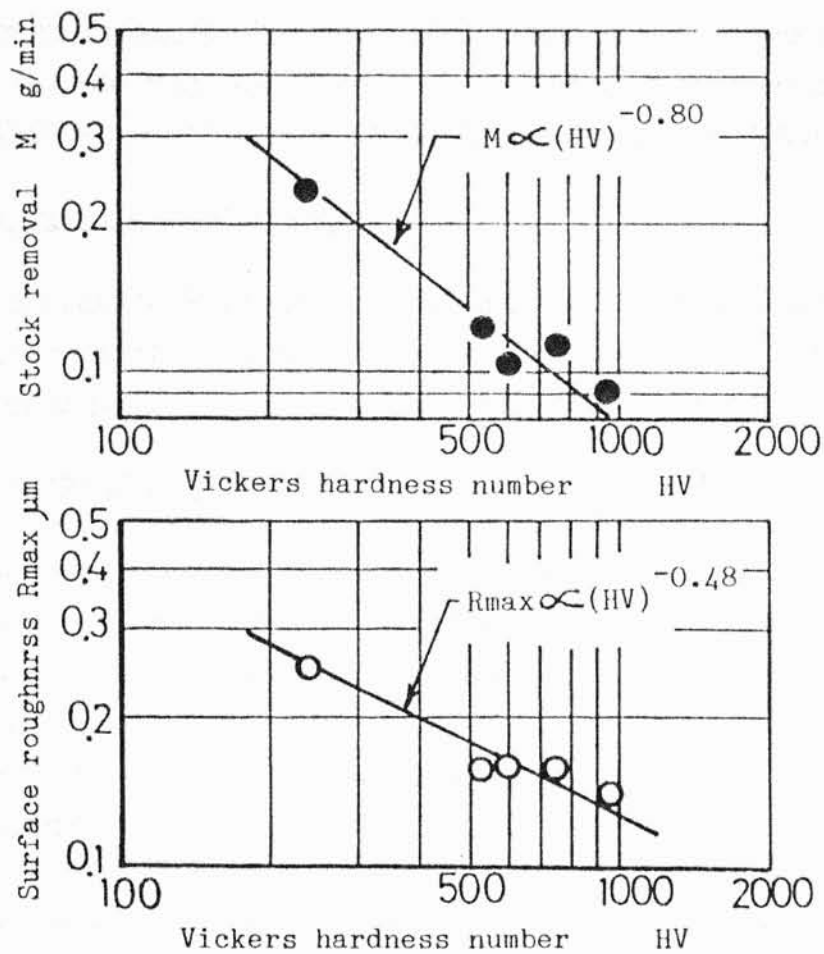


Figure 2.42: Variation of stock removal, and temperature of the workpiece with finishing time using stearic acid (5wt%) as a lubricant [Shinmura et al 1986]



Effects of vickers hardness number on
stock removal and surface roughness
[Experimental conditions]

Workpiece:SK3,31mm in dia.,45mm in length ;
circumferential speed of workpiece:62m/min ;
working clearance:1mm ; magnetic flux density:
1.2T ; finishing time:2min ; machining fluid:
straight oil type grinding fluid,10wt.% supplied ;
magnetic abrasives:see Fig.2.3 ; without vibration

Figure 2.43: Effects of vickers hardness number on stock removal and surface roughness [Shinmura, 1987b]

Residual Stress

Shinmura measured the residual stresses on a polished surface of steel, with an X ray spectroscopy [Shinmura, 1987b]. Compressive stresses of 230 MPa and 160 MPa were observed for steel and brass, respectively.

Thickness of damaged layer

With a micro Vickers hardness tester, the hardness of a polished surface was measured under different testing loads (25g - 1000g). Changing of hardness by change of test load shows that the surface condition was changed by polishing.

2.7 APPLICATIONS:

Depending on design of the device and finishing conditions, the MAF method allows finishing of shafts, axles, rods, bushes, rings with diameters from 1 to 2000 mm and lengths from 5 to 2000 mm. The process is applicable to finishing of parts that have fillets, annular grooves, threads, shoulders, and spherical and conic surfaces (Figures 2.1, 2.4, and 2.9); pipe edges, with inside and outside surfaces to 200 mm from the edge; plane surfaces with grooves and shoulders to a depth of 1 mm; ferromagnetic and nonferromagnetic narrow bands (to 40 mm) and wires with thickness to 5-6 mm; edges of sheets; inside surfaces of thin (to 1-2 mm) nonferrous tubes. The magnetic abrasive finishing process has been investigated for different applications, such as roller finishing [Shinmura et al., 1985a], edge finishing such as deburring and precision rounding off [Shinmura et al., 1985b, 1986a], plane finishing [Shinmura et al., 1985c, 1989a, 1989b], interior finishing of tube [Shinmura et al., 1985a, 1989c], and spherical finishing of ball valves and hinges [Shinmura et al., 1985a].

Typical industrial applications of this process are [Shinmura et. al. 1985a]:

- Finishing of the surface and the end face of the pumping gear
- Edge finishing of gears of hydraulic gear pumps
- Finishing of metal molds
- Finishing of flatwears

- Finishing of bearing race surfaces
- For removing grinding burr of precision a cutting tool such as reamer, broach, hob or tap.
- Surface finishing of the dies for rubber products
- Edge finishing of camshafts
- Finishing of cutting tools, including taps, feed screws, and worms
- Finishing of small parts with complicated shapes, printed circuit boards

CHAPTER 3

ANALYTICAL MODELLING

3.0 Introduction

Although the magnetic abrasive finishing process has been investigated by many researchers [Baron 1987, Shinmura et al 1984-94], study on the effect of various parameters on the material removal rate and surface finish is far from complete. This is especially so with nonmagnetic work materials, including nonmagnetic ceramics. The understanding of the magnetic field density distribution in the magnetic abrasive region and the magnetic forces developed on the surface of the rollers, which affect the surface finish and the material removal rate obtainable by the process, have not been studied in detail. Continuous efforts in this direction will give new insights into the many facets of the process, thereby improving the performance and versatility of the process.

As described in Chapter 2, Takazawa et al [Takazawa et al, 1983] attempted to optimize different magnetic head designs in terms of finishing efficiency and material removal rate. This was done by building different magnetic heads and evaluating their relative performance. However this is a trial and error process which is time consuming and expensive. Finite element analysis is preferable because it overcomes the need to actually build various designs. The performance of different designs can be simulated and the more promising ones can be built and tested. This investigation is aimed at optimizing the magnetic head design to achieve the desired magnetic pressure exerted by the magnetic abrasives on the surface of the roller for high removal rate and /or best finish.

In this chapter the principles used from the theory of magnetism to address this problem are first presented. Next, the finite element analysis of the magnetic abrasive finishing system using ANSYS (5.0 version) program is described. Also, the procedures used for the characterization of the magnetic head, using

both experimental and FEM approaches are described. Finally, the finite element analysis is used to estimate the magnetic field distribution and the magnetic force exerted on the workpiece by the magnetic abrasives for different magnetic head geometries.

3.1 THEORY:

Electromagnetic fields are governed by the following Maxwell's equations:

$$\nabla \times \{H\} = \{J\} \quad (3.1)$$

$$\nabla \cdot \{B\} = 0 \quad (3.2)$$

where $\nabla \times$ is the curl operator

$\nabla \cdot$ is the divergence operator

$\{H\}$ is the magnetic field intensity vector

$\{B\}$ is the magnetic flux density vector

$\{J\}$ is the current density vector,

Also, $\{J\} = \{J_s\} + \{J_e\}$

where $\{J_s\}$ is the fixed source current density vector

$\{J_e\}$ is the induced eddy current density vector

The above field equations are supplemented by the following constitutive relationship that describes the behavior of electromagnetic materials. For problems concerning saturable material without permanent magnets, the constitutive relation for the magnetic fields is given by

$$\{B\} = [\mu] \{H\} \quad (3.3)$$

where $[\mu]$ is the magnetic permeability matrix which in general is a function of $\{H\}$

$$[\mu] = \begin{bmatrix} \mu_{xx} & 0 & 0 \\ 0 & \mu_{yy} & 0 \\ 0 & 0 & \mu_{zz} \end{bmatrix}$$

The magnetic permeability can also be written as

$$[\mu] = \mu_0 [\mu_r]$$

where μ_0 is the permeability of free space, and

$[\mu_r]$ is the relative permeability matrix

Rewriting the general constitutive equation in terms of magnetic reluctivity, it becomes

$$\{H\} = [v] \{B\} \quad (3.4)$$

where $[v]$ is the reluctivity matrix $= [\mu]^{-1}$

The magnetic flux density B is the first derived result. It is defined as the curl of the magnetic vector potential. This evaluation is performed at the integration points using the element shape functions.

Magnetic Forces:

Magnetic forces are computed by elements using the vector potential method (PLANE13). Maxwell stress tensor is used to determine forces on ferromagnetic regions. For the 2-D application, this method uses extrapolated field values and results in the following numerically integrated surface integral:

$$\{F^{mx}\} = \frac{1}{\mu_0} \int_s [A_n]^T \begin{bmatrix} T_{11} & T_{12} \\ T_{21} & T_{11} \end{bmatrix} \begin{Bmatrix} n_1 \\ n_2 \end{Bmatrix} ds \quad (3.5)$$

where: $T_{11} = B_x^2 - 1/2 |B|^2$

$$T_{12} = B_x B_y$$

$$T_{21} = B_y B_x$$

$$T_{22} = B_y^2 - 1/2 |B|^2$$

n_1 is the component of unit vector normal in the x-direction

n_2 is the component of unit vector normal in the y-direction

ds is the surface area of the element face

The magnetic permeability can also be written as

$$[\mu] = \mu_0 [\mu_r]$$

where μ_0 is the permeability of free space, and

$[\mu_r]$ is the relative permeability matrix

Rewriting the general constitutive equation in terms of magnetic reluctivity, it becomes

$$\{H\} = [v] \{B\} \quad (3.4)$$

where $[v]$ is the reluctivity matrix $= [\mu]^{-1}$

The magnetic flux density B is the first derived result. It is defined as the curl of the magnetic vector potential. This evaluation is performed at the integration points using the element shape functions.

Magnetic Forces:

Magnetic forces are computed by elements using the vector potential method (PLANE13). Maxwell stress tensor is used to determine forces on ferromagnetic regions. For the 2-D application, this method uses extrapolated field values and results in the following numerically integrated surface integral:

$$\{F^{mx}\} = \frac{1}{\mu_0} \int_s [A_n]^T \begin{bmatrix} T_{11} & T_{12} \\ T_{21} & T_{22} \end{bmatrix} \begin{Bmatrix} n_1 \\ n_2 \end{Bmatrix} ds \quad (3.5)$$

where: $T_{11} = B_x^2 - 1/2 |B|^2$

$$T_{12} = B_x B_y$$

$$T_{21} = B_y B_x$$

$$T_{22} = B_y^2 - 1/2 |B|^2$$

n_1 is the component of unit vector normal in the x-direction

n_2 is the component of unit vector normal in the y-direction

ds is the surface area of the element face

$$|B|^2 = B_x^2 + B_y^2$$

3.2 A Simple Model for the Magnetic Abrasive Finishing System

The magnetic abrasive finishing system described in Chapter 1 (Figure 1.2) can be modelled using a simple magnetic circuit as shown in Figure 3.1.

In Figure 3.1 NI is the magnetomotive force (MMF) that generates the magnetic flux Ψ_c in the magnetic core.

l_c , μ_c , and s_c are the length, magnetic permeability and cross sectional area of the ferromagnetic core, respectively

l_a , μ_a , and s_a are the length, magnetic permeability and crosssectional area of the ferromagnetic abrasives, respectively

l_g , μ_0 , and s_g are the length, magnetic permeability and crosssectional area of the air gap respectively

Reluctance of the ferromagnetic core, $R_c = l_c / \mu_c s_c$

Reluctance of the ferromagnetic abrasives, $R_a = l_a / \mu_a s_a$

Reluctance of the air gap, $R_g = l_g / \mu_0 s_g$

The following assumptions are made in the analysis:

- Flux leakage is neglected, which means that the total flux is confined within the ferromagnetic core.
- Fringe effects are neglected, which means the air gap is sufficiently narrow so that the total flux in the ferromagnetic core will continue to flow across the air gap and the magnetic abrasives, without resulting in any magnetic field loss from fringe effects. Hence,

$$\Psi_c = \Psi_a + \Psi_g$$

The above magnetic circuit is solved using the electric circuit analogy. The following equations can be derived from the circuit:

$$NI = R_c \Psi + R_a \Psi_1 \quad (3.6a)$$

$$NI = R_c \Psi + R_g(\Psi - \Psi_1) \quad (3.6b)$$

Solving the above two equations for Ψ , the total flux is given by,

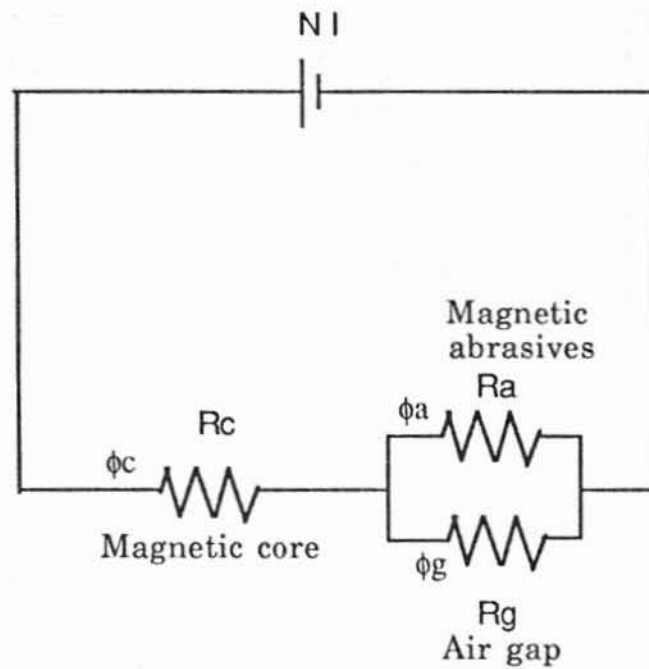


Figure 3.1 Simple model of the magnetic abrasive finishing system using a magnetic circuit

$$\Psi = \frac{R_a + R_g}{R_a R_g + R_g R_c + R_c R_a} N I \quad (3.7)$$

The magnetic field density in the abrasive region is given by the relation

$$B_a = \frac{\Psi_a}{S_a} = \frac{R_g / S_a}{R_a R_g + R_g R_c + R_c R_a} N I \quad (3.8)$$

Properties	Abrasive	Air	Magnetic core
Length (la)	0.017 m	0.0065 m	0.984 m
Magnetic permeability	1.8×10^{-6}	1.256×10^{-6}	0.3936×10^{-3}
Crosssectional Area (w * l)	$1.6 \times 10^{-4} \text{ m}^2$	6.8×10^{-4}	$2 \times 10^{-3} \text{ m}^2$

Table 1: The properties of the materials considered in a simple model of the MAF apparatus.

Substituting the above values in equation 3.8 we get,

$$B_a = 0.27 \text{ T.}$$

The calculated value of the magnetic flux density (0.27 T) is less than the measured value in the magnetic abrasives region (0.4 T). This is due to the fact that the magnetic poles are of converging shape which concentrates the magnetic field in the abrasive region and minimal leakage of the field takes place, surrounding the air gap present between the magnetic heads. However, the above analysis of the magnetic abrasive finishing apparatus using complex magnetic head shapes is rather complicated. Finite element analysis is best suited for this purpose as any complicated shape of the magnetic head can be effectively modelled and the exact nature of the magnetic field density distribution in the abrasive region can be determined. In the following sections details of the finite element analysis of the magnetic abrasive finishing process are given.

3.3 FINITE ELEMENT ANALYSIS:

Finite element analysis (using the 2-D static magnetic analysis in ANSYS 5.0 version) is used for modelling the magnetic abrasive finishing of nonmagnetic rollers. Figure 3.2 shows the geometry of the two dimensional model used in the finite element analysis. The following assumptions are made in this analysis,

- The purpose of the current carrying coils is to generate the magnetic field in the magnetic head region. It in no way influences the distribution of magnetic field, when it is rotated through 90° for the purpose of modelling.
- The thickness of the parts such as magnetic core in the experimental set up is not considered for the purpose of two-dimensional analysis.
- Any eddy current loss, if present, in the current carrying coil is neglected.

3.3.1 ANSYS ANALYSIS

The procedure for a typical ANSYS (5.0 version) analysis is classified into three distinct steps:

- 1 To build the model
- 2 To apply loads and obtain the solution
- 3 To review the results

3.3.1.a To build the model:

Specifying Element types

Magnetic abrasive finishing of a nonmagnetic roller is modelled using the following two basic elements:

1. Infin 9: Used for the boundary element type
2. Plane 13: Magnetic (permeable regions), current conducting regions, permanent magnet regions, and air (free) space.

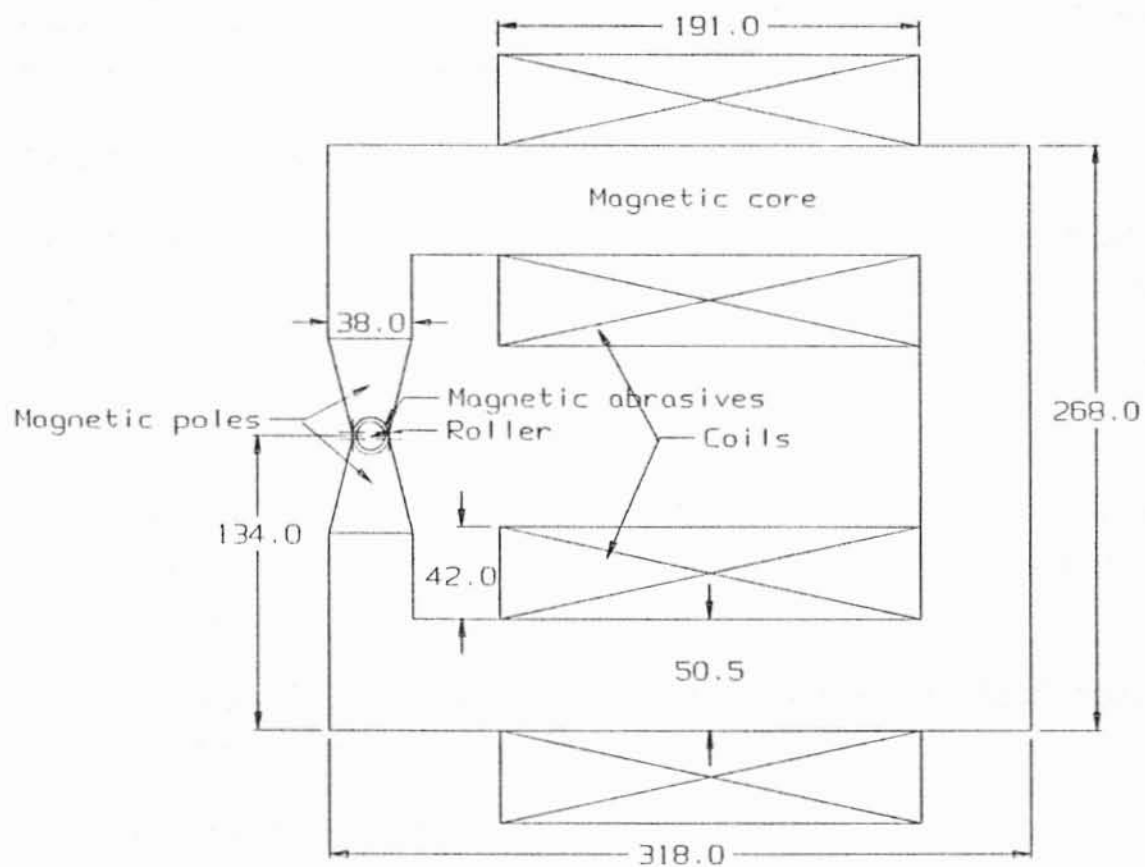


Figure 3.2: Two dimensional geometry of MAF apparatus used in the finite element analysis (dimensions are in mm)

Specifying Material Properties of various elements of MAF

The model consists of any or all of the following regions: air, non-magnetic regions (nonmagnetic stainless steel/ceramic roller), magnetic saturable materials (iron core, magnetic abrasives), current conducting regions (coil), and permanent magnets. The linear material properties of air and current-conducting regions such as relative magnetic permeability (equal to 1) is specified. Any non-magnetic material present in the cell has been assigned relative permeability of 1. For saturable materials, the nonlinear properties such as B-H curve is specified using TB commands. Figures 3.3 and 3.4 show typical B-H plots of iron core (0.16% carbon steel) and magnetic abrasive material (KMX80). They show that the iron core and the magnetic abrasives do not attain saturation at the operating condition of magnetic flux density (0.4 T). This leaves the scope for the further increase in the magnetic field.

Creating the Model Geometry

The 3-D magnetic roller finishing apparatus is converted to 2-D by rotating the coils in the plane perpendicular to the axis of the polishing rod. As pointed out earlier, this does not affect the analysis.

A common modeling session follows this general outline:

- Begin planning the approach: After determining appropriate element types, establishing an appropriate geometry, ANSYS session is initiated
- Execute PREP7 to initiate the model building session. Solid modeling procedure is used for the present analysis
- Establish a working plane
- Generate basic geometric features such as areas, lines, and keypoints using geometric primitives and Boolean operators

The main objective of the model generation is to generate a finite element model, consisting of nodes and elements that adequately describes the model geometry. The finite element model is created using solid modeling approach.

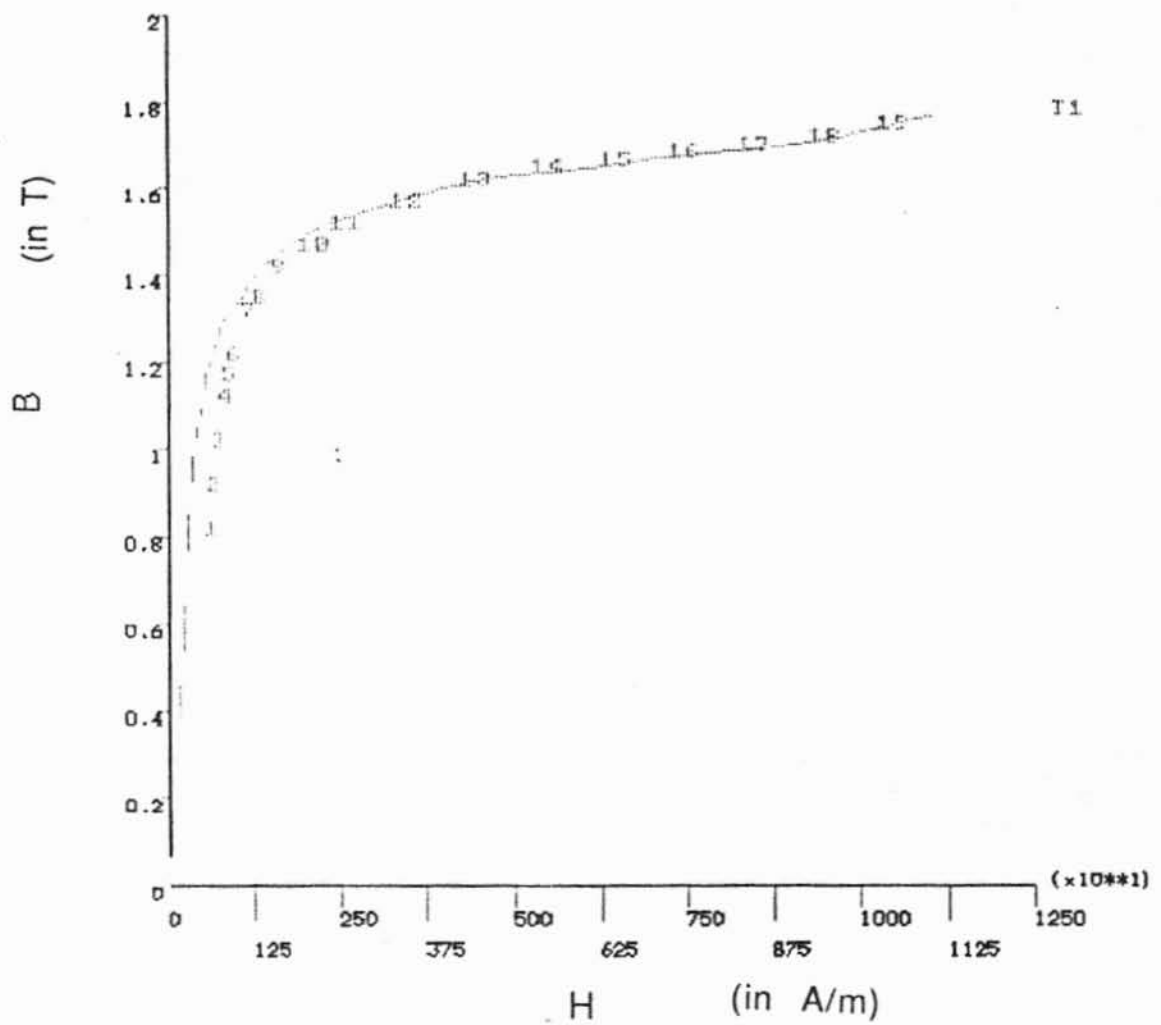


Figure 3.3: B-H plot of iron core (0.16%C steel)

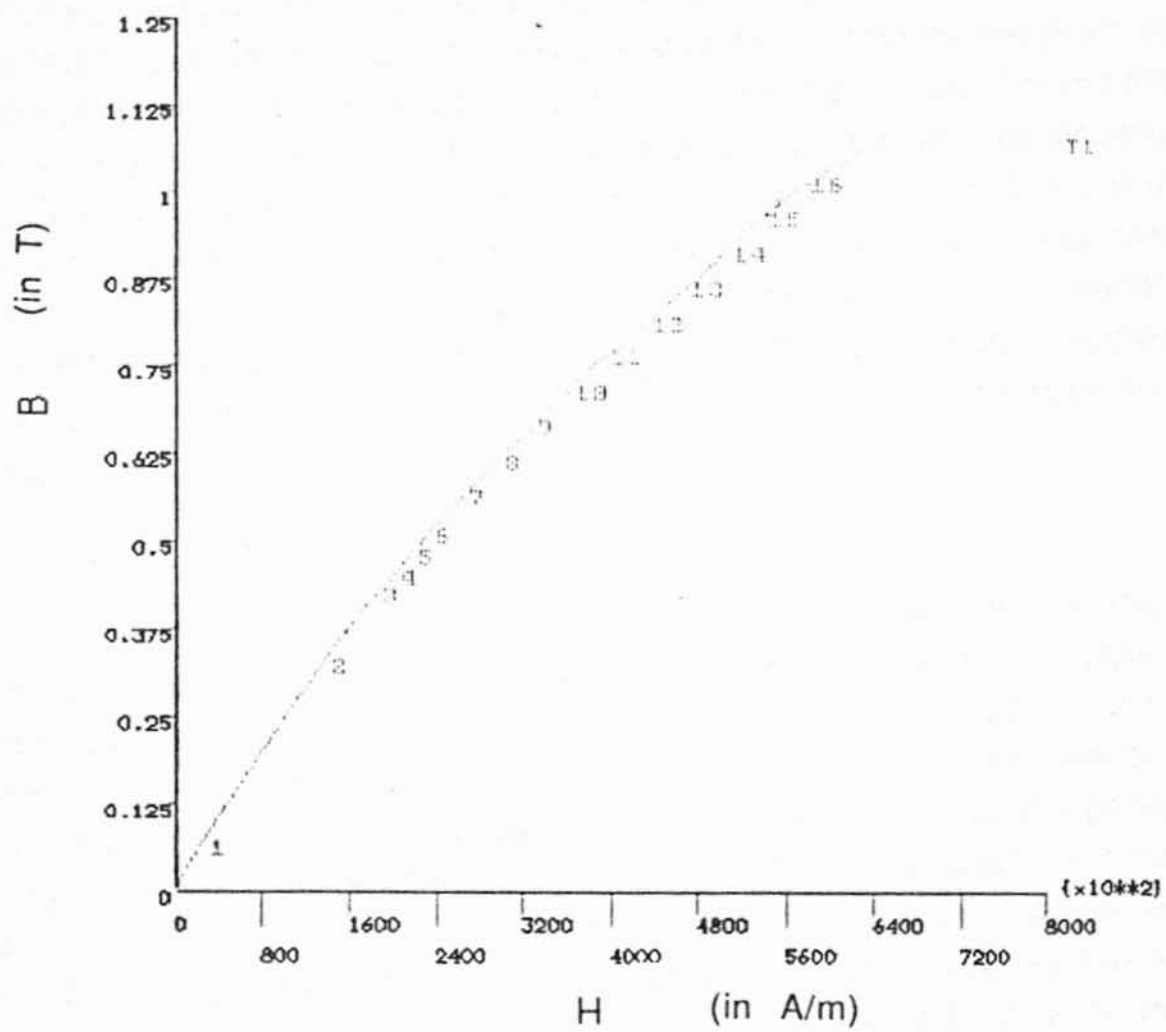


Figure 3.4: B-H plot magnetic abrasives (KMX80)

The geometric boundaries of the model are first defined. The ANSYS program is then instructed to automatically mesh the geometry with nodes and elements. By this procedure, the size and shape of the elements can be controlled. This helps in obtaining a more detailed FEM of the various elements of the model, such as the magnetic abrasive region and the magnetic heads. In the present modelling, the sizes of the elements in the abrasive and magnetic regions were specified to be 2 mm, as opposed to the element size in rest of the model which is 20 mm. Figure 3.5 is a finite element model for the complete cell. It shows the coarse element distribution in the magnetic core region and in the copper coils. The fine element distribution at the nonmagnetic workpiece is depicted in Figure 3.6. From this, it is clear that the complicated shapes of the magnetic head can be effectively modelled using a finer element distribution. Materials with different magnetic properties are numbered from 1 to 3 in these figures. Material 1, 2 and 3 indicate nonmagnetic region, magnetic iron core, and magnetic abrasives respectively.

3.3.1.b To apply loads and obtain the solution:

In this step, the analysis type and analysis options are defined. Here, static (or steady state) analysis is used. Newton-Raphson descent 'on' option is used as an analysis option to customize the analysis type. Once the analysis type and options are defined, loads are applied as a source current density of the electromagnet used for the generation of the magnetic field. The present analysis is done for the source current density of 150 kA/m^2 through the current carrying coils. Figure 3.7 shows the variation of magnetic field density with current density through the current carrying coils. Load step options are specified which involve breaking the load into a series of 5 load increments. Convergence tolerances (0.01%) for equilibrium iterations are specified. The automatic time stepping option is used, in addition, to vary the time step size during the nonlinear portions of the system's response. Finally, SOLVE command is executed to initiate the ANSYS solution.

3.3.1.c To review the results:

Once the solution is obtained, ANSYS postprocessor (POST1) is used to review the results. This step can be used to view the following results:

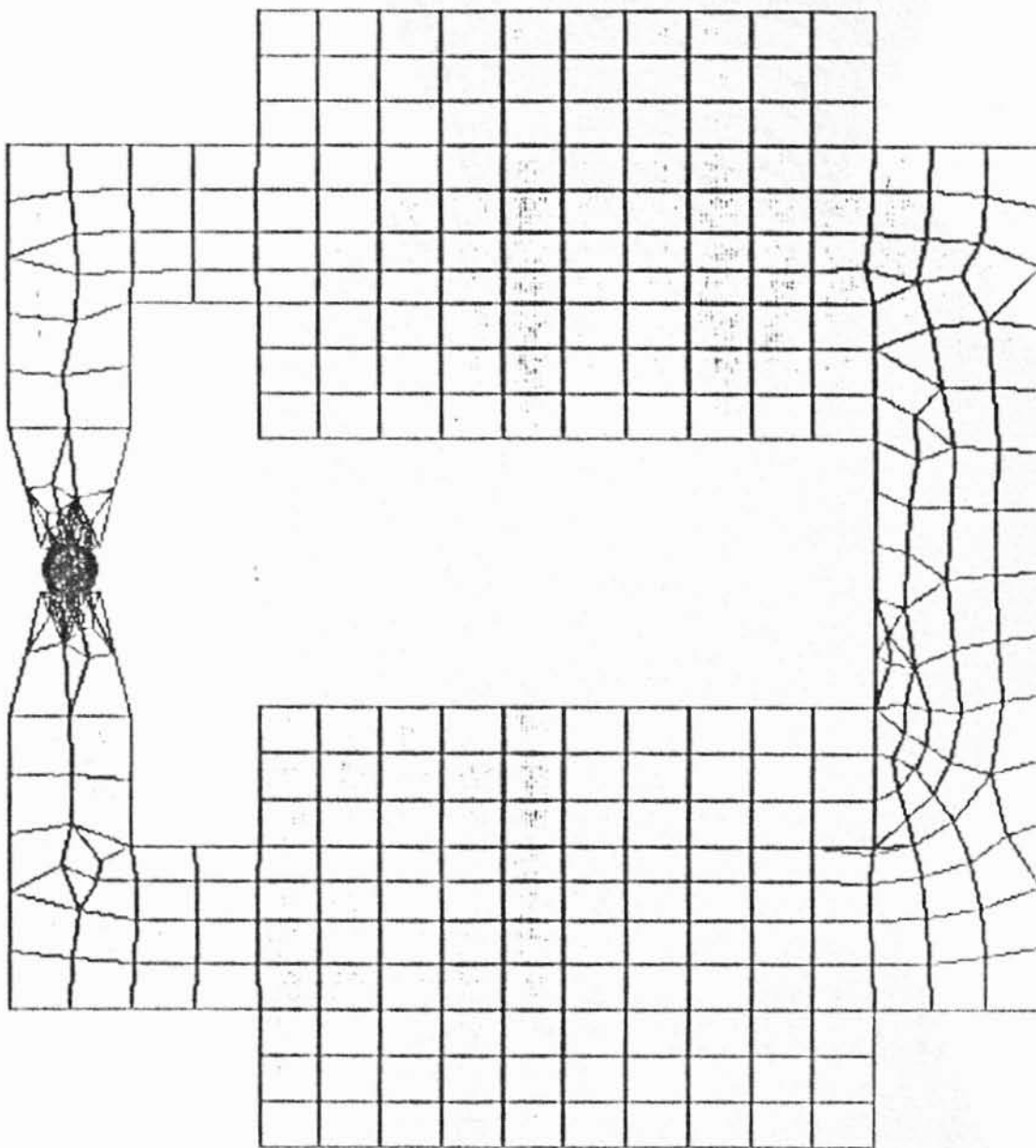


Figure 3.5 The finite element model for the complete magnetic abrasive finishing cell.

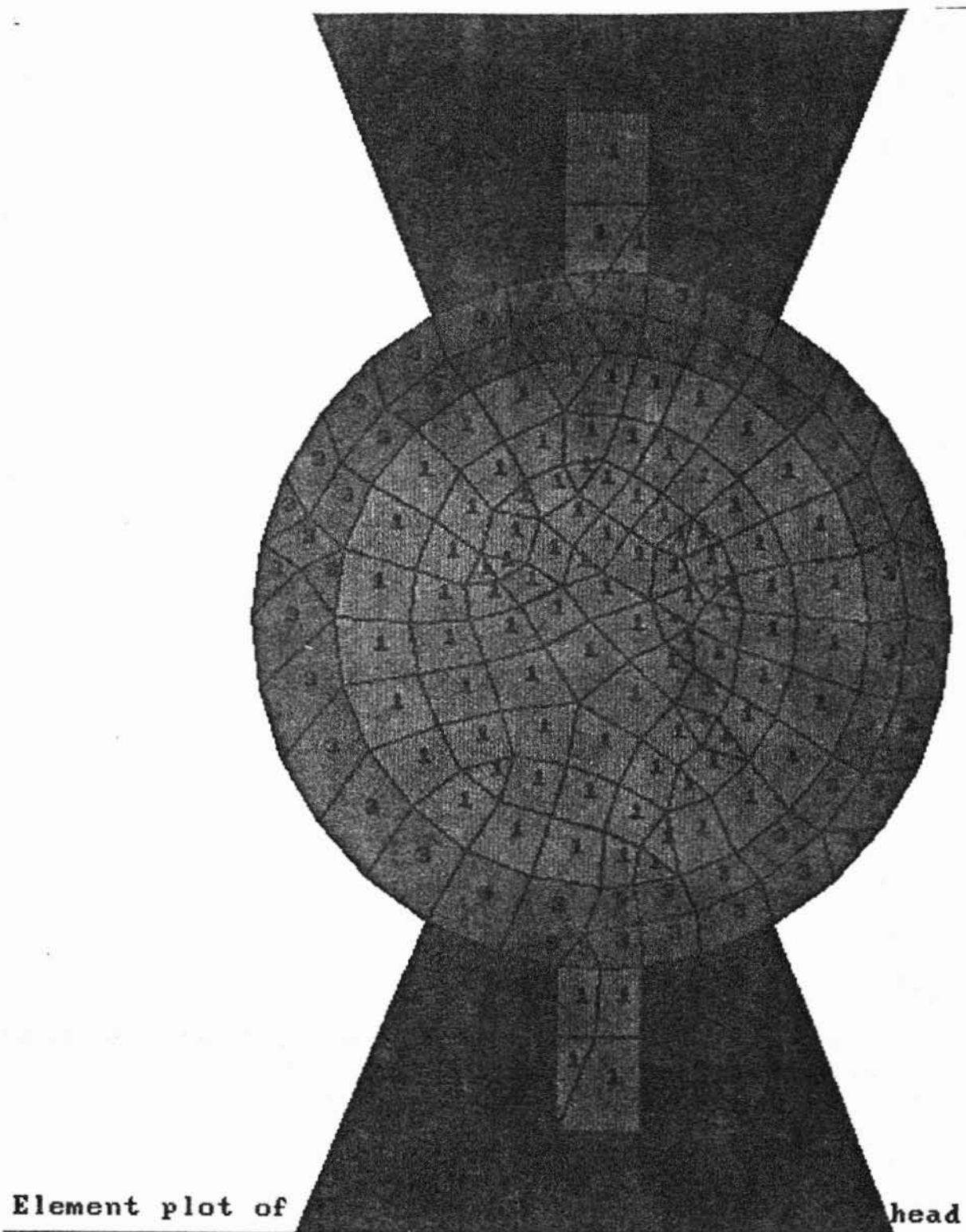


Figure 3.6: The fine element distribution of the finite element model at the nonmagnetic workpiece

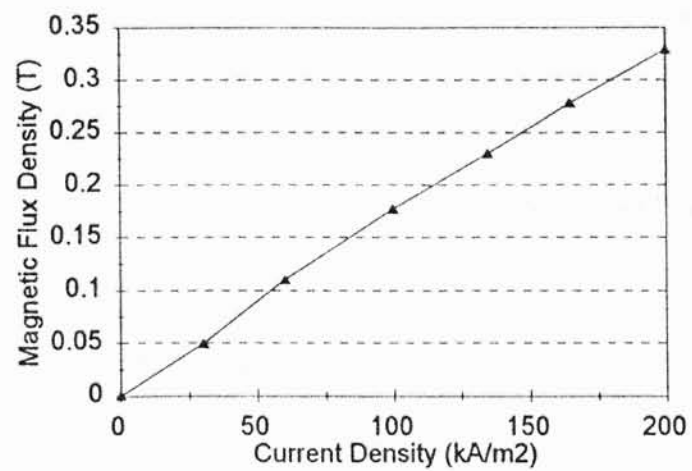


Figure 3.7: The variations of magnetic field density with different current densities through the current carrying coils in MAF process

- Flux lines (flux paths)
- Contour displays of flux density, field density, and source current density
- Vector displays of flux density, and field intensity

As the distribution of magnetic field density controlling the magnetic force is affected by the shape of the magnetic pole, consideration is given to it when designing the MAF system. Various magnetic head designs considered in the finite element analysis of the magnetic abrasive finishing process are shown in Figure 3.8. The magnetic pole shape is governed by the included angle of the magnetic head, presence of any air slot in the magnetic head (including its geometry), and converging shape of the magnetic head.

The results of this analysis can be used to predict the magnetic field distribution and the magnetic force distribution on the surface of the roller, which are responsible for the finishing action during polishing. This, in turn, helps in evaluating the capacity of the magnetic field source to carry out the finishing operation.

3.4 Magnetic force distribution on the nonmagnetic roller

To calculate the magnetic force on the roller, the pressures acting on the abrasives at the abrasive-magnetic pole interface and the roller-abrasive interface at each nodal point are calculated using Maxwell stress tensor approach. Using equation 3.5, the nodal pressure at each interface is integrated with respect to the surface area on which these forces act

The nodal pressures in both normal and tangential directions are given by,

$$\sigma_r(\text{abrasive-roller}) = \frac{1}{2\mu_0}(B_r^2 - B_\theta^2) \quad (3.9a)$$

and

$$\sigma_\theta(\text{abrasive-roller}) = \frac{1}{\mu_0}(B_r B_\theta) \quad (3.9b)$$

Head Design	Characteristics	Diagram
A	<ul style="list-style-type: none"> •No slot in the magnetic head •Included angle of the magnetic abrasive on the surface of the roller is 40° 	
B	<ul style="list-style-type: none"> •Rectangular slot in the magnetic head •Included angle of the magnetic abrasive on the surface of the roller is 180° 	
C	<ul style="list-style-type: none"> •No slot in the magnetic head •Included angle of the magnetic abrasive on the surface of the roller is 180° 	

Figure 3.8: Various head designs used in the finite element analysis of MAF process contd...


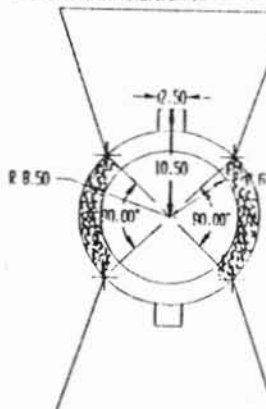
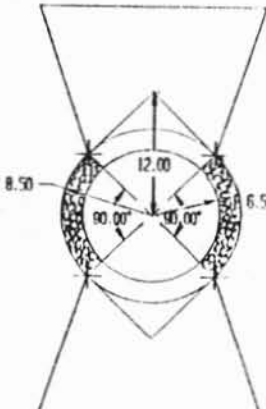
Head Design	Characteristics	Diagram
D	<ul style="list-style-type: none"> •No slot in the magnetic head •Included angle of the magnetic abrasive on the surface of the roller is 300° 	
E	<ul style="list-style-type: none"> •Rectangular slot in the magnetic head •Included angle of the magnetic abrasive on the surface of the roller is 180° 	
F	<ul style="list-style-type: none"> •Triangular slot in the magnetic head •Included angle of the magnetic abrasive on the surface of the roller is 180° 	

Figure 3.8: Various head designs used in the finite element analysis of MAF process contd...

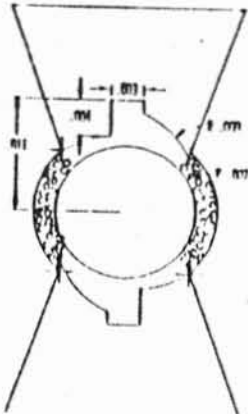
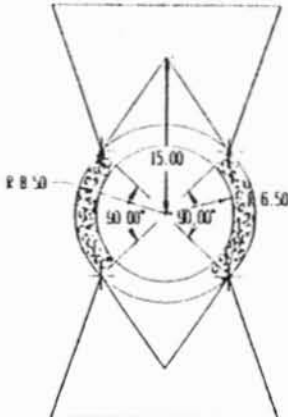
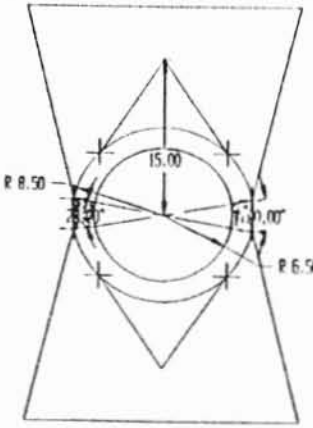
Head Design	Characteristics	Diagram
G	<ul style="list-style-type: none"> •Rectangular slot in the magnetic head with variable air gap •Included angle of the magnetic abrasive on the surface of the roller is 180° 	
H	<ul style="list-style-type: none"> •Triangular slot in the magnetic head •Included angle of the magnetic abrasive on the surface of the roller is 180° 	
I	<ul style="list-style-type: none"> •Triangular slot in the magnetic head •Included angle of the magnetic abrasive on the surface of the roller is 40° 	

Figure 3.8: Various head designs used in the finite element analysis of MAF process contd...

Head Design	Characteristics	Diagram
J	<ul style="list-style-type: none"> •No slot in the magnetic head •Included angle of the magnetic abrasive on the surface of the roller is 120° 	

Figure 3.8: Various head designs used in the finite element analysis of MAF process

Where μ_0 is the permeability of free space
 B_r and B_θ are the magnetic field densities in the radial and tangential directions respectively at the node under consideration
 $\sigma_{r(\text{abrasive-roller})}$ is the normal stress between the abrasive and the roller interface
 $\sigma_{\theta(\text{abrasive-roller})}$ is the tangential stress between the abrasive and the roller interface

$$\sigma_{r(\text{pole-abrasive})} = \frac{1}{2\mu_{\text{abrasive}}} (B_r^2 - B_\theta^2) \quad (3.10a)$$

and

$$\sigma_{\theta(\text{pole-abrasive})} = \frac{1}{\mu_{\text{abrasive}}} (B_r B_\theta) \quad (3.10b)$$

Where μ_{abrasive} is the permeability of free space
 $\sigma_{r(\text{pole-abrasive})}$ is the normal stress between the pole and the abrasive, and
 $\sigma_{\theta(\text{pole-abrasive})}$ is the tangential stress between the pole and the abrasive.

The net force exerted by the abrasive on the roller is the difference between the forces acting on the abrasive-roller interface and abrasive-magnetic pole interfaces.

$$\sigma_{r(\text{net})} = \sigma_{r(\text{abrasive-roller})} - \sigma_{r(\text{pole-abrasive})} \quad (3.11a)$$

$$\sigma_{\theta(\text{net})} = \sigma_{\theta(\text{abrasive-roller})} - \sigma_{\theta(\text{pole-abrasive})} \quad (3.11b)$$

3.4 Characterization of the magnetic heads

The magnetic force exerted by the abrasives on the roller is measured using a 350 ohm strain gage formed in 1/4 bridge. The strains developed on the surface of the roller are measured using a strain gage indicator. Before the strain gage indicator can be used, it is calibrated using static loads for the given

experimental set up. The strain gage is fixed to the strain indicator and a known force is applied at the other end of the apparatus. The plot of the known force vs the strain gage indicator reading gives the calibration curve as shown in Figure 3.9.

If the abrasives surround the workpiece, then due to symmetry the tangential and normal forces cancel out with that of the diametrically opposite point. Hence, the net force measured by the dynamometer in the X-direction and Y-direction is zero.

In order to estimate the forces acting on the roller, two set of experiments were performed.

In experiment 1, the abrasives surround the roller only on the top part of the roller (Figure 3.10). In this case, the horizontal (X-component) forces cancel out and the net force acting on the roller is in the Y-direction.

In experiment 2, the abrasives surround the roller only on the left part of the roller, i. e. the abrasives are present only on one of the magnetic poles (Figure 3.11). In this case, the vertical (Y-component) forces cancel out and the net force acting on the roller is in the X-direction.

In all these experiments 3 gm of KMX80 magnetic abrasive was used.

Head designs C, D, E, I and J were selected for the above experiments to investigate the effect of length of magnetic conducting path on the magnetic pressure exerted on the surface of the roller. These head designs results in the 180° , 300° , 180° , 40° , and 60° included angles of the magnetic abrasives on the surface roller. Figure 3.12 shows the variation of measured values of the action force, F , exerted by the magnetic abrasives on the roller surface using experiment 1. F follows a parabolic behavior with increase in the magnetic field density. Also, F increase with increases in the included angle of the magnetic head upto a certain value (upto an included angle of 120°) and then decreases with further increase in the angle. This indicates that the optimal included angle of the magnetic head is necessary to generate the required magnetic pressure exerted by the magnetic abrasives on the surface of the roller.

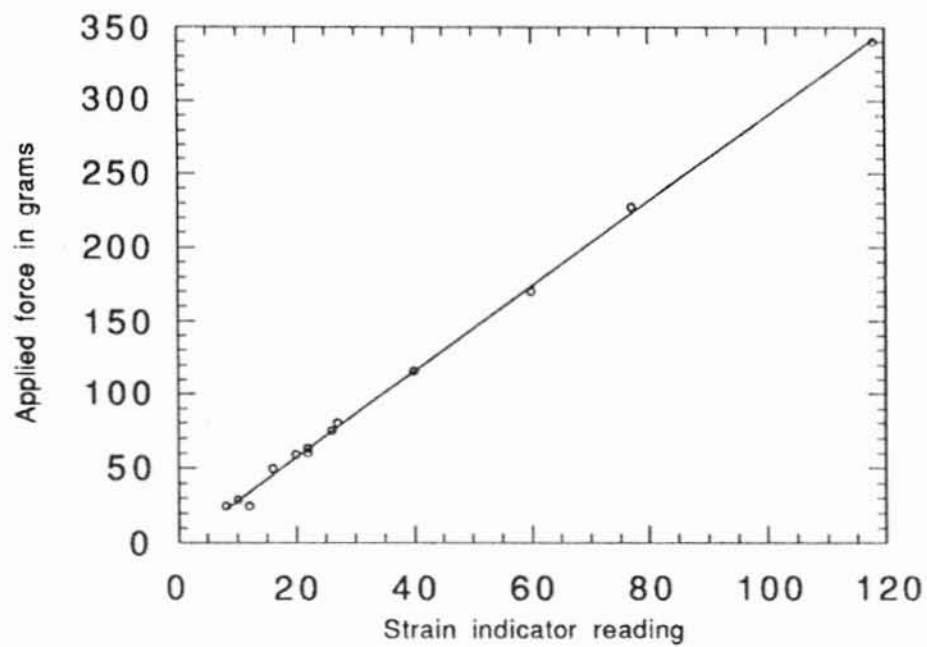


Figure 3.9: Calibration curve for strain gage (350 ohm) using strain gage indicator

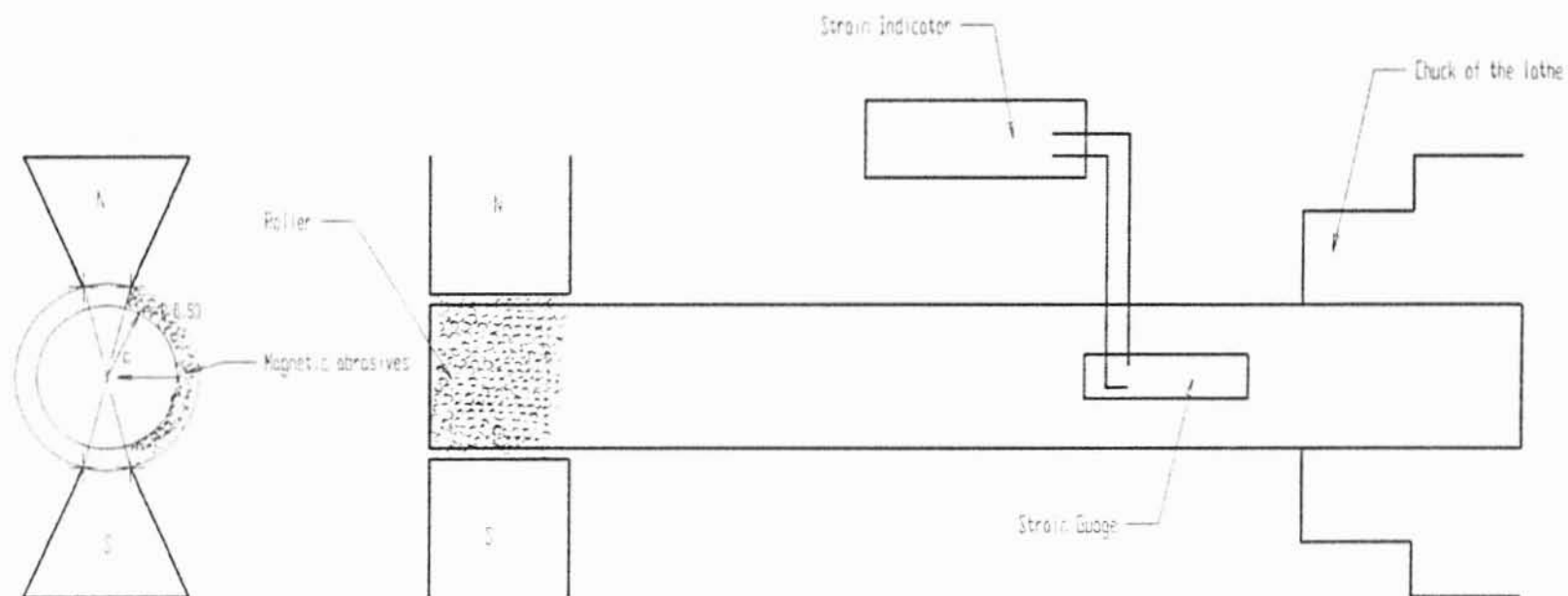


Figure 3.10: Set up for the measurement of the action force F exerted by the magnetic abrasives on the roller surface using Experiment 1

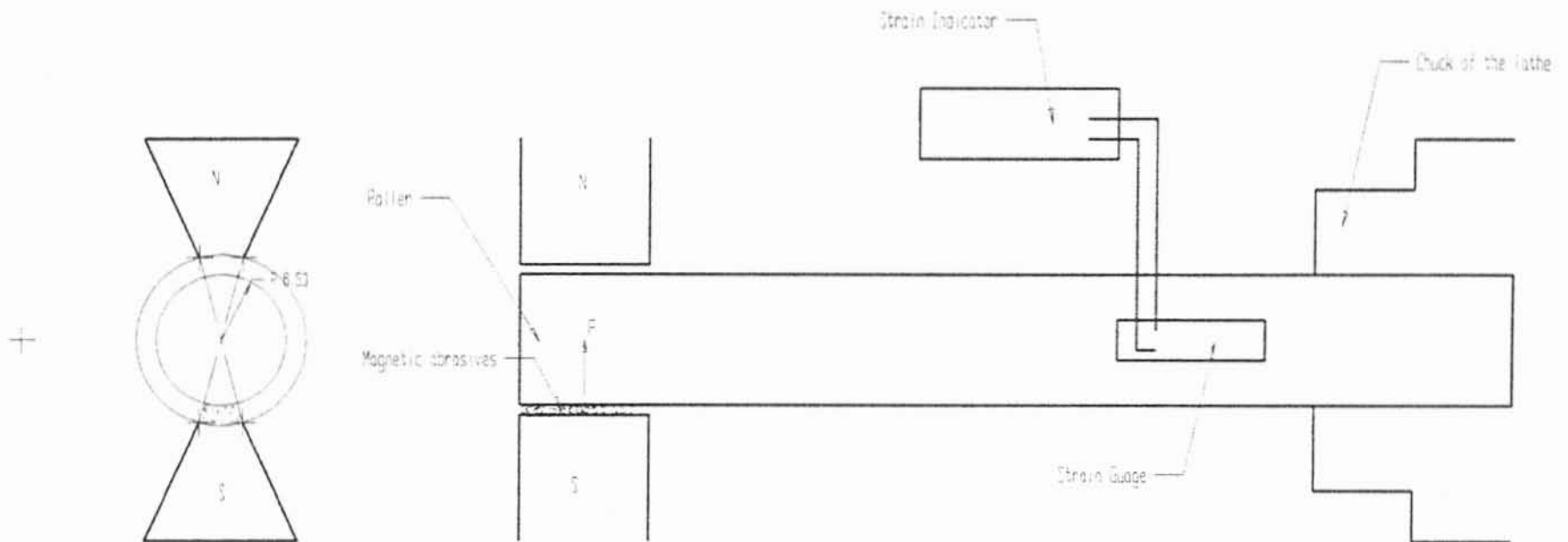


Figure 3.11: Set up for the measurement of the action force F exerted by the magnetic abrasives on the roller surface using Experiment 2

Characterisation of the magnetic head using experiment (I)

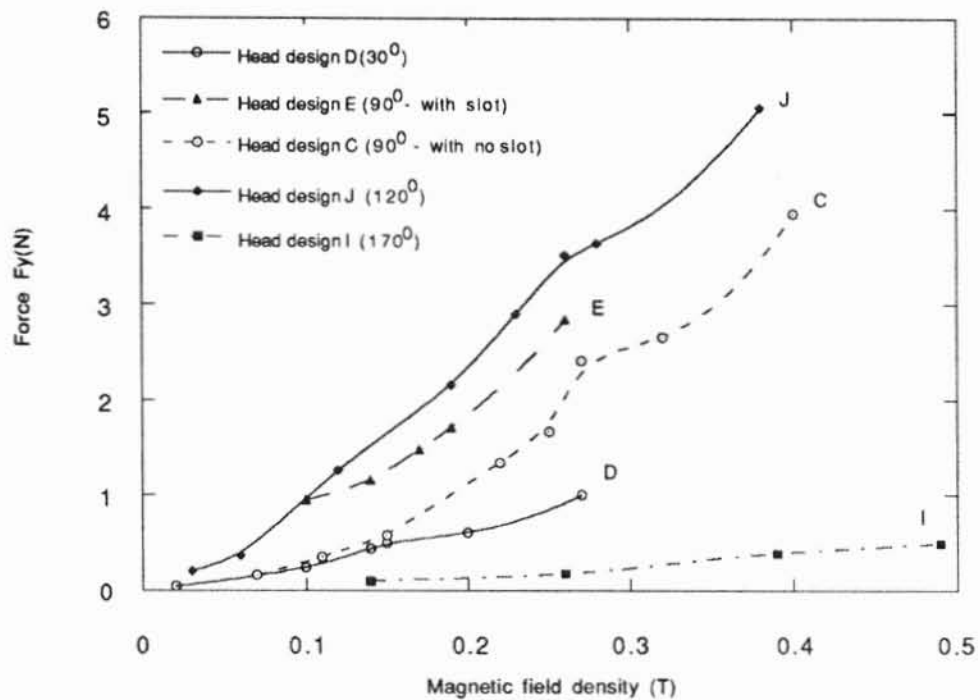


Figure 3.12: Variation of the action force F exerted by the magnetic abrasives on the roller surface using Experiment 1 for different head designs of various included angles with magnetic field density

The magnetic heads are characterized using Experiment 1 as well as simulation for the head designs E and I. Similarly, the magnetic heads are characterized using experiment 2, as well as simulation for head design E. Figures 3.13 - 3.15 show the variation of total force exerted on the roller by the magnetic abrasives, for each case at different magnetic field densities. It can be seen that the total force obtained from the simulation in the first case is lower than that obtained from experiment 1 (Figures 3.13, 3.15). This can possibly be due to the fact that in the presence of a magnetic field density, the abrasives are firmly held between the magnetic poles with the shear forces. Consequently, a rigid abrasive brush is formed. Unfortunately, the shear forces are not considered in the ANSYS analysis and the force interactions only due to the magnetic field is considered. However, in experiment 2, the forces obtained from the simulation studies closely match the experimental results at all magnetic field densities (Figure 3.14). The magnitude, of forces obtained from these experiments, also agrees with the experimental results reported by [Shinmura, 1987b].

The magnetic pressure exerted by the magnetic abrasives on the roller is calculated using the expression:

$$P = \frac{F}{\frac{\pi \times d \times l}{4}} \quad (3.12)$$

Where, P is the normal pressure (N/m²)

F is the force measured in the experiment (N)

d is the diameter of the roller (m)

l is the length of the roller in contact (m)

It is found that the magnetic pressures exerted by the magnetic head designs C, D, E, I and J are 58 kN/m², 9 kN/m², 45 kN/m², 33 kN/m², and 98 kN/m² respectively. It is found that more magnetic abrasives are in contact in the case of head designs C and E compared to head design I and J. Thus the design J gives the very high magnetic pressures but at relatively low contact length on

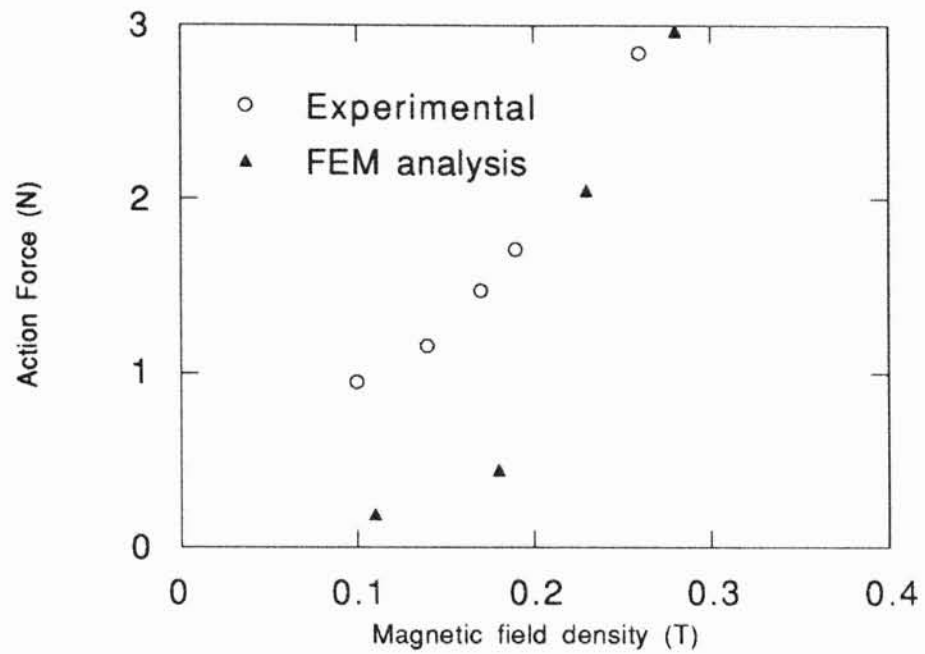


Figure 3.13: Variation of the action force F exerted by the magnetic abrasives on the roller using Experiment 1 for head design E with magnetic field density

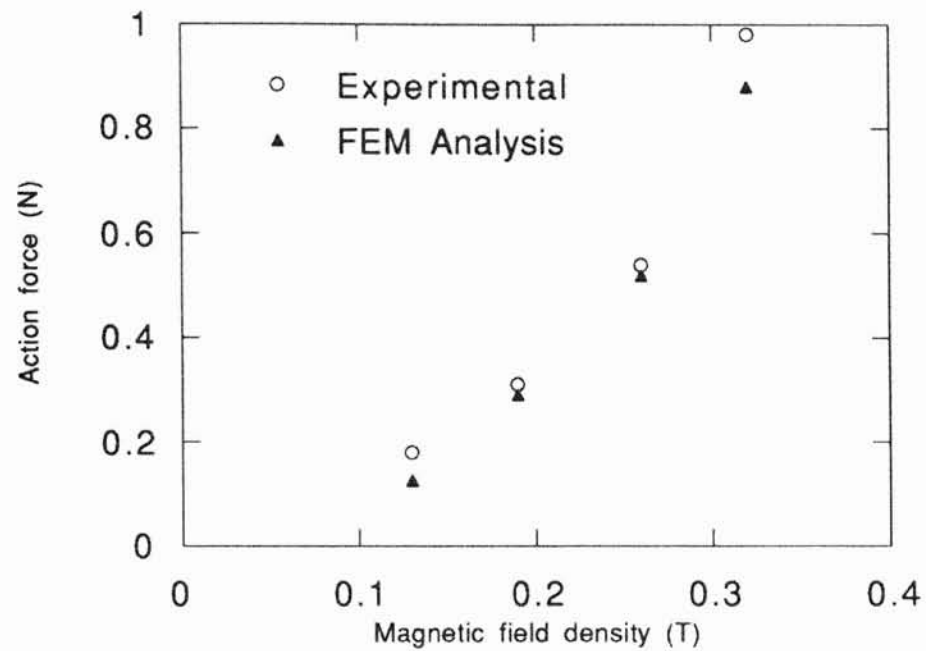


Figure 3.14: Variation of the action force F exerted by the magnetic abrasives on the roller surface using Experiment 2 for head design E with magnetic field density

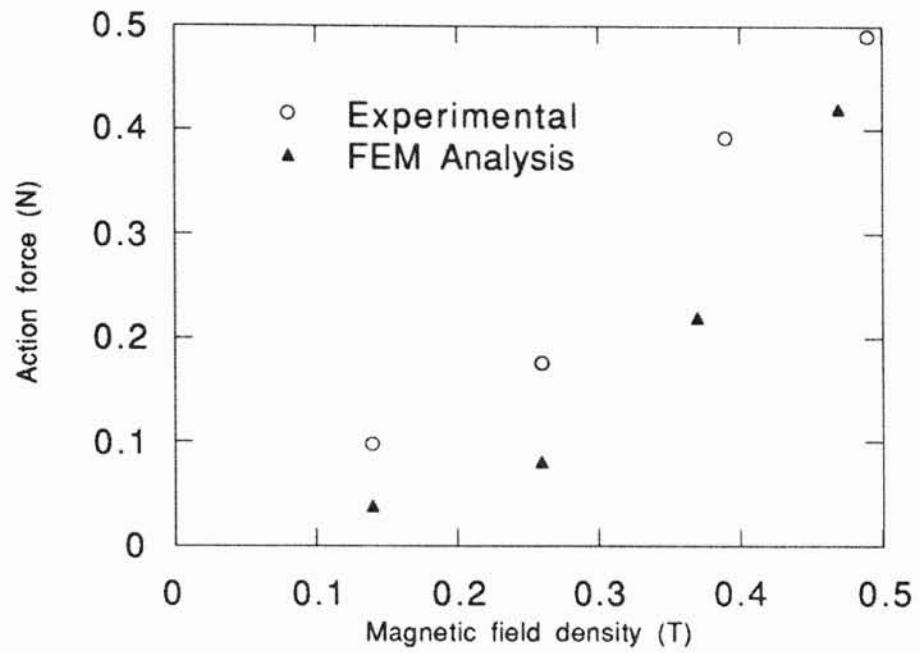


Figure 3.15: Variation of the action force F exerted by the magnetic abrasives on the roller surface using Experiment 1 for head design I with magnetic field density

the roller surface. The design C gives lower magnetic pressure, but at relatively larger contact length on the roller surface.

3.5 Determination of the cutting force

The ANSYS analysis was used for the determination of the total cutting force (F_c) exerted on the roller for a given magnetic field density and head geometry. The total friction force F_c generated in MAF process is given by,

$$F_c = \int_s |\tau + \mu_f \sigma| d\epsilon \quad (3.13)$$

where μ_f is the frictional force.

As the experiment was carried out in dry conditions, the coefficient of friction was assumed to be 0.5 [Tipnis, 1980]. Experiments were carried out to measure the material removal rate on nonmagnetic stainless steel rollers using head design E. The following conditions were used during the experiments:

Rotational speed of the roller: 2000 rpm

Magnetic field density : 0.0965, 0.174, 0.254, and 0.324T.

Duration of polishing: 3 minutes

The material removal rate for the finishing process was noted at the end of three minutes for different magnetic flux densities. The abrasives were uniformly stirred during polishing at the end of each minute, so that new abrasives stay in contact with the workpiece. The variation of the material removal rate with the cutting force (F_c) shows that the material removal rate is directly proportional to the cutting force (Fig.3.16a).

Effect of axial vibration on the action force

Experiments were conducted to investigate the effect of axial vibration and weight of abrasives used, on the action force, F , exerted by the abrasives on the surface of the roller for experiment 1. The action force is found to increase substantially with the introduction of axial vibration (Figure 3.16b). This can be due to the fact that the vibration can enhance interlinking among the abrasives

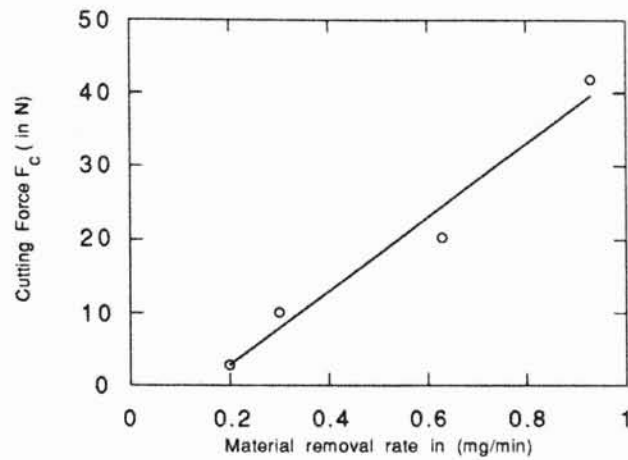


Figure 3.16a: Variation of material removal rate with the cutting force exerted by the abrasives on the surface of the roller in case of head design E.

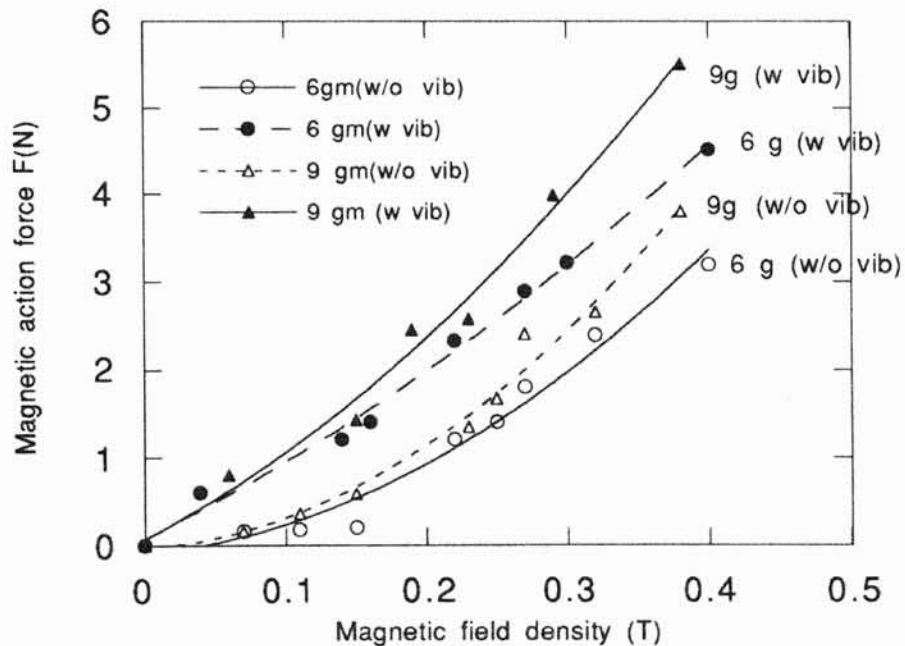


Figure 3.16b: Variation of action force with magnetic field density for various weights of magnetic abrasives used with/without axial vibration on the surface of the roller

between the N and S poles, thus increasing the packing density. Also, with increase in weight of the abrasives, the F also increased. This can be due to the increase in the packing density of the abrasives in the air gap between the N and S poles.

3.6 Development of design principles for the magnetic head used in MAF

An attempt was made to develop design principles for the magnetic head used in MAF process. This study has resulted in the following:

- i) An understanding of the effect of magnetic head geometry on the distribution of magnetic forces, and magnetic flux density at the abrasive/roller interface region.
- ii) Generation of the magnetic head design principles capable of providing optimum magnetic field density distribution in the abrasive region, and the maximum force generation in the cell for best material removal rate and/or finish.

Magnetic head geometry:

Various magnetic head designs used in the FEM analysis are shown in Figure 3.8. The following considerations are given in the design of the magnetic head.

- To increase the normal pressure exerted by the magnetic abrasives on the roller
- To achieve an optimum arc length sustained by the magnetic abrasives on the roller

The magnetic head designs were investigated in terms of magnetic forces that can be achieved near the magnetic abrasive and roller interface, to achieve maximum material removal rate. For each magnetic head design, the variation of the magnetic flux density and the magnetic force along the interface was evaluated using finite element analysis. Also, the magnetic head designs were investigated in terms of the total cutting force, using equation (3.8). To achieve the uniform surface finishing, it is desirable to have a uniform magnetic flux density distribution around the workpiece in the abrasives. This will enable all

the abrasives to take part in the finishing process equally, so that they wear uniformly. This would improve the efficiency of the finishing process.

Results of Finite Element Analysis

The normal and tangential component of the magnetic flux density and magnetic stress plots resulted from the finite element analysis are presented in Figures 3.17 through Fig. 3.52. These plots are for the magnetic flux density and magnetic stress at the abrasive - roller interface. Table 2 shows the maximum normal and tangential component of the magnetic field density and stress exerted by the magnetic abrasives on the surface roller. The results of this analysis are discussed in the following section.

3.7 Discussion:

From the two dimensional FEM analysis, the magnetic field in the abrasive region near the air gap within the magnetic head is found to be weaker than the magnetic field in the rest of abrasive region (Figure 3.17). This is because the magnetic flux flows through the shorter and magnetically conducting path in the abrasive region and avoids the air gap. This, subsequently, results in the agglomeration of magnetic abrasives in the region away from the magnetic head. It appears that the main cutting action takes place in the region away from the magnetic head. From the investigation of the Maxwell forces exerted on the surface of the workpiece by the abrasives, it appears that the forces are high at the surface where the maximum magnetic field exists, which is at the midpoint between the north and south pole. The forces drop at the point nearest to the magnetic head due to the presence of the air gap. For the material removal to take place, it is necessary to obtain high normal and tangential components of the force. The normal component of the force can effectively dig in the valleys on the surface of the roller, which can be subsequently removed by the tangential component of the force. Therefore, design of the poles should be changed so that a higher normal force is distributed over a larger area, for achieving better surface finish faster. From the experiments and simulation studies performed for the calculation of the forces on the roller, it is observed that the magnetic force varies parabolically with the magnetic field density. The magnetic force obtained from the simulation studies is less than that obtained

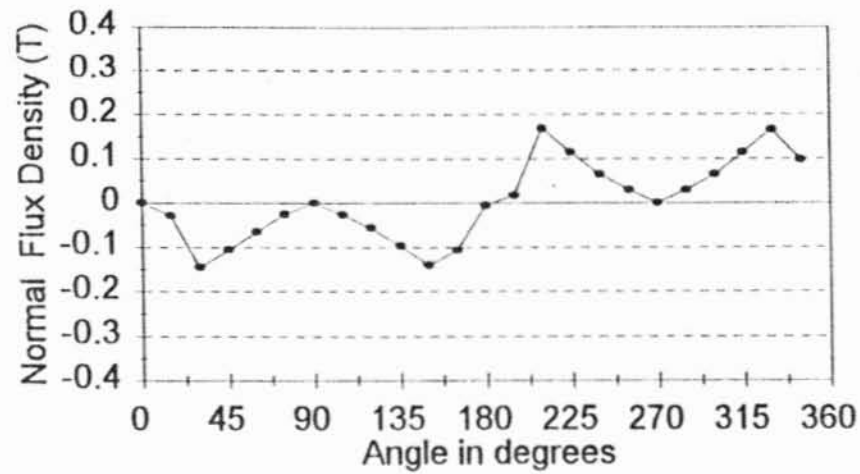


Figure 3.17 Normal magnetic field density at the roller - abrasive interface for head design A (included angle 170°)

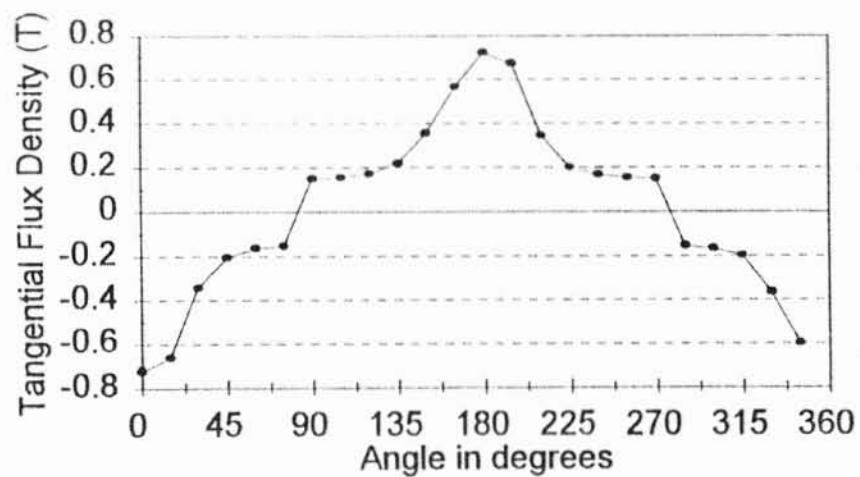


Figure 3.18 Tangential magnetic field density at the roller - abrasive interface for head design A (included angle 170°)

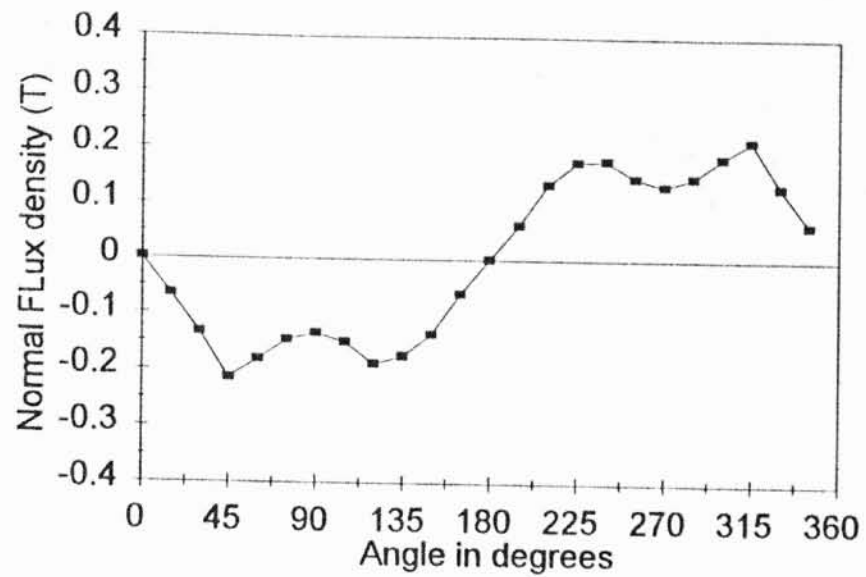


Figure 3.19 Normal magnetic field density at the roller - abrasive interface for head design B (included angle 90°)

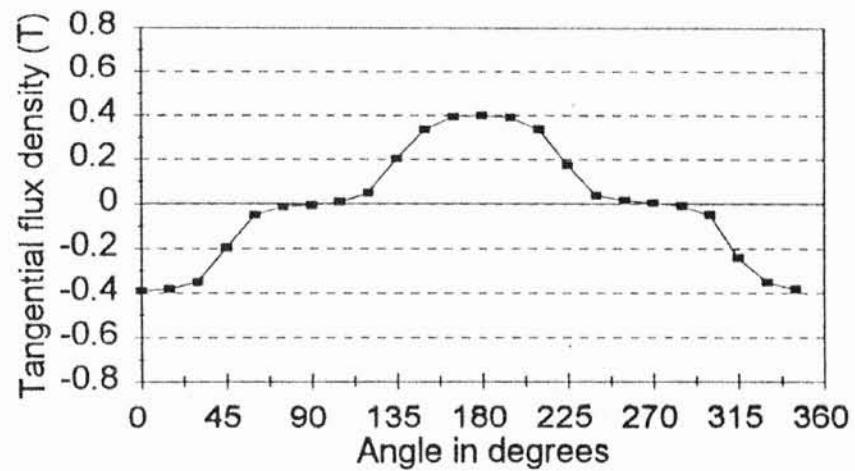


Figure 3.20 Tangential magnetic field density at the roller - abrasive interface for head design B (included angle 90°)

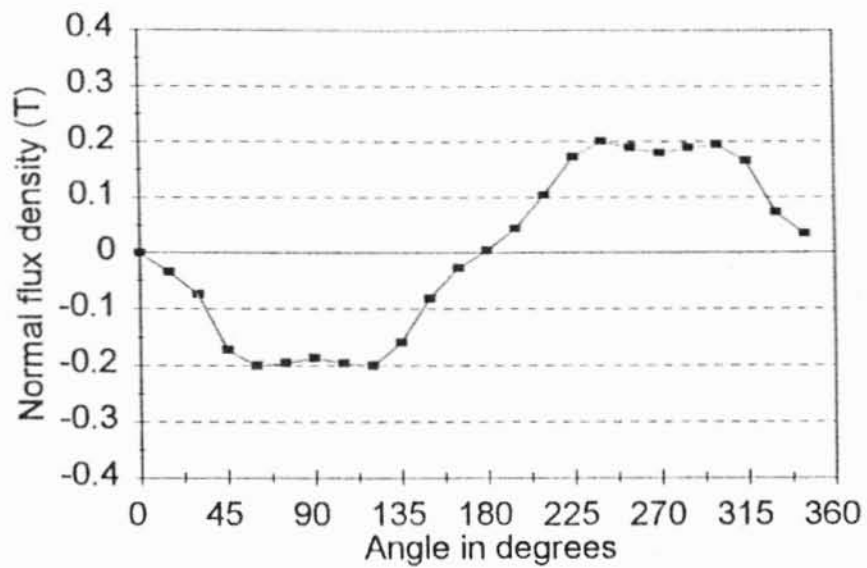


Figure 3.21 Normal magnetic field density at the roller - abrasive interface for head design C (included angle 90°)

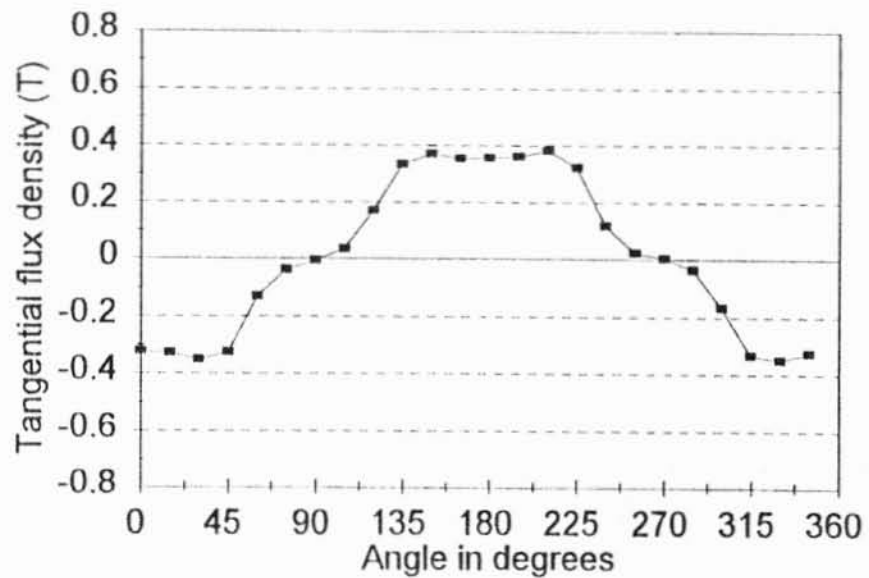


Figure 3.22 Tangential magnetic field density at the roller - abrasive interface for head design C (included angle 90°)

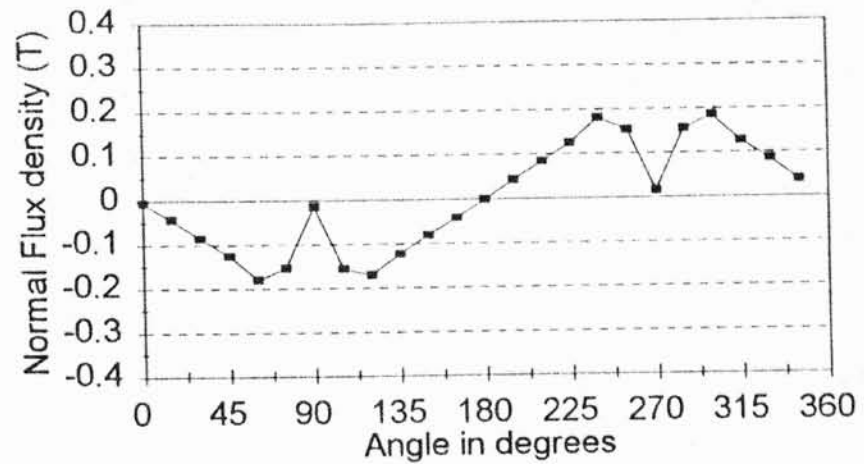


Figure 3.23 Normal magnetic field density at the roller - abrasive interface for head design D (included angle 30°)

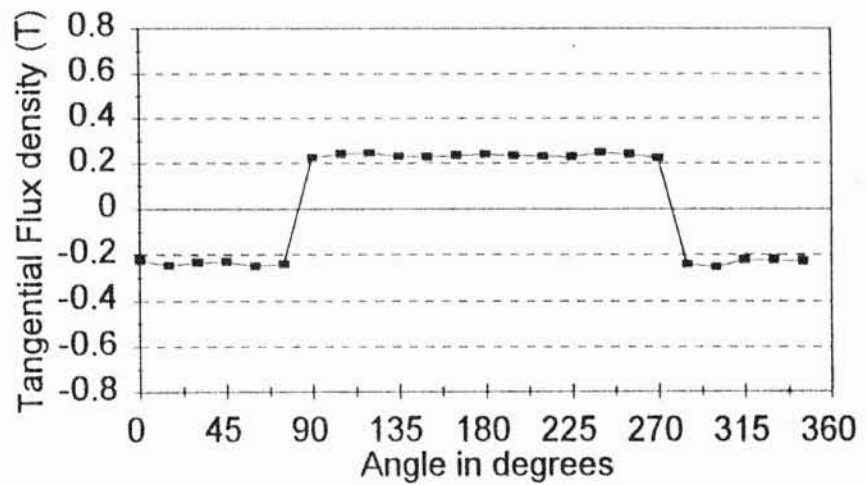


Figure 3.24 Tangential magnetic field density at the roller - abrasive interface for head design D (included angle 30°)

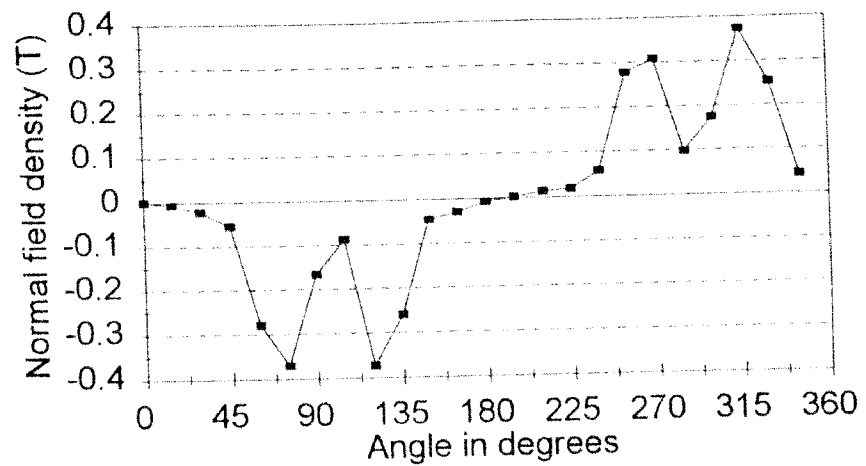


Figure 3.25 Normal magnetic field density at the roller - abrasive interface for head design E (included angle 90°)

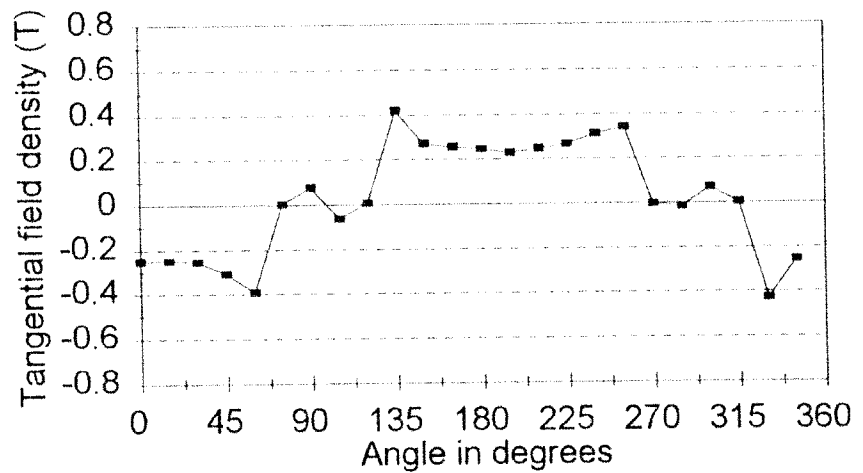


Figure 3.26 Tangential magnetic field density at the roller - abrasive interface for head design E (included angle 90°)

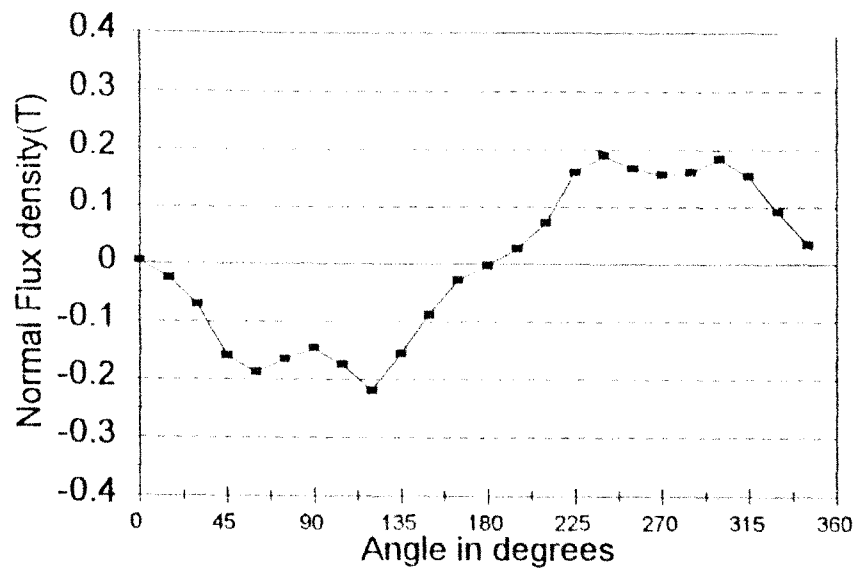


Figure 3.27 Normal magnetic field density at the roller - abrasive interface for head design F (included angle 90°)

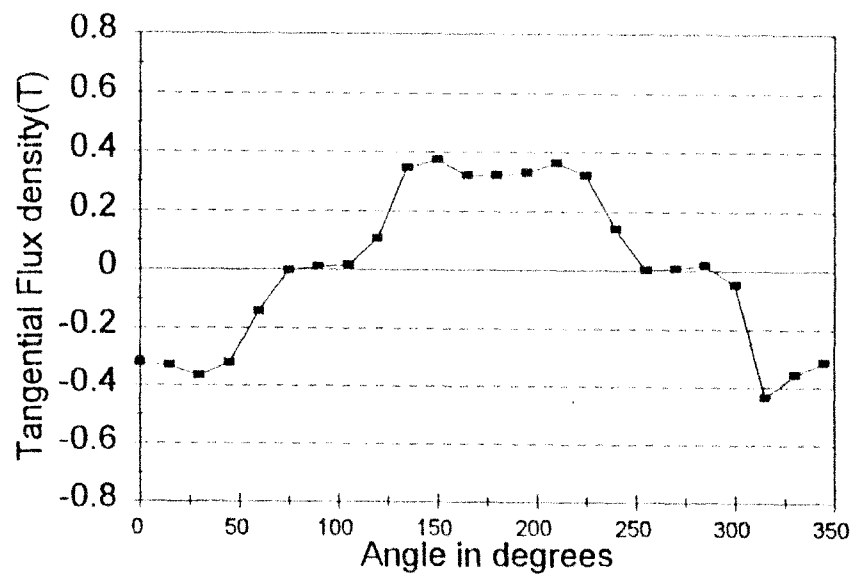


Figure 3.28 Tangential magnetic field density at the roller - abrasive interface for head design F (included angle 90°)

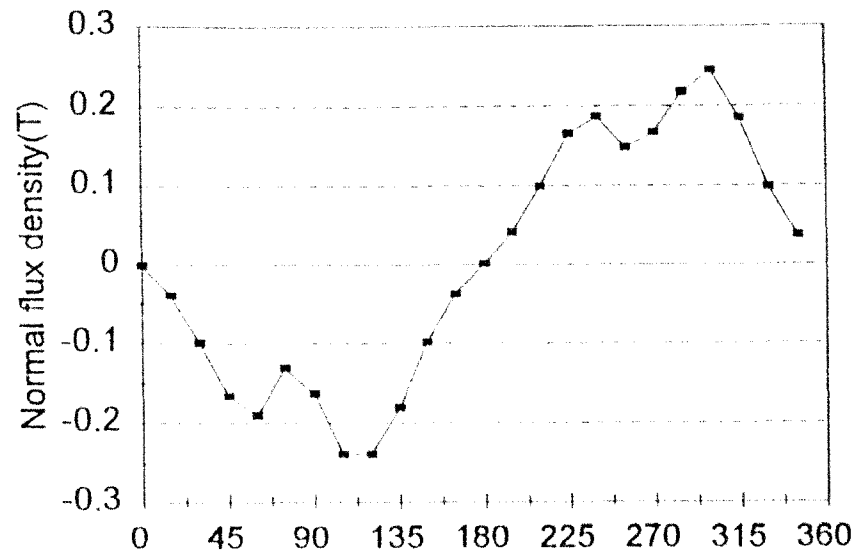


Figure 3.29 Normal magnetic field density at the roller - abrasive interface for head design G (included angle 90°)

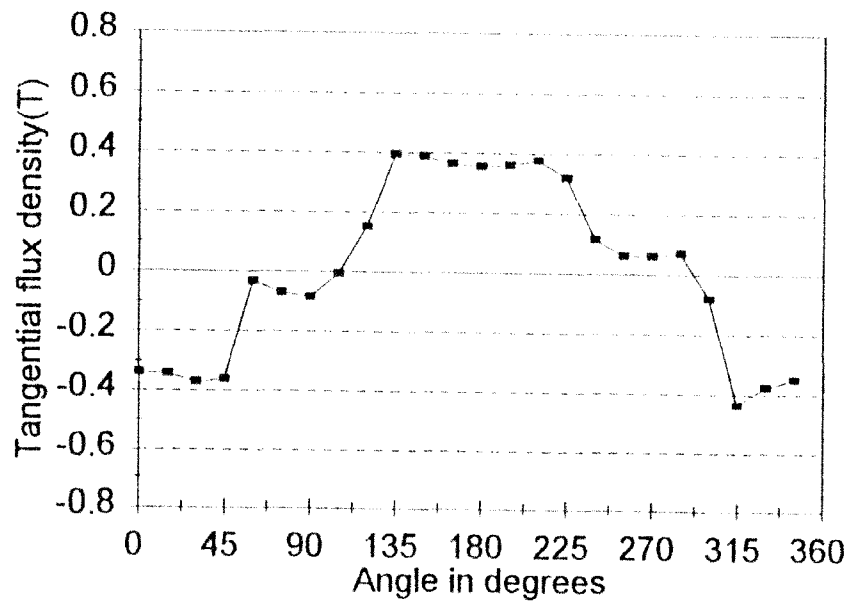


Figure 3.30 Tangential magnetic field density at the roller - abrasive interface for head design G (included angle 90°)

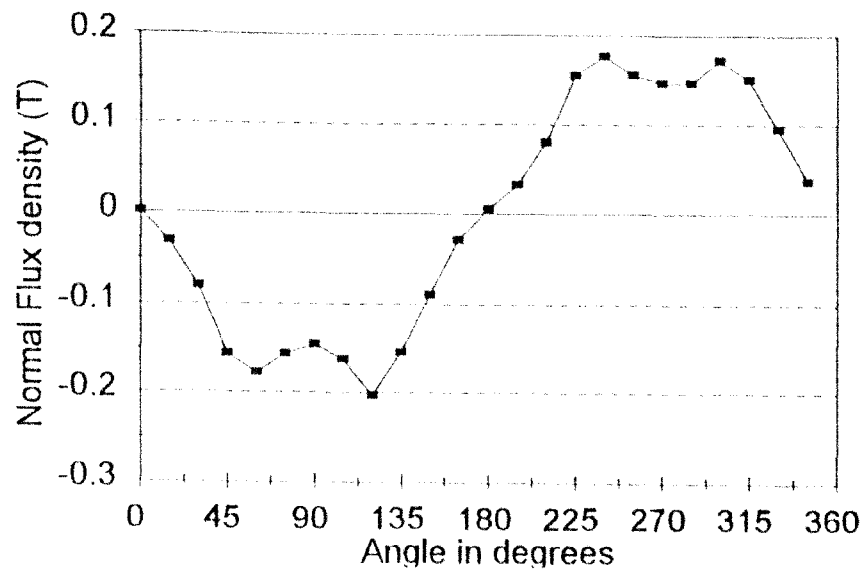


Figure 3.31 Normal magnetic field density at the roller - abrasive interface for head design H (included angle 90°)

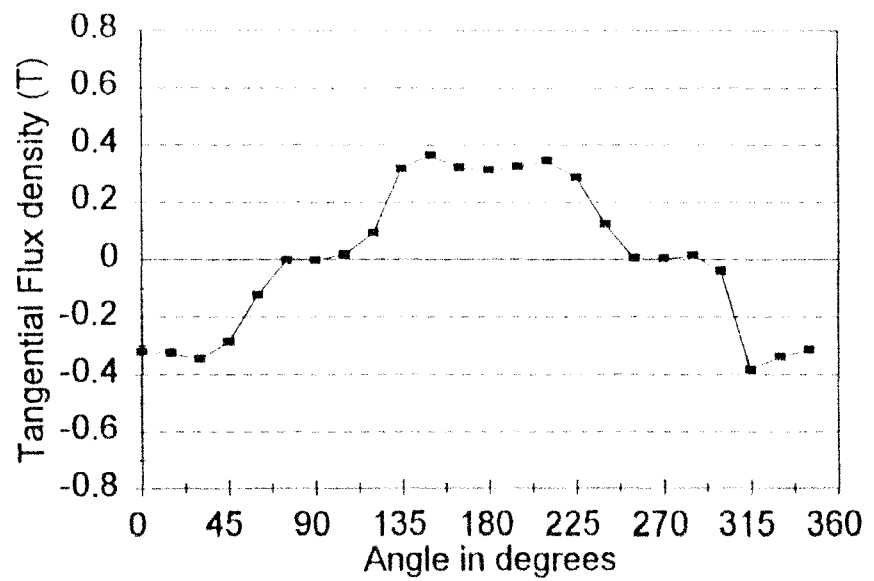


Figure 3.32 Tangential magnetic field density at the roller - abrasive interface for head design H (included angle 90°)

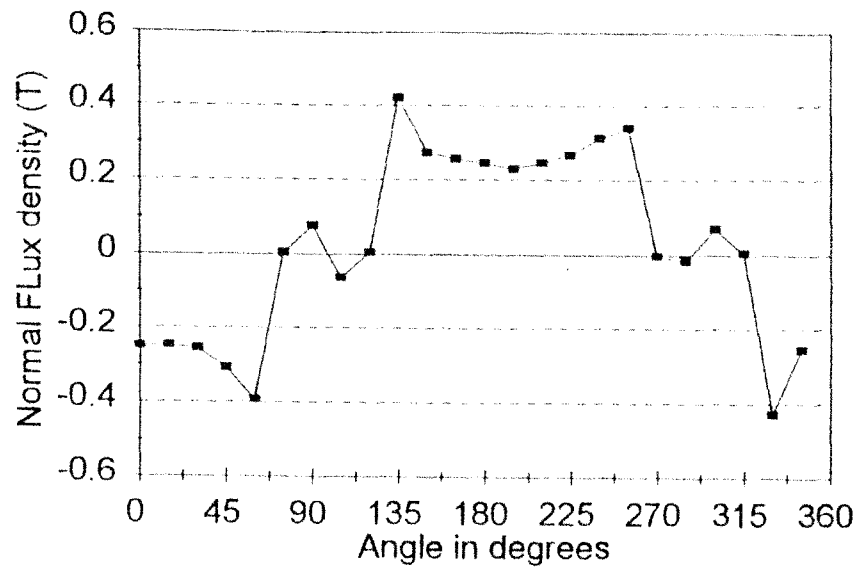


Figure 3.33 Normal magnetic field density at the roller - abrasive interface for head design I (included angle 170°)

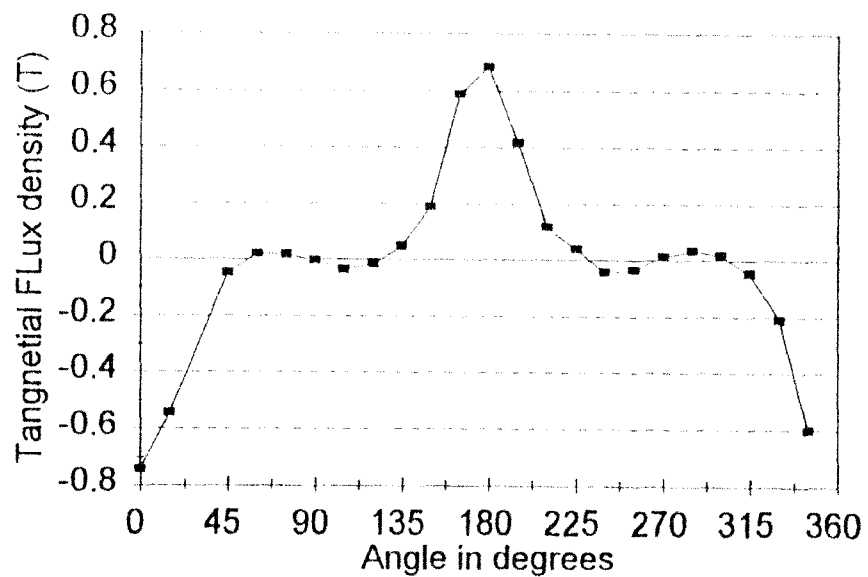


Figure 3.34 Tangential magnetic field density at the roller - abrasive interface for head design I (included angle 170°)

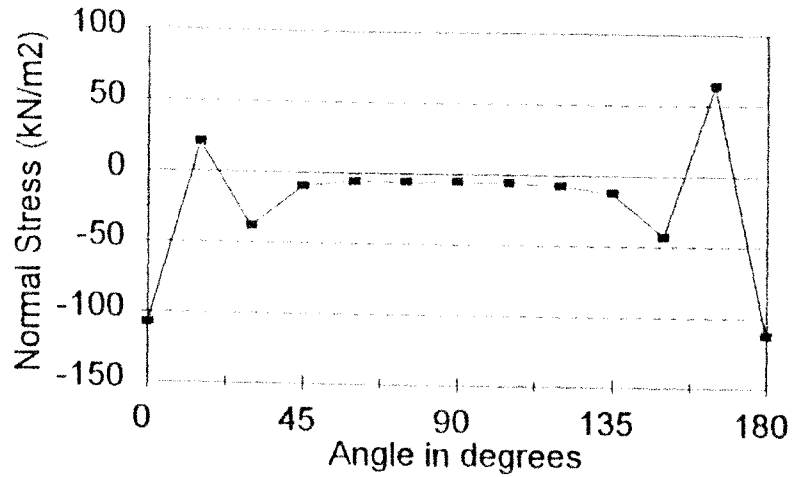


Figure 3.35 Normal stress distribution at the roller - abrasive interface for head design A (included angle 170°)

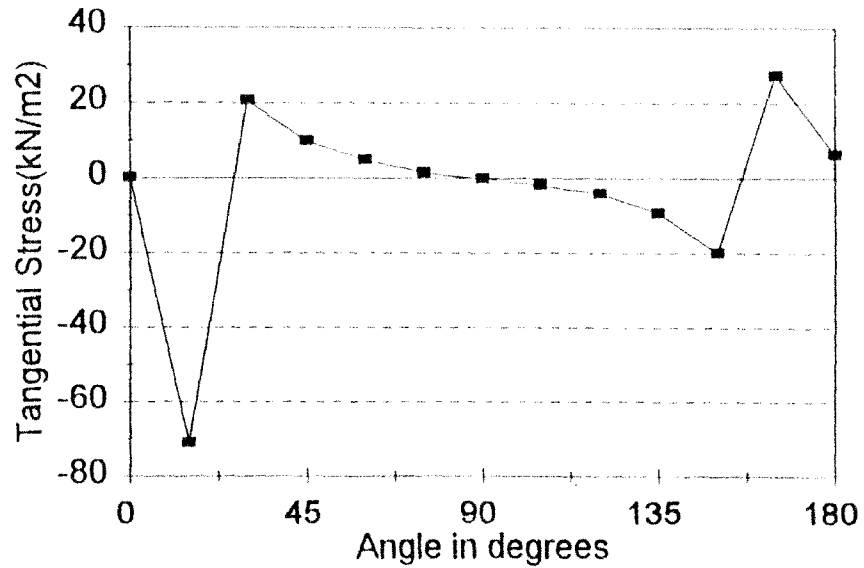


Figure 3.36 Tangential stress distribution at the roller - abrasive interface for head design A (included angle 170°)

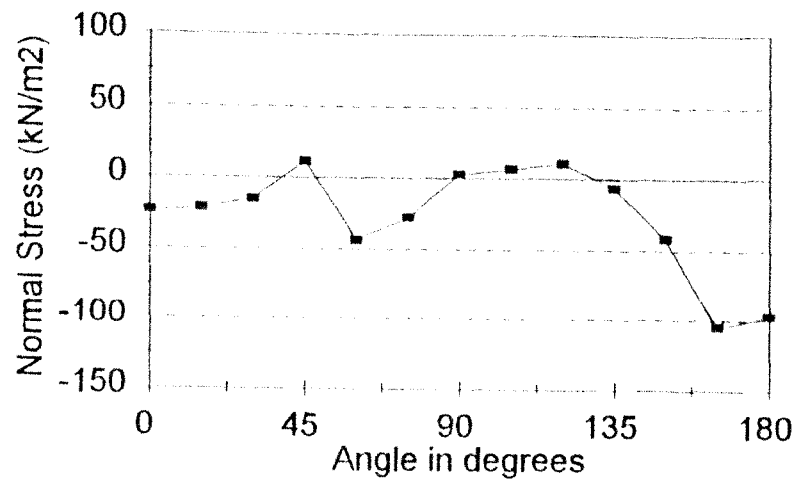


Figure 3.37 Normal stress distribution at the roller - abrasive interface for head design B (included angle 90°)

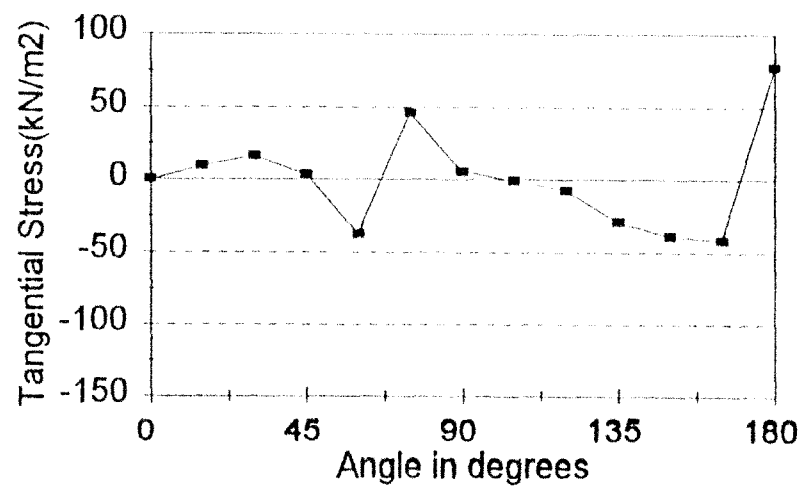


Figure 3.38 Tangential stress distribution at the roller - abrasive interface for head design B (included angle 90°)

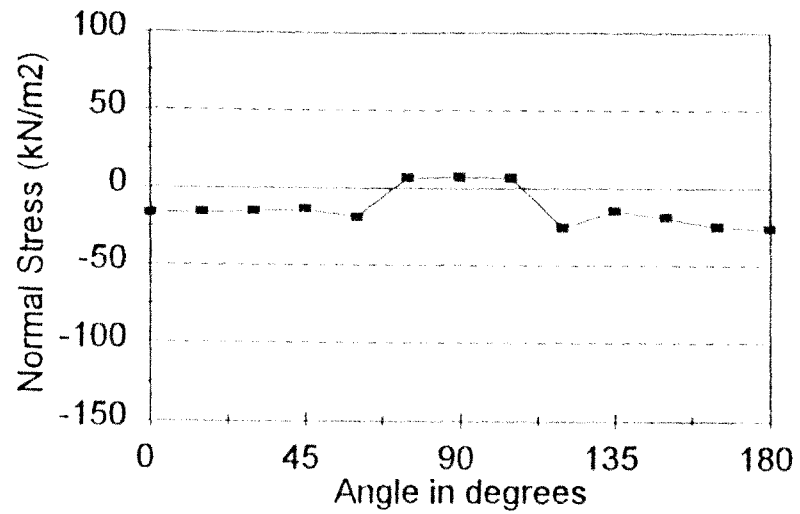


Figure 3.39 Normal stress distribution at the roller - abrasive interface for head design C (included angle 90°)

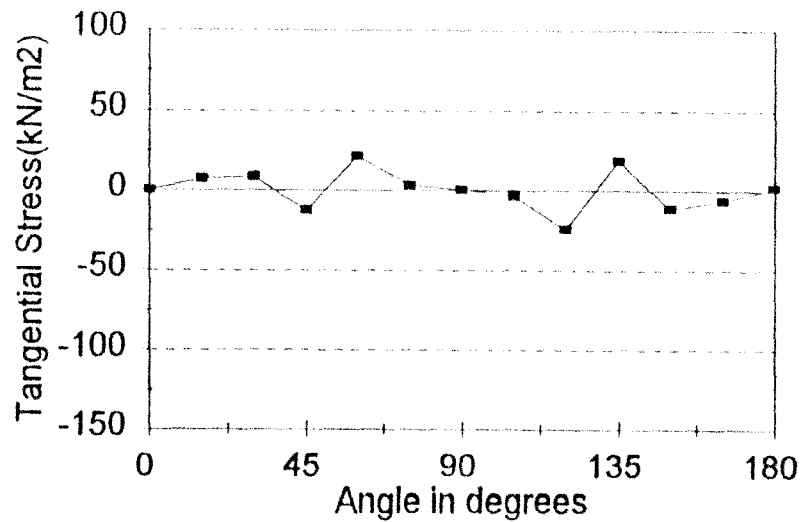


Figure 3.40 Tangential stress distribution at the roller - abrasive interface for head design C (included angle 90°)

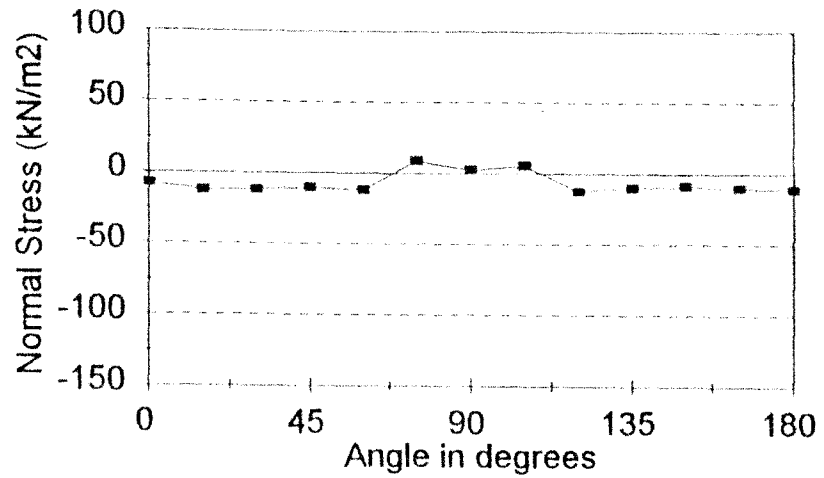


Figure 3.41 Normal stress distribution at the roller - abrasive interface for head design D (included angle 30°)

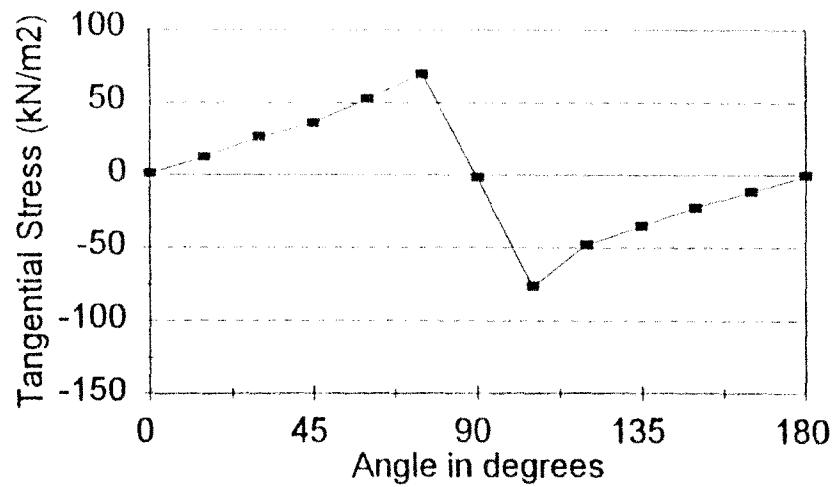


Figure 3.42 Tangential stress distribution at the roller - abrasive interface for head design D (included angle 30°)

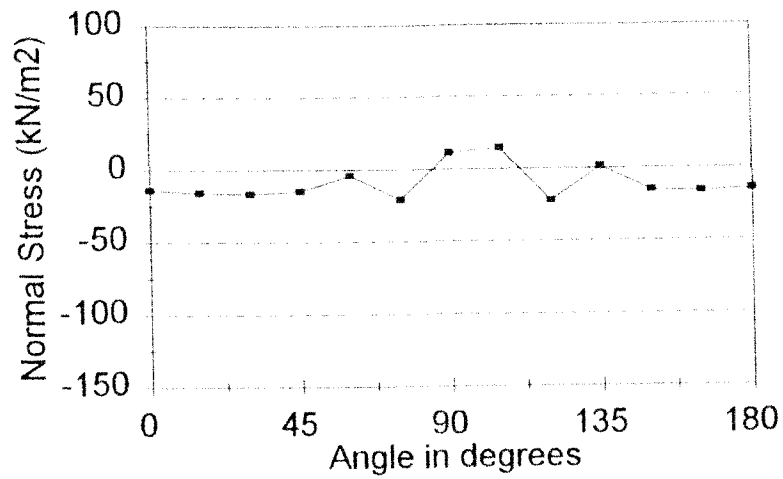


Figure 3.43 Normal stress distribution at the roller - abrasive interface for head design E (included angle 90°)

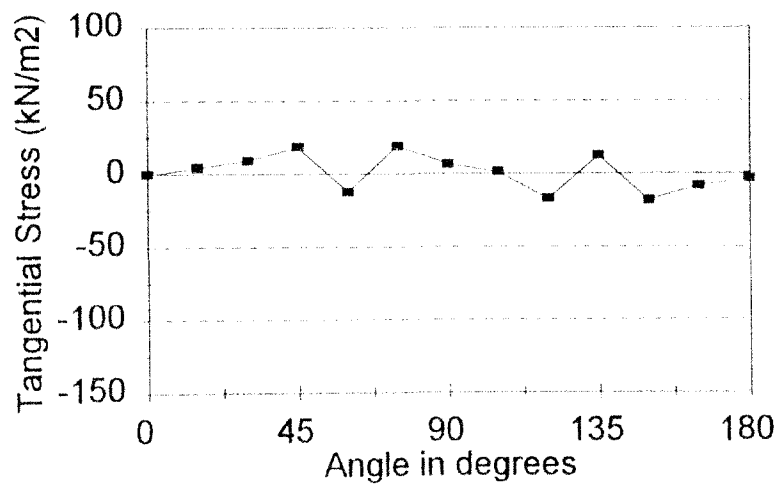


Figure 3.44 Tangential stress distribution at the roller - abrasive interface for head design E (included angle 90°)

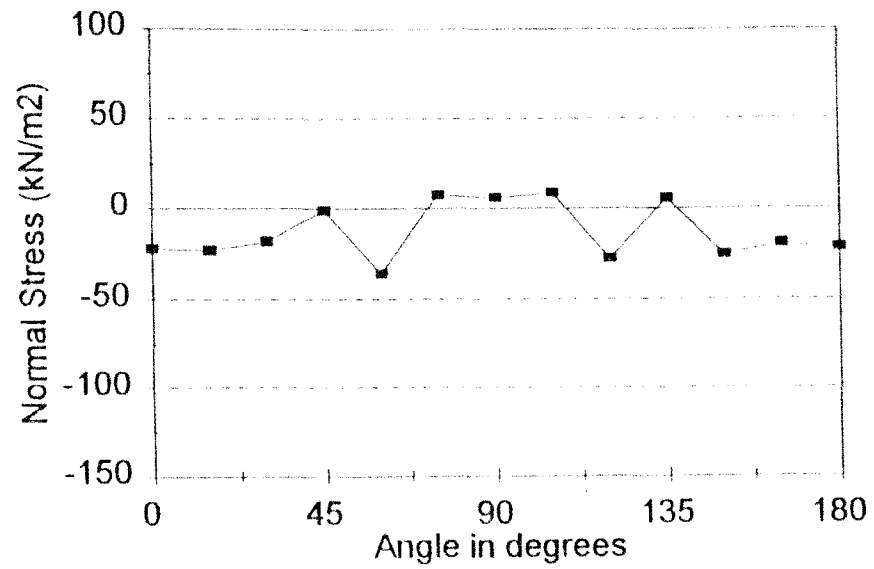


Figure 3.45 Normal stress distribution at the roller - abrasive interface for head design F (included angle 90°)

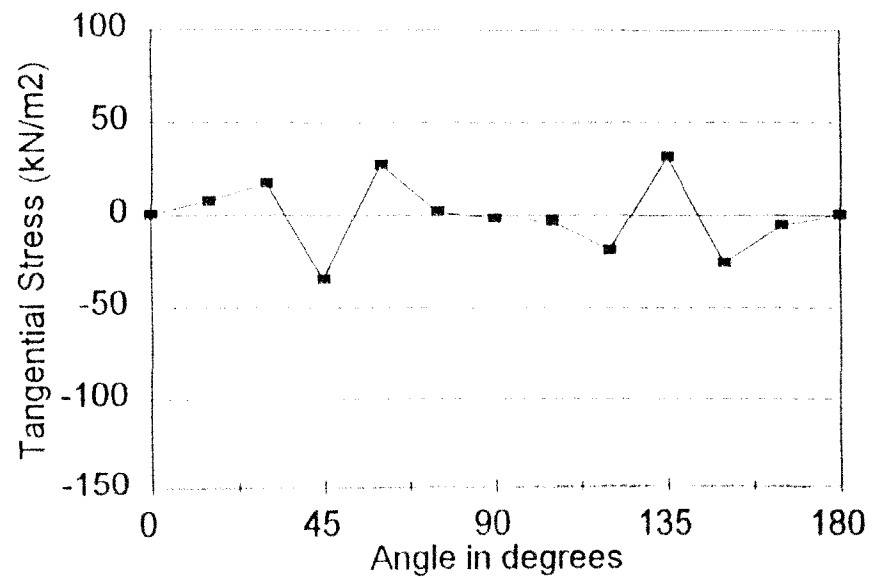


Figure 3.46 Tangential stress distribution at the roller - abrasive interface for head design F (included angle 90°)

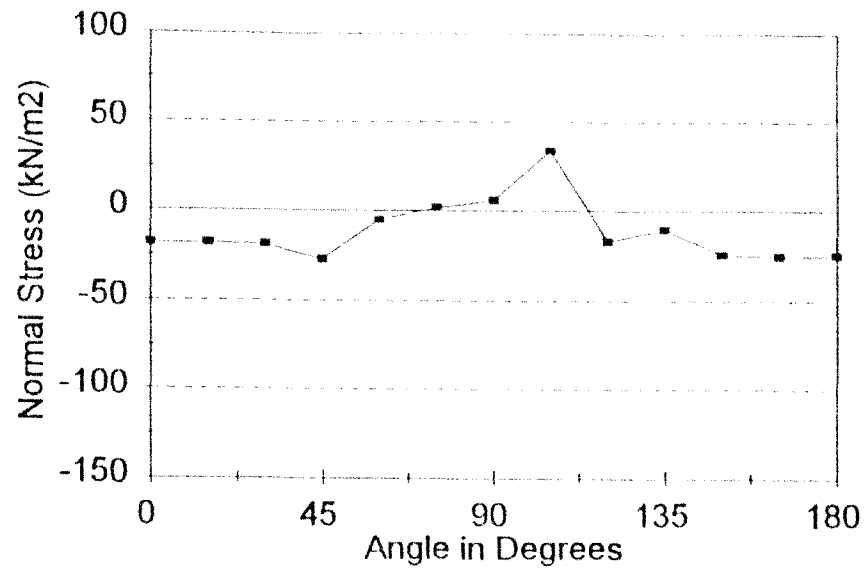


Figure 3.47 Normal stress distribution at the roller - abrasive interface for head design G (included angle 90°)

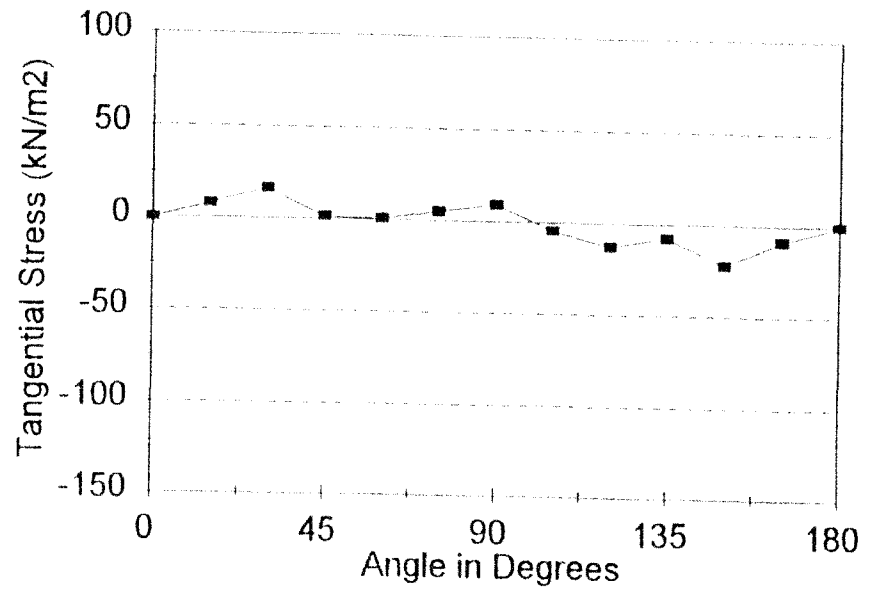


Figure 3.48 Tangential stress distribution at the roller - abrasive interface for head design G (included angle 90°)

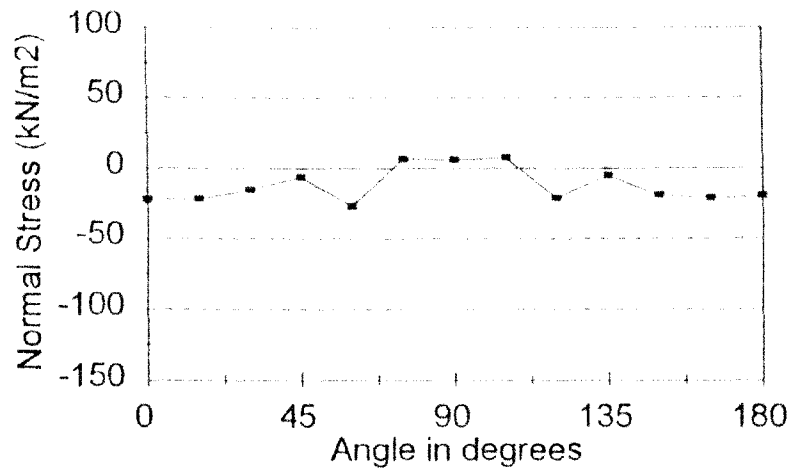


Figure 3.49 Normal stress distribution at the roller - abrasive interface for head design H (included angle 90°)

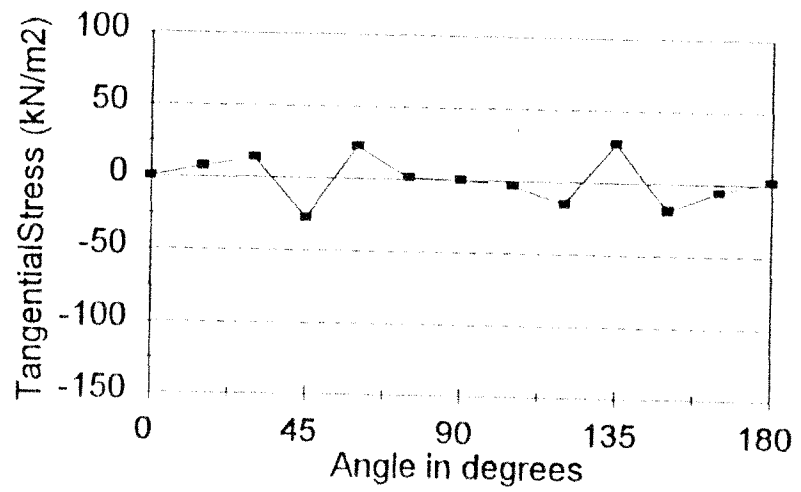


Figure 3.50 Tangential stress distribution at the roller - abrasive interface for head design H (included angle 90°)

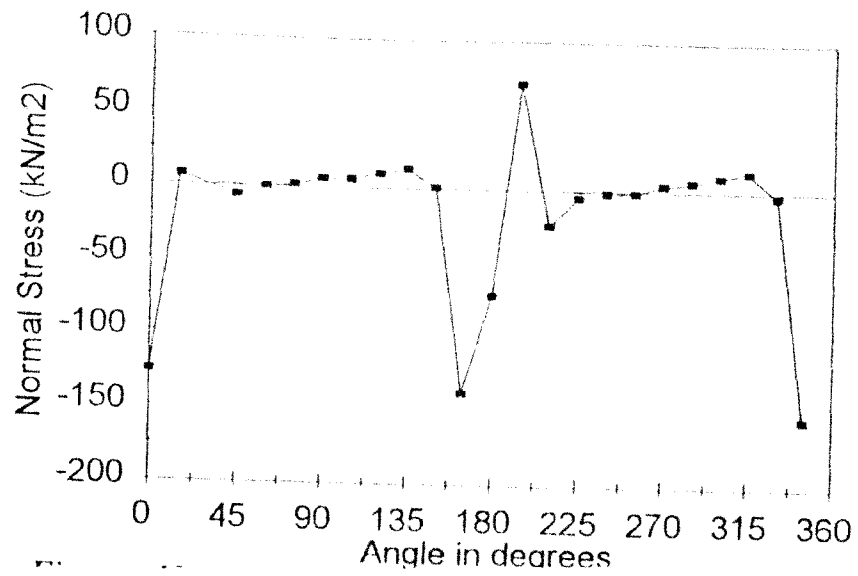


Figure 3.51 Normal stress distribution at the roller - abrasive interface for head design I (included angle)

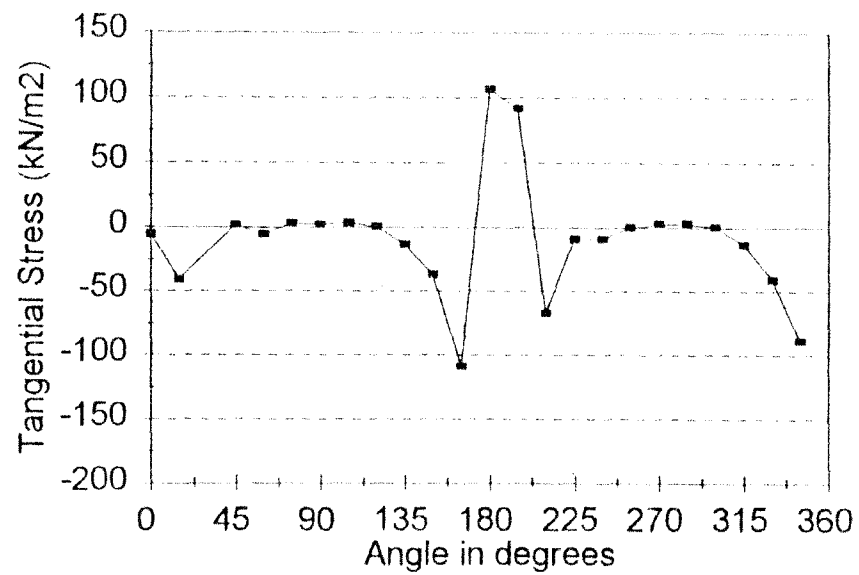


Figure 3.52 Tangential stress distribution at the roller - abrasive interface for head design I (included angle 170°)

Table 2: Summary of results from the FEM analysis of the magnetic abrasive finishing process using various magnetic heads.

Head design	Arc length of the abrasive (mm)	Maximum normal field density (T)	Maximum tangential field density (T)	Maximum total field density (T)	Maximum normal stress (kN/m ²)	Cutting Force (N)
A	4.54	0.18	0.72	1.8	112	33.3
B	20.4	0.22	0.4	0.4	97	51.1
C	20.4	0.35	0.4	0.5	26	20.83
D	34	0.26	0.38	0.46	13	54.8
E	27.2	0.27	0.34	0.36	25	20.29
F	20.4	0.42	0.52	0.6	41	23.88
G	20.4	0.37	0.46	0.51	30	20.31
H	20.4	0.37	0.44	0.54	34	20
I	4.54	0.57	0.92	0.97	154	67.64

from experimental values at low current density. While at higher current density, the experimental value closely match the simulation results.

Effect of different variables involved in the design of magnetic heads

Effect of air slot:

The air slot results in the main cutting action taking place in the region away from the magnetic head, as explained in the previous paragraph. The air slot forces the magnetic flux to converge and flow through the magnetic head. This results in a lower normal magnetic field density in the region of the air slot. However, the magnetic field density is more in the adjacent regions closer to the magnetic heads. In case of head E, the normal field density in the region of the air slot is 0.09 T as compared to 0.38 T in the adjacent regions. However, in the absence of an air slot, as in head C, the magnetic field density is found to be 0.2 T.

Effect of magnetic conducting path:

The longer magnetically conducting path results in lower normal stress and lower tangential field density. The analysis of three different heads A, C and D with varying included angle (160° , 60° , 30°) shows that a maximum tangential magnetic flux density of 0.72 T exists at the corner of head A, as compared to 0.25 and 0.34 T in the cases of head D and C, respectively. Also, the maximum normal stress of 112 KPa is observed in the head A, as compared to 13 and 26 Kpa in case of head D and C, respectively. The reason for this may be the following: The permeability of iron is higher than that of the abrasive. The flux prefers to pass through the shorter and magnetically conducting path in the magnetic head region, as compared to the abrasive region.

Effect of converging shape of the magnetic head:

The converging shape of the magnetic head results in the higher normal field density in the region near the magnetic head. The analysis of head E and head B shows that the normal magnetic flux density (0.27 T) in head E is higher than that in head B (0.22 T). This is due to the fact that the converging shape of the

magnetic head forces the magnetic flux to converge, iron being more magnetically conductive than air.

Effect of the sharpness in the corner of the magnetic head:

A sharp corner in the magnetic head results in higher normal and tangential stresses on the surface of the roller. An analysis of heads E and F shows that in the case of the head E where smooth corner exists, the maximum normal stress is 25 KPa while in the case of head F, it is 41 KPa. This is due to the magnetic flux concentration at the sharp corner of head F.

Wedging effect of the abrasive

A wedging effect in the abrasive finishing can be created by providing a magnetic head such that the air gap with variable width exists between the head and the surface of the roller. This results in an appreciable increase in the finishing action of the abrasives. As the FEM analysis is particularly concerned with generation of magnetic force in the abrasive region, the wedging force could not be investigated.

The FEM analysis of head F shows an improvement in the magnetic flux density and normal stress in the region near the magnetic head as compared to head E. The tangential flux density in head F, with lowest width of air gap, is found to be 0.43 T, as compared to that in head E which is 0.34 T. Also, the maximum normal stress was higher in head F (41 Kpa), compared to head E (25 KPa).

CHAPTER 4

EXPERIMENTAL APPROACH

In MAF process, in order to efficiently generate a smooth finished surface from a rough ground surface, it is necessary to understand and optimize the effect of the process parameters on finishing characteristics. This chapter describes the experimental set up and test conditions used in the investigation. It discusses the studies conducted to analyze the effect of process parameters on finishing characteristics.

4.1 Experimental Apparatus:

Figure 4.1 shows the MAF apparatus mounted on a Hardinge precision lathe. Figure 4.2 is a close-up of the apparatus showing key elements. The specifications of the equipment and test conditions used in the investigation are given in Table 3. An electromagnet is used for the generation of the magnetic field. Current is passed through the copper coil, wound in the form of a solenoid, for generating the magnetic field in the magnetic core. As discussed in Chapter 3, the magnetic heads are so designed that the magnetic field is concentrated and minimum leakage of the field takes place surrounding the air gap between the magnetic heads. A pneumatic air vibrator is used to supply the vibratory motion to the magnetic head. A nonmagnetic stainless steel roller is clamped to the chuck of the lathe to provide the rotary motion. The lathe can be operated upto about 3000 rpm. Above this speed, the performance of the lathe becomes unsteady.

Magnetic Abrasives:

In the MAF process, the magnetic abrasive agglomerate is used where the finishing pressure is exerted by the magnetic field. Figure 4.3 shows a SEM micrograph of the magnetic abrasive used which consists of iron particles with grain size 80-400 μm with finer aluminium oxide abrasive particles (grain size 1-10 μm) embedded on it. A working clearance of roughly 5 times the abrasive

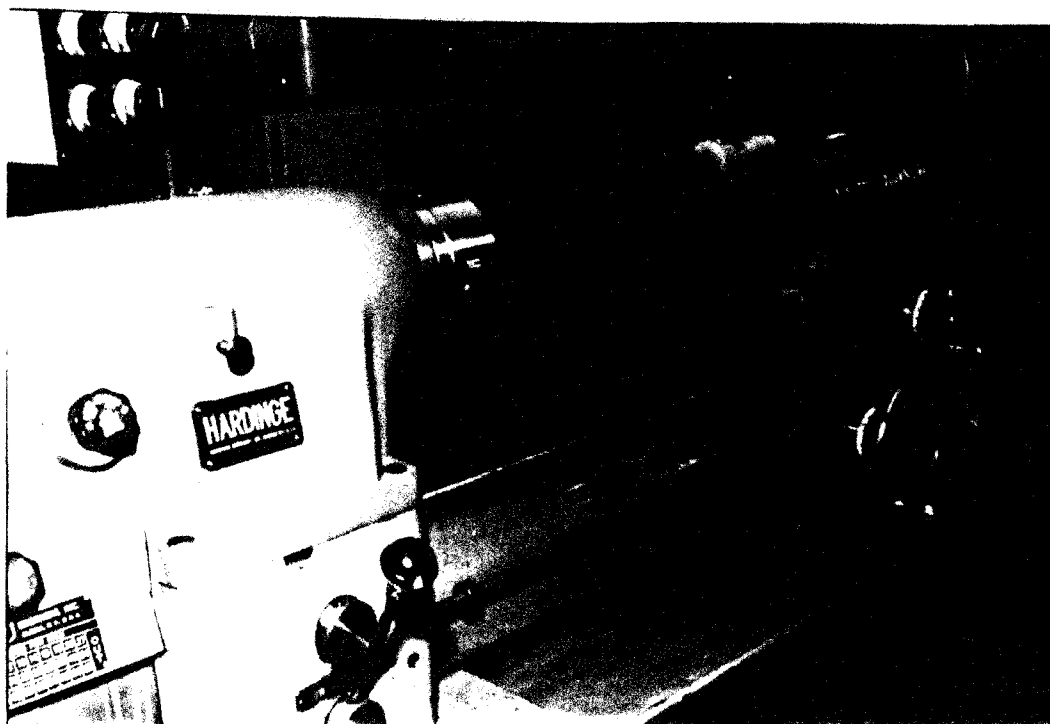


Figure 4.1 Photograph of the magnetic abrasive finishing apparatus used for polishing of rollers.

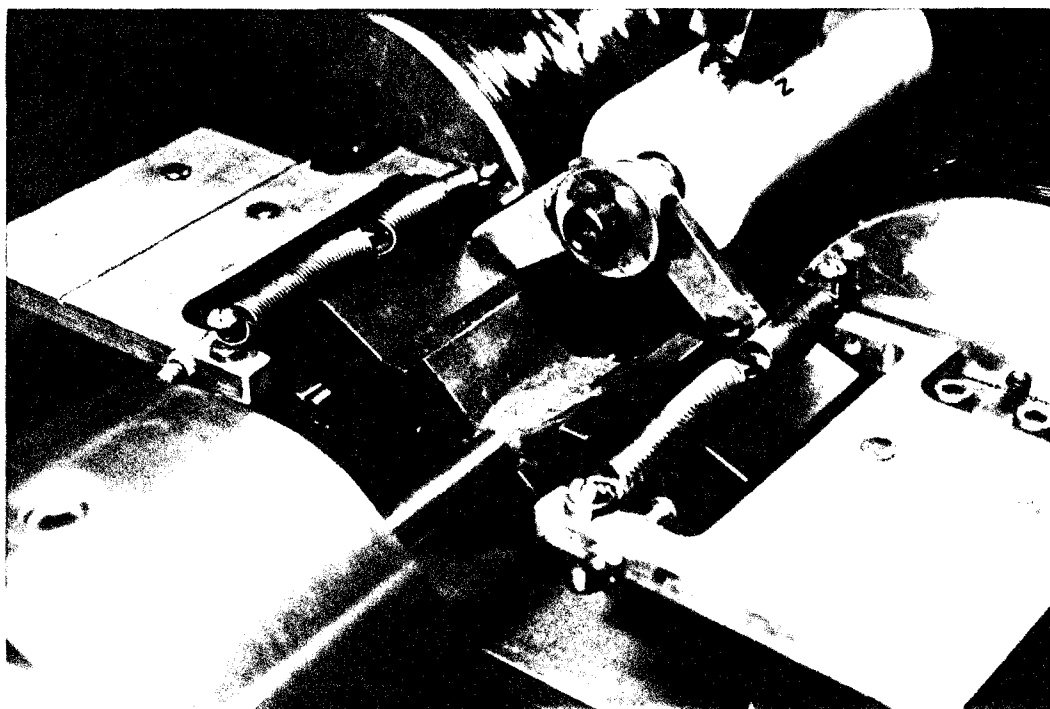


Figure 4.2 Close-up of the magnetic abrasive finishing apparatus showing roller, flexible magnetic abrasive brush, magnetic poles

Table 3: Specifications of the Magnetic Abrasive Finishing equipment (MAF) and test conditions used in the investigation

Workpiece material	Non-magnetic stainless steel rods
Workpiece size	13 cm long , 5-15 mm diameter cylindrical roller with length of polishing 45 mm/batch
Surface speed of the roller	500, 1000, 2000, 3000 rpm (corresponding to 0.32, 0.65, 1.3, and 1.92 m/s)
Current through the coil	0.5, 1, 2A
Magnetic field density	0.1-0.4 T
Magnetic pressure	10-40 Kpa
Vibrational frequency of the magnetic heads	15 - 25 Hz
Magnetic core	0.16% carbon steel
Magnetic abrasives	Al ₂ O ₃ abrasives of size 5-10 μ m bonded on the iron particles of size 100-400 μ m. Abrasives : KMX80, M5, 400/5 μ m, SiC
Lubricant	Oil, Zinc Stearate

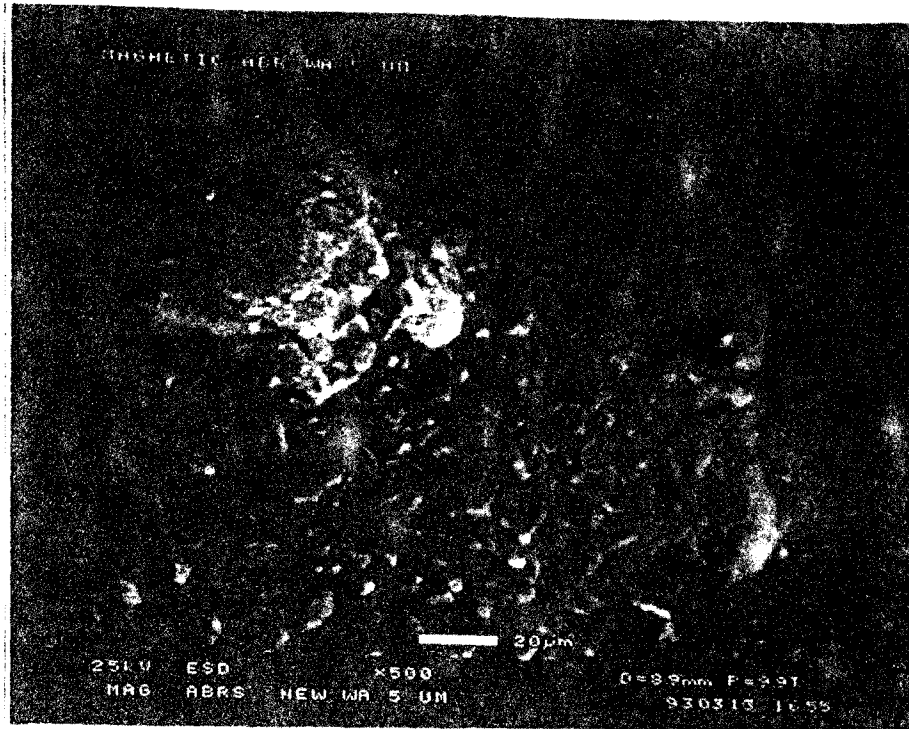


Figure 4.3a SEM micrograph of magnetic abrasive (400/5 μm)

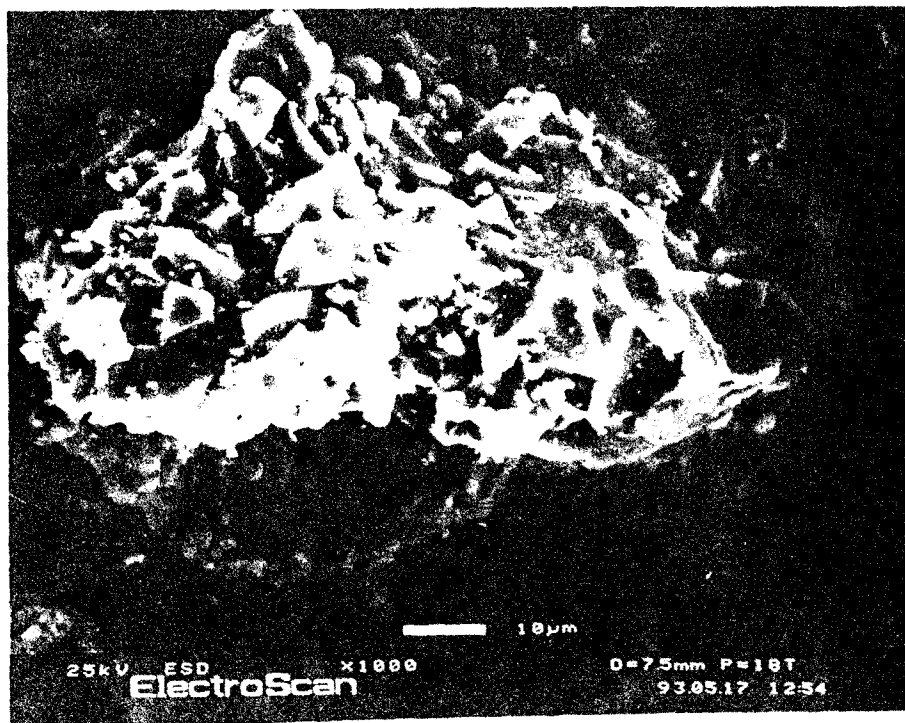


Figure 4.3b SEM micrograph of magnetic abrasive (KMX 80)

particle size is provided between the work surface and the magnetic pole. These magnetic abrasives we obtained were made as follows: pure iron powder and aluminium oxide powder with grain size 5 μm were mixed with a weight ratio of 4:1 and sintered under high temperature conditions (about 1600K), high pressure (5 MPa) and in an inert gas atmosphere. After that the sintered material was crushed mechanically and controlled to a specific particle sizes by screening.

4.2 Experimental Procedure:

The cylindrical roller to be polished is held in the chuck of the lathe. Current is passed through the copper coil wound in the form of a solenoid to generate the magnetic field. The magnetic field generated within the magnetic core passes through the magnetic head gap between the N and S poles. Magnetic abrasive is introduced in the head gap. Due to the presence of the field, the abrasives get aligned in the direction of the field forming a flexible magnetic abrasive brush. The magnetic head gap controls the resistance met by the magnetic flux, to flow across the abrasive region between the magnetic heads. If the magnetically conducting path is longer, then the corresponding drop in the magnetic flux intensity is expected to be large, resulting in low density in the abrasive region. The magnetic head gap is fixed to be 5 times the abrasive size used in the experiment. The roller is given rotary motion by rotating the chuck of the lathe at the desired speed. It is then introduced in to the magnetic field by moving the magnetic heads relative to the rotating workpiece. A small clearance between the magnetic head and chuck of the lathe is necessary to avoid accidental collision. The length of the magnetic head used is 45 mm. Hence, only 45 mm length of the workpiece can be polished at a time. The vibratory motion is provided to the magnetic head with the help of an air pneumatic vibrator. The surface finishing operation is carried out by the flexible magnetic abrasive brush.

The magnetic abrasive is stirred at an interval of one minute to achieve uniform distribution of the abrasives. The workpiece is taken out at regular intervals for surface characterization using Talysurf and Talyrond.

4.3 Characterization Equipment

An Environmental Scanning Electron Microscope (ESEM) is used for the characterization of the magnetic abrasives used in the apparatus. The finishing efficiency of the process is very much influenced by the size and shape of the abrasives used.

Form Talysurf and Talyrond 250 are used for the characterization of the polished surfaces. The surface characterization procedure, using the above equipments, is explained in detail in the Appendix A.

4.4 Results and Discussion

Figure 4.4a shows the Talysurf traces of the as-received, ground stainless steel rod and the same rod finished by magnetic field assisted polishing. The roughness of the ground surface (R_a) is about $0.2198\text{ }\mu\text{m}$ (220 nm) while that of the polished surface is about 7.6 nm. Figure 4.4b shows the photograph of the as-received, ground stainless steel rod and the same rod finished by magnetic field assisted polishing showing a mirror finished surface.

4.4.1 Finishing of nonmagnetic stainless steel rollers

The nonmagnetic stainless steel rollers were polished under various polishing conditions. The following variables are studied:

- 1 Time duration of finishing process
- 2 Abrasive size
- 3 Lubricant
- 4 Source current density
- 5 Workpiece rotational speed
- 6 Combined effect of rotational speed and axial vibration

These are discussed briefly in the following:

4.4.1.1 Time duration of finishing process:

The finished surface is characterized using Talysurf and Talyrond at time intervals of 1/2, 1, 2, 3, 5 and 10 minutes. Figure 4.5 shows the Talysurf traces of

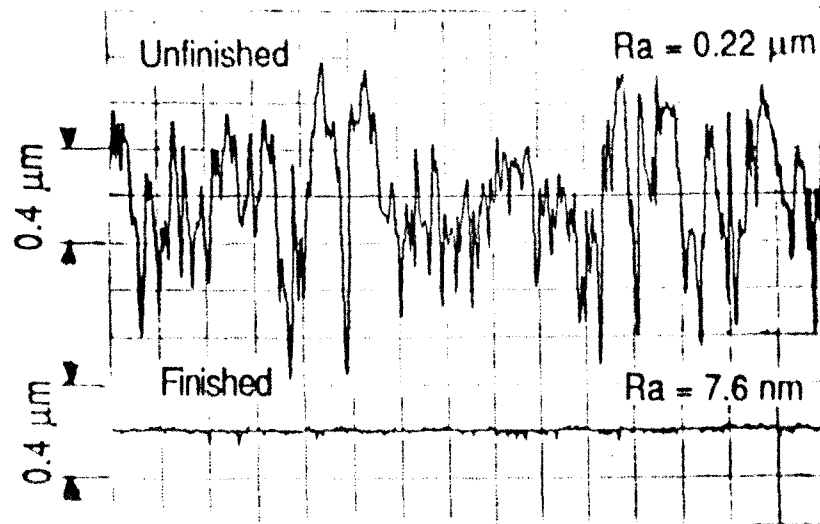


Figure 4.4a Talysurf traces of the as-received, ground stainless steel rod and the same finished by magnetic filed assisted polishing. surfaces showing improvement in the finish between the ground and polished surfaces.

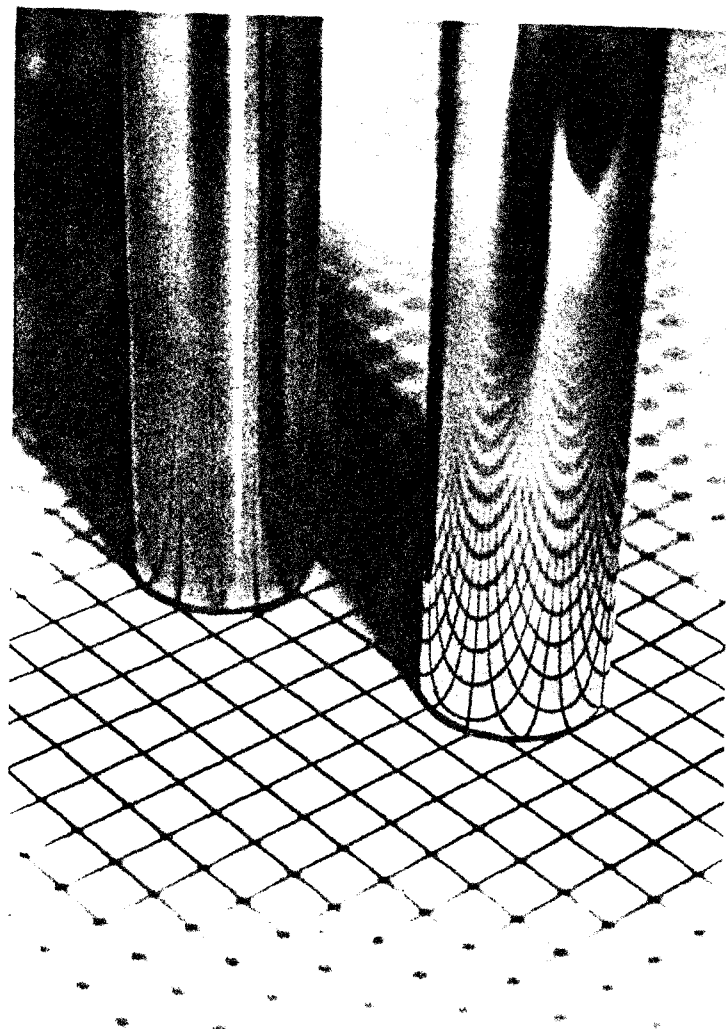


Figure 4.4b Photograph of the as-received, ground stainless steel rod and the same finished by magnetic field assisted polishing

the stainless steel roller depicting the surface finish obtained in the MAF process, with the time of polishing. It is observed that the improvement in surface finish decreases as duration of polishing increases. Also, the removal rate decreases with the duration of the process. The as received, ground surface of the stainless steel rod consists of valleys and peaks, the maximum height/depth of which are depicted by the values R_p and R_v shown on the talysurf traces in Figure 4.5(a). During MAF, initially the rounding of the peaks on the surface of the roller takes place, which is a very fast process. Subsequently, magnetic abrasives cut these round peaks during polishing. However, to remove the valleys on the surface, the material removal has to be significant enough for the abrasives to reach the bottom most level.

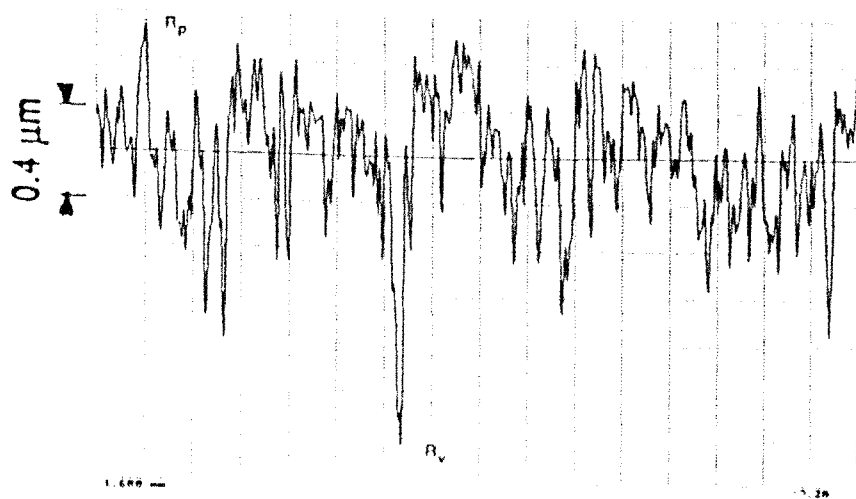
Figure 4.6 shows the effect of duration of polishing on the surface roundness. It is observed that surface roundness improves during finishing upto a certain extent, beyond which it saturates.

4.4.1.2 Abrasive size:

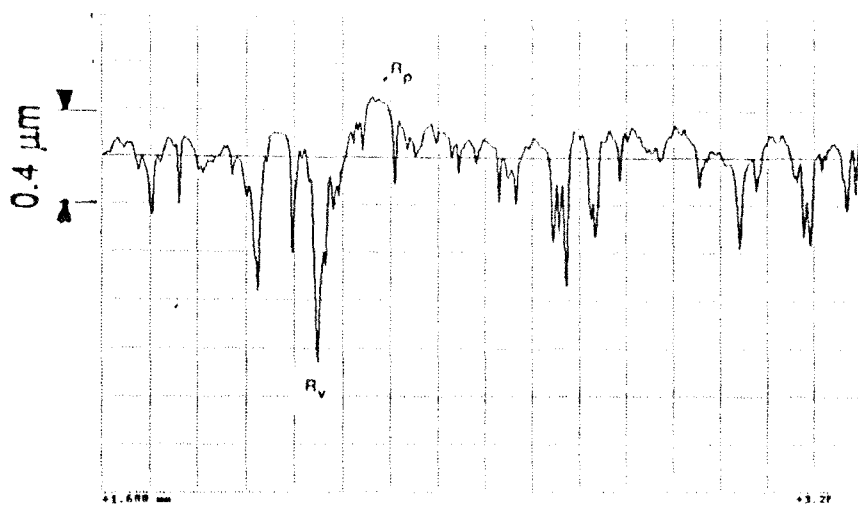
The abrasives used in the present investigations are KMX80 and 400/5 μm abrasives. It is observed that surface finish is better with 400/5 μm abrasive than that to KMX80 (Fig. 4.7).

4.4.1.3 Lubricant:

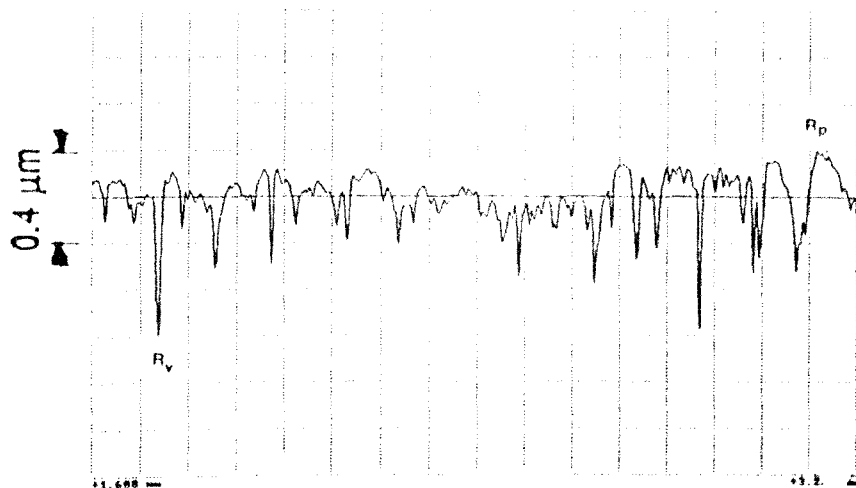
Zinc Stearate is used as a solid lubricant to enhance the surface finishing efficiency of the process. The lubricant makes the abrasive brush more flexible and enhances its ability to produce a better finish. Figure 4.8 shows the surface finish that can be achieved on nonmagnetic stainless steel roller at the end of 10 minutes, with different amounts of lubricant. It appears that increasing the zinc stearate content, up to about 5 wt %, gives a better surface finish in a shorter time beyond which the finishing efficiency decreases. This may be attributed to the excessive flexibility in the abrasive brush beyond a certain wt % of the lubricant, which prevents the abrasives from cutting against the surface of the roller.



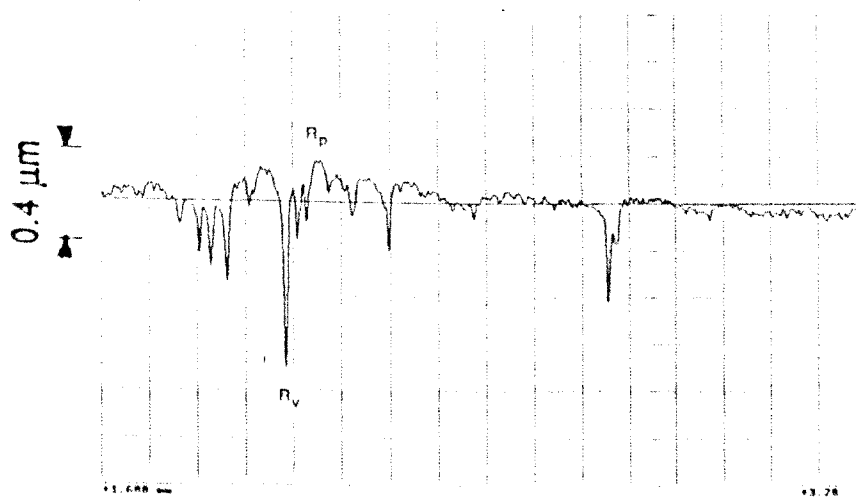
(a) Time = 0 minute $R_a = 0.21 \mu\text{m}$ $R_p = 0.54 \mu\text{m}$ $R_v = 1.3 \mu\text{m}$



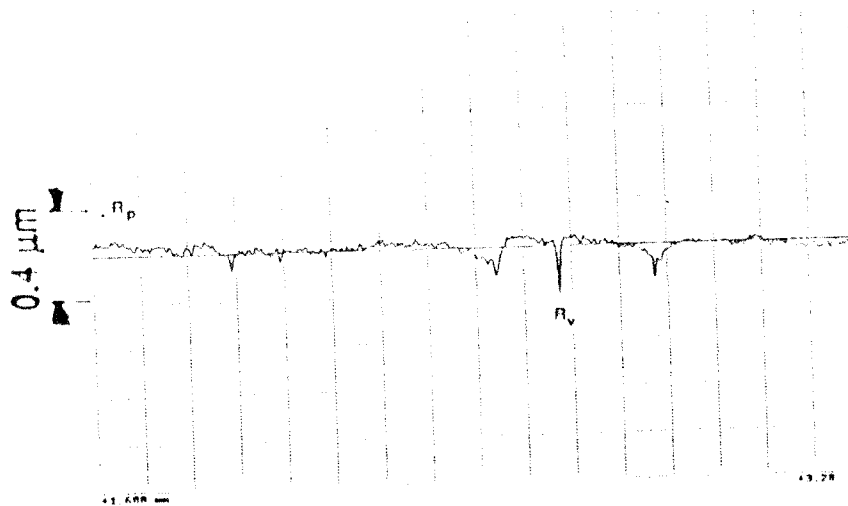
(b) Time = 1/2 minute $R_a = 0.096 \mu\text{m}$ $R_p = 0.257 \mu\text{m}$ $R_v = 0.863 \mu\text{m}$



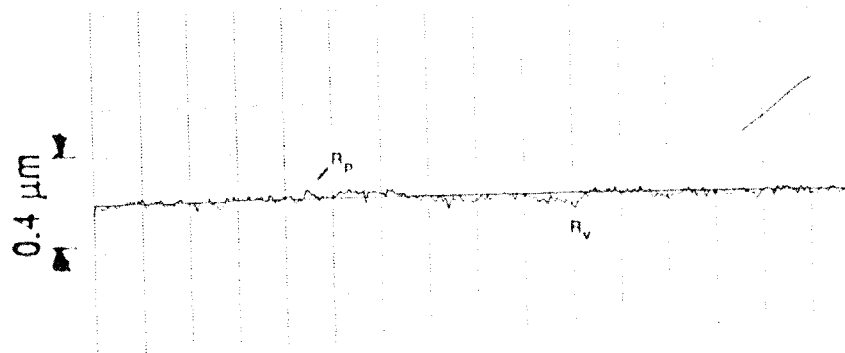
(c) Time = 1 minute $R_a = 0.078 \mu\text{m}$ $R_p = 0.201 \mu\text{m}$ $R_v = 0.59 \mu\text{m}$



(d) Time = 2 minute $R_a = 0.05 \mu\text{m}$ $R_p = 0.1774 \mu\text{m}$ $R_v = 0.702 \mu\text{m}$

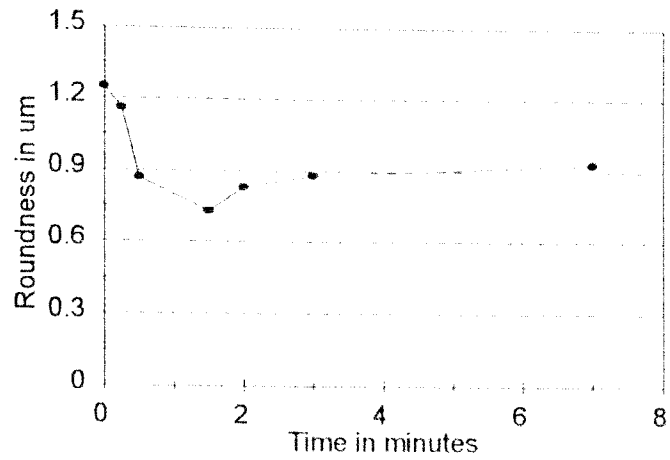


(e) Time = 3 minute $R_a = 0.022 \mu\text{m}$ $R_p = 0.07 \mu\text{m}$ $R_v = 0.199 \mu\text{m}$



(f) Time = 5 minute $R_a = 0.012 \mu\text{m}$ $R_p = 0.037 \mu\text{m}$ $R_v = 0.068 \mu\text{m}$

Figure 4.5 Figures showing the Talysurf traces of the stainless steel roller depicting the surface finish obtained in the magnetic abrasive finishing process at varying polishing time (a) 0 minute (b) 1/2 minute (c) 1 minute (d) 2 minute (e) 3 minute (f) 5 minute



Testing Conditions:

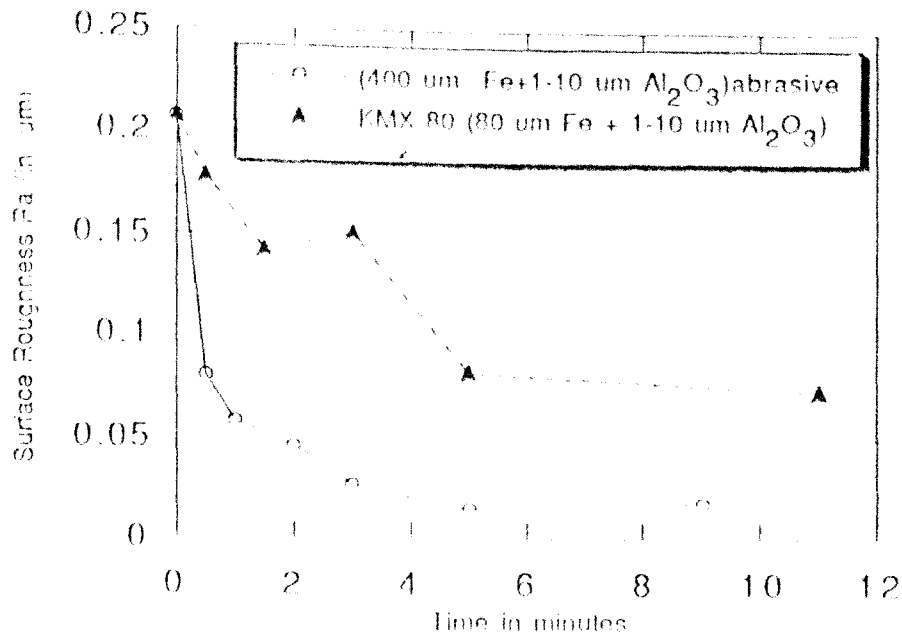
Surface Speed: 1.3 m/s

Lubricant: Zinc Stearate (8wt%)

Flux Density: 0.37 T

Abrasive: KMX80

Figure 4.6 Variation of surface roundness (O) with finishing time



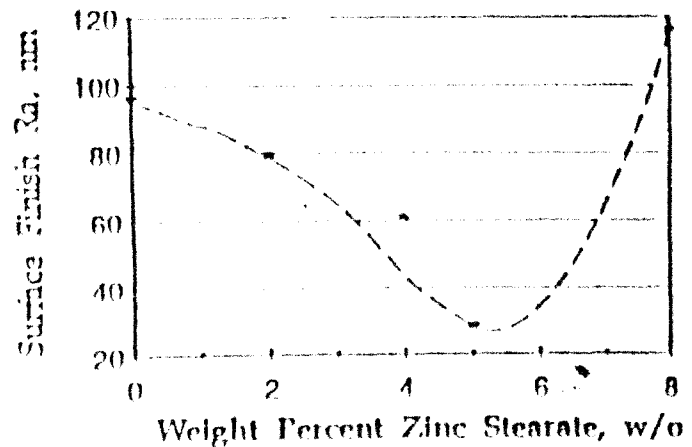
Testing Conditions:

Surface Speed: 1.3 m/s

Lubricant: Zinc Stearate (8wt%)

Flux Density: 0.37 T

Figure 4.7 Variation of the surface finish (Ra) with finishing time for KMX80 and 400/5 μm abrasives



Testing Conditions:

Surface Speed: 1.3 m/s

Abrasive: KMX80

Flux Density: 0.37 T

Figure 4.8 Variation of surface finish (Ra) with 0 w/o, 2W/o, 5 w/o and 8 w/o of zinc stearate.

4.4.1.4 Source current density:

The source current density plays an important role in generating the magnetic field between the magnetic poles which in turn controls the magnetic force exerted by the abrasives on the rollers. Figure 4.9 shows the variations of magnetic field density within the magnetic abrasives with source current in the copper coil. A higher tangential magnetic flux density in the magnetic head results in stiffer magnetic brushes. By controlling the source current density, both surface removal and surface finish can be controlled. A set of experiments was conducted with KMX80 abrasives. The source currents used were 1A and 2A corresponding to the magnetic flux density of 0.25T and 0.37T. Figure 4.10 shows the variation in surface finish obtained with different magnetic field densities in the abrasive region. Higher magnetic flux density (0.37T) resulted in better surface finish (R_a 73 nm), as compared to a lower magnetic flux density (0.25T).

4.4.1.5 Workpiece rotational speed:

The workpiece rotational speeds used in the experiment are 1000, 2000 and 3000. This corresponds to surface speeds of the workpiece of 0.68, 1.34 and 1.68 m/s respectively. Increase in the rotational speed of the workpiece resulted in better surface finish with lesser time. This could be due to the increased finishing distance with time. At a rpm of 3000, the surface finish obtained was 39 nm (Figure 4.11).

4.4.1.6 Combined effect of rotational speed and axial vibration:

The surface finish and material removal rate, obtained in the magnetic abrasive finishing process, depend on the workpiece rotational speed and the axial vibration of the magnetic heads. If the workpiece is rotated, keeping the magnetic heads stationary, circumferential grooves will be formed on the surface of the roller. By introducing axial vibration, the relative velocity of the magnetic abrasive with respect to the surface of the roller can be changed. This results in cross hatched patterns. By varying the rotational speed and the axial vibration, the direction of the cross hatched patterns can be changed.

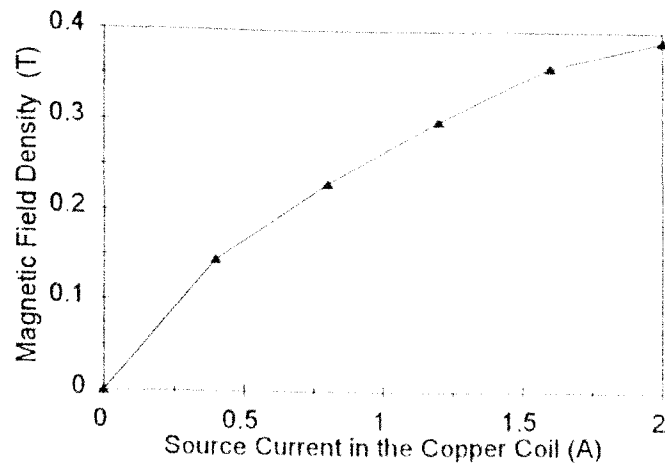
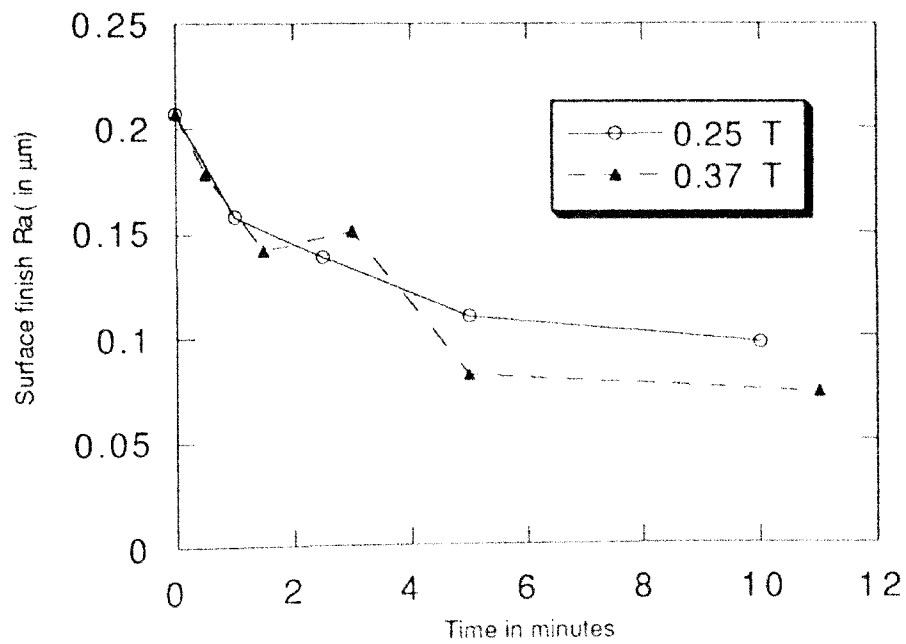


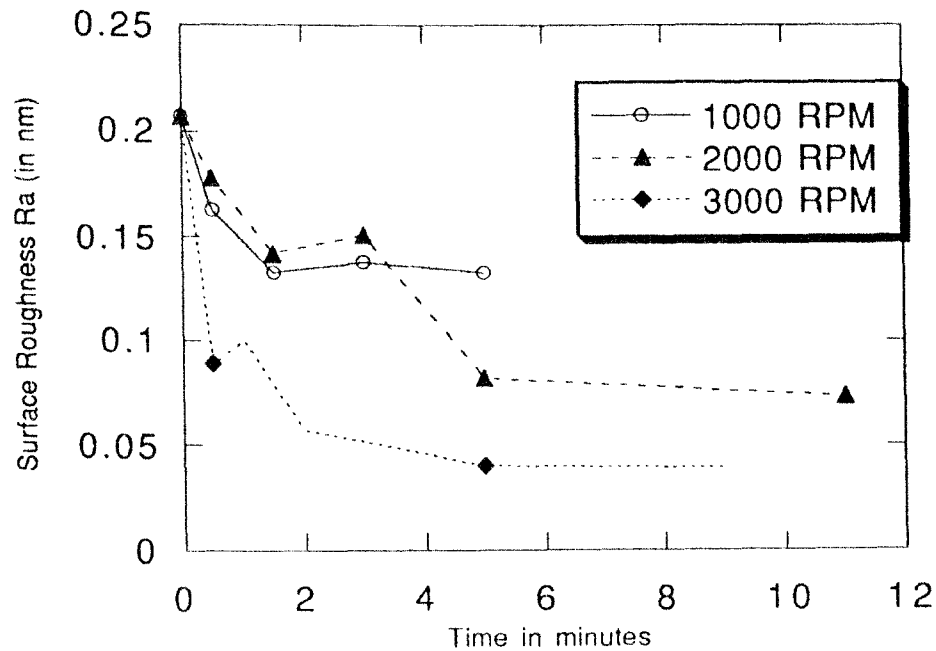
Figure 4.9 Variation in the magnetic field density within the magnetic abrasives with the source current density in the copper coil



Testing Conditions:
 Surface Speed: 1.3 m/s
 Abrasive: KMX80

Lubricant: Zinc Stearate (8wt%)

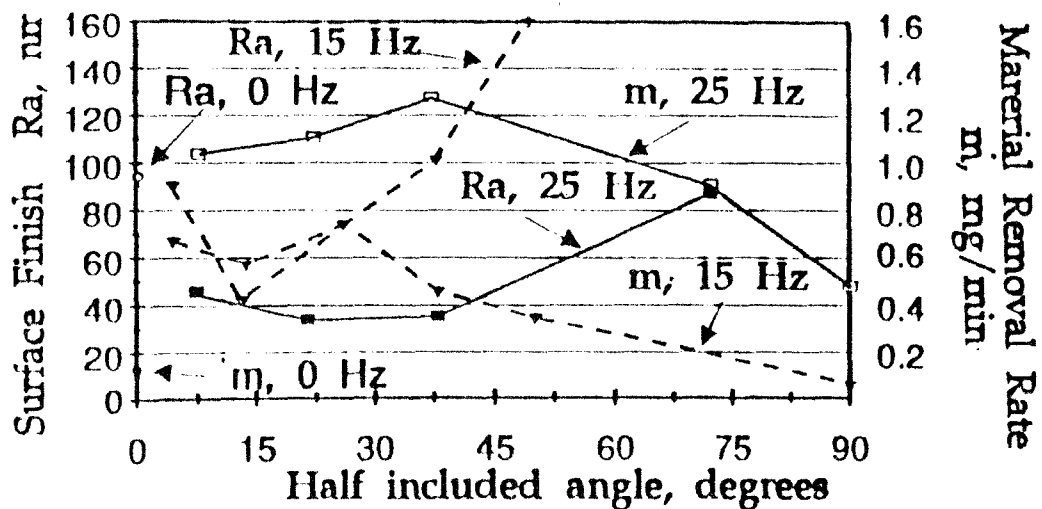
Figure 4.10 Variation of surface finish (Ra) with finishing time for various magnetic flux densities.



Testing Conditions:
 Abrasive: KMX80
 Flux Density: 0.37 T

Lubricant: Zinc Stearate (8wt%)

Figure 4.11 Variation of surface finish (Ra) with finishing time for various rotational speed of the workpiece



Test Conditions:

Surface Speed: 1.3 m/sec
 Flux Density: 0.37 T

Abrasive: 80 w% Fe (40#) + 20 w% M5
 Lubricant: 3 w% Zinc stearate

Figure 4.12 Variation of removal rate and surface finish after finishing for 5 min. with half included angle.

The vibration of the magnetic head is assumed to be sinusoidal. Hence the vibrational velocity of the magnetic head is given by,

$$V_{\text{vib}} = a \omega \cos(\omega t)$$

where,

a is the half the amplitude of the vibration of the magnetic head

ω ($2 \pi f$) is the angular velocity of vibration

f is the frequency of vibration

The rotational speed of the surface of the roller is given by

$$V_{\text{rot}} = \pi d N/60$$

where,

d is the diameter of the roller

N is rotational speed (rpm)

The half included angle of the cross hatched pattern is given by,

$$\begin{aligned} \theta &= \tan^{-1} \left(\frac{(V_{\text{vib}})_{\text{max}}}{V_{\text{rot}}} \right) \\ &= \tan^{-1} \left(\frac{120 a f}{d N} \right) \end{aligned}$$

The effect of half included angle on the variation of material removal rate and surface finish is shown in Figure 4.12. It is observed that a better surface finish and material removal rate can be achieved with a high frequency of vibration (25Hz) at a given half included angle. Also, it appears that best surface finish and maximum material removal rate occur at half included angle between 25° to 35° .

4.4.2 Polishing of Si_3N_4 rollers using different head designs:

Using the process principles developed for nonmagnetic stainless steel roller by experimental and analytical methods, the polishing of Si_3N_4 rollers were investigated next. The typical test conditions used for the polishing of Si_3N_4 rollers is described in Table 4.

Table 4: The specifications of the Magnetic Abrasive Finishing equipment and test conditions used for polishing Si₃N₄ rollers

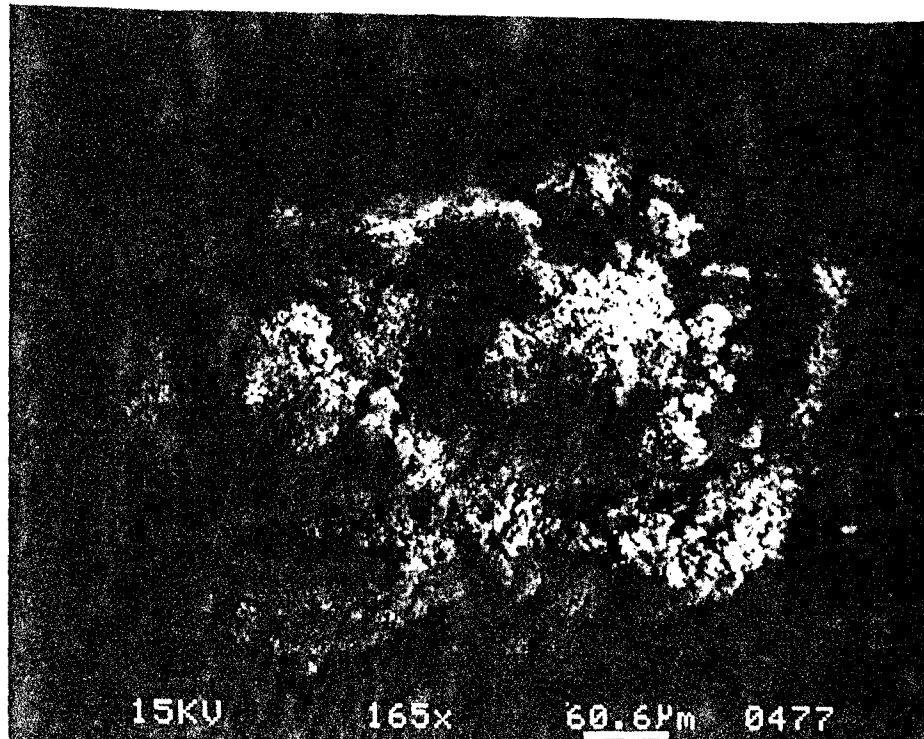
Workpiece material	Si ₃ N ₄ rollers
Workpiece size	20 mm long , 13 mm diameter cylindrical roller
Surface speed of the roller	500, 1000, 2000, 2500 rpm (corresponding to 0.32, 0.65, 1.3, and 1.62 m/s)
Current through the coil	2A
Magnetic field density	0.26 - 0.4 T
Magnetic pressure	10-40 Kpa
Vibrational frequency of the magnetic heads	25 Hz
Magnetic core	0.16% carbon steel
Magnetic abrasives	Cr ₂ O ₃ abrasives of size 4 μm mixed with the iron particles (40#).
Lubricant	nil

4.4.2.1 Magnetic abrasives:

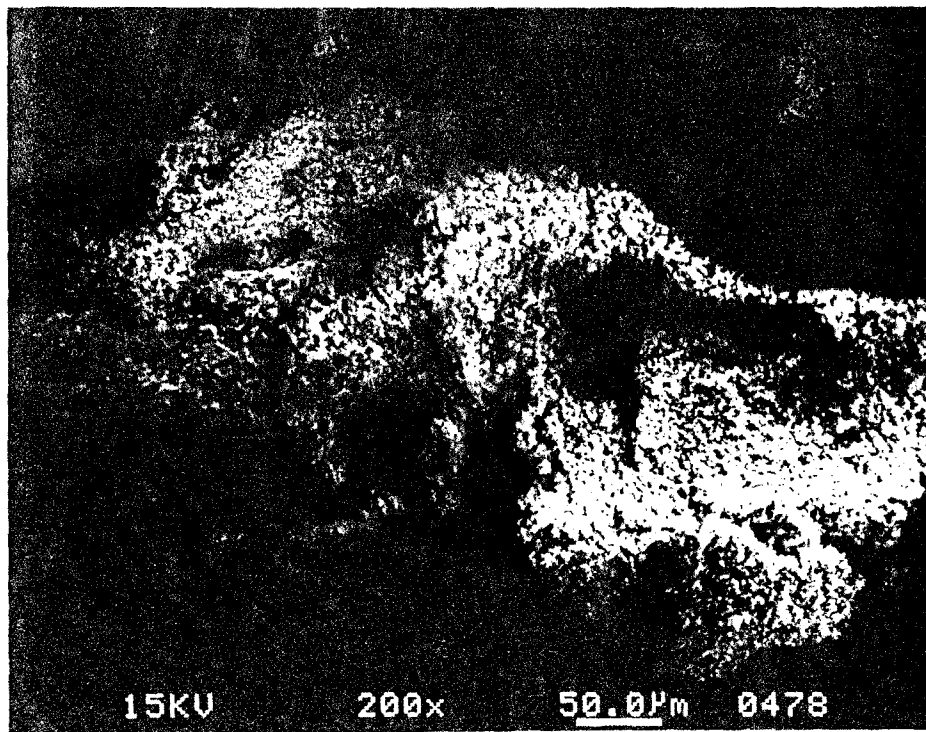
The magnetic abrasive used in these experiments is of an unbonded type. Fe powder (40#) and Cr_2O_3 abrasive ($4\text{ }\mu\text{m}$) were mixed 3:1 by weight. Methanol was added to the mixture and the resulting mixture was stirred well for an hour, in a rotating container mounted on a lathe at 125 rpm. Methanol appeared to enhance the bonding between the loose Cr_2O_3 abrasive and Fe particles. Figure 4.13 shows the SEM micrographs of unbonded abrasives thus prepared, before using them for polishing. From the micrograph it is clear that the abrasive particles uniformly coated the surface of the Fe particles. Figure 4.14 shows the SEM micrographs of unbonded abrasives after it is used for 1 hour for polishing of Si_3N_4 rollers. The Fe surface appears to be depleted of the abrasive concentration, thus diminishing the cutting action of the magnetic abrasives and rendering it ineffective. Therefore, during the polishing experiment it is advisable that the magnetic abrasives be changed periodically. The abrasive particles appeared to be rounded off, indicating the presence of the rolling motion between the abrasive and the Fe particles, and also between the abrasive and the workpiece. The sharp edges of the abrasive particles take part actively in the finishing action. However, as the particles are rounded they are rendered ineffective after a period of time.

4.4.2.2 Polishing of Si_3N_4 rollers with different magnetic head designs:

Experiments were conducted with different magnetic head designs to examine the effect of the included angle of the magnetic head, and the rotational velocity of the workpiece, on the surface finish and the material removal rate obtained. Figures 4.15-4.17 show the effect of rotational velocity on the material removal rate in the case of different head designs. From Figures 4.15-4.17 it is clear that at low rpm, namely 500 and 1000, the material removal attains saturation after polishing for 30-45 minutes. However, at higher rotational speed of the workpiece (2000-2500 rpm), the material removal shows a different behavior. In case of head designs D and J with included angles of 30° , and 150° respectively, the material removal rate appears to increase continuously at higher rotational velocity of the workpiece (2500 RPM). In the case of head design C, the material removal appears to be negative after prolonged polishing for an hour with the formation of scale on the surface of the roller.

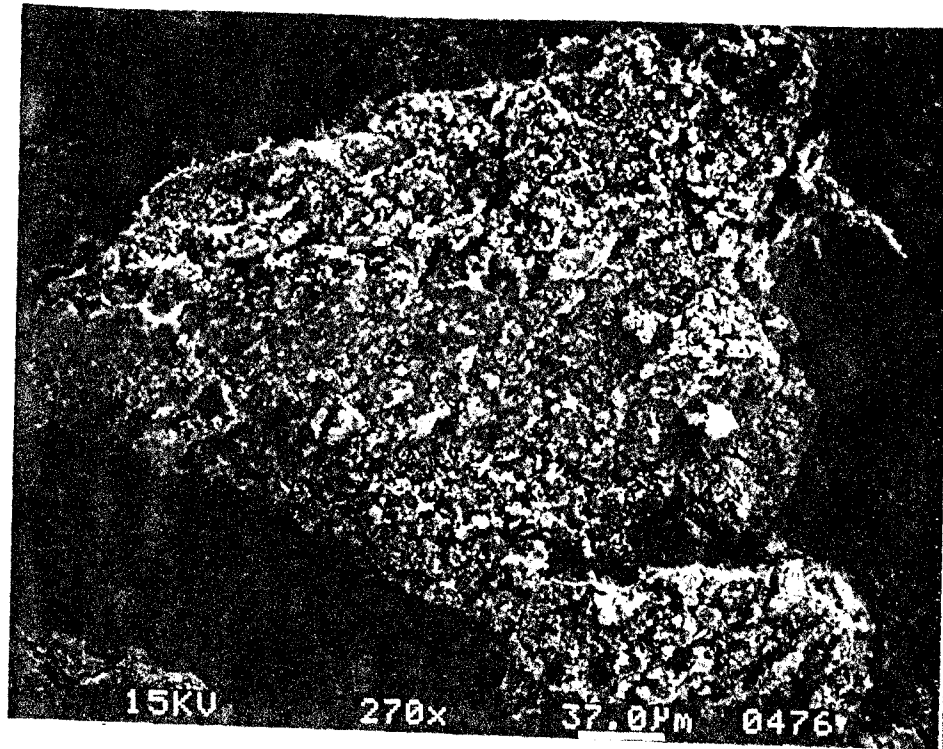


(a)

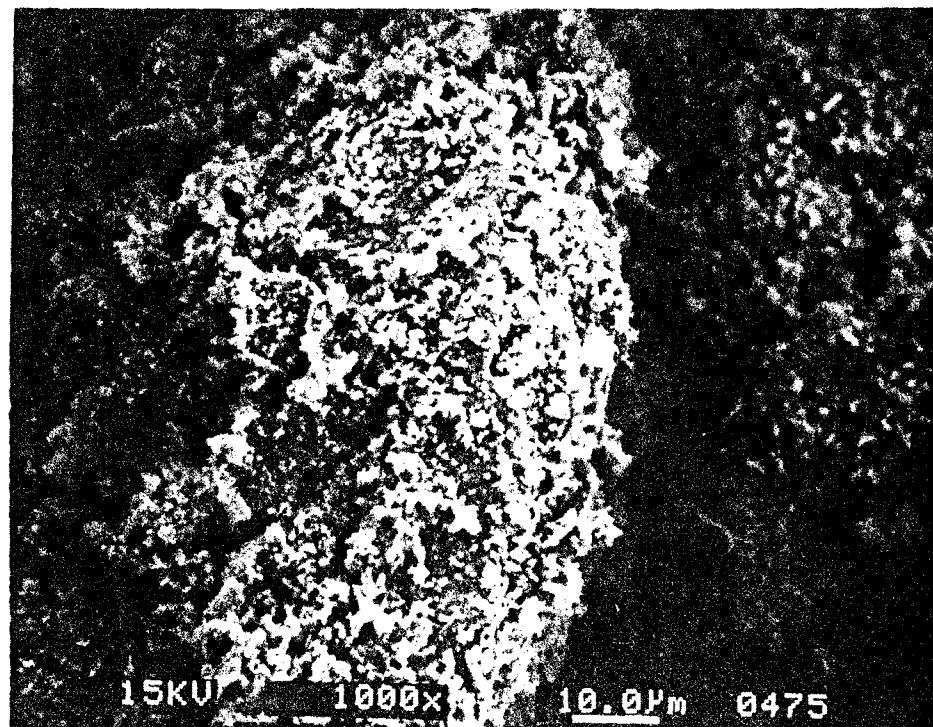


(b)

Figure 4.13 SEM micrograph of unused magnetic abrasives (Fe (40#, 75%) + Cr_2O_3 (4µm, 25%)) at 200X, and 165X magnifications



(a)



(b)

Figure 4.14 SEM micrograph of used magnetic abrasives (Fe (40#, 75%) + Cr_2O_3 (4 μm , 25%)) at 270X, and 1000X magnifications

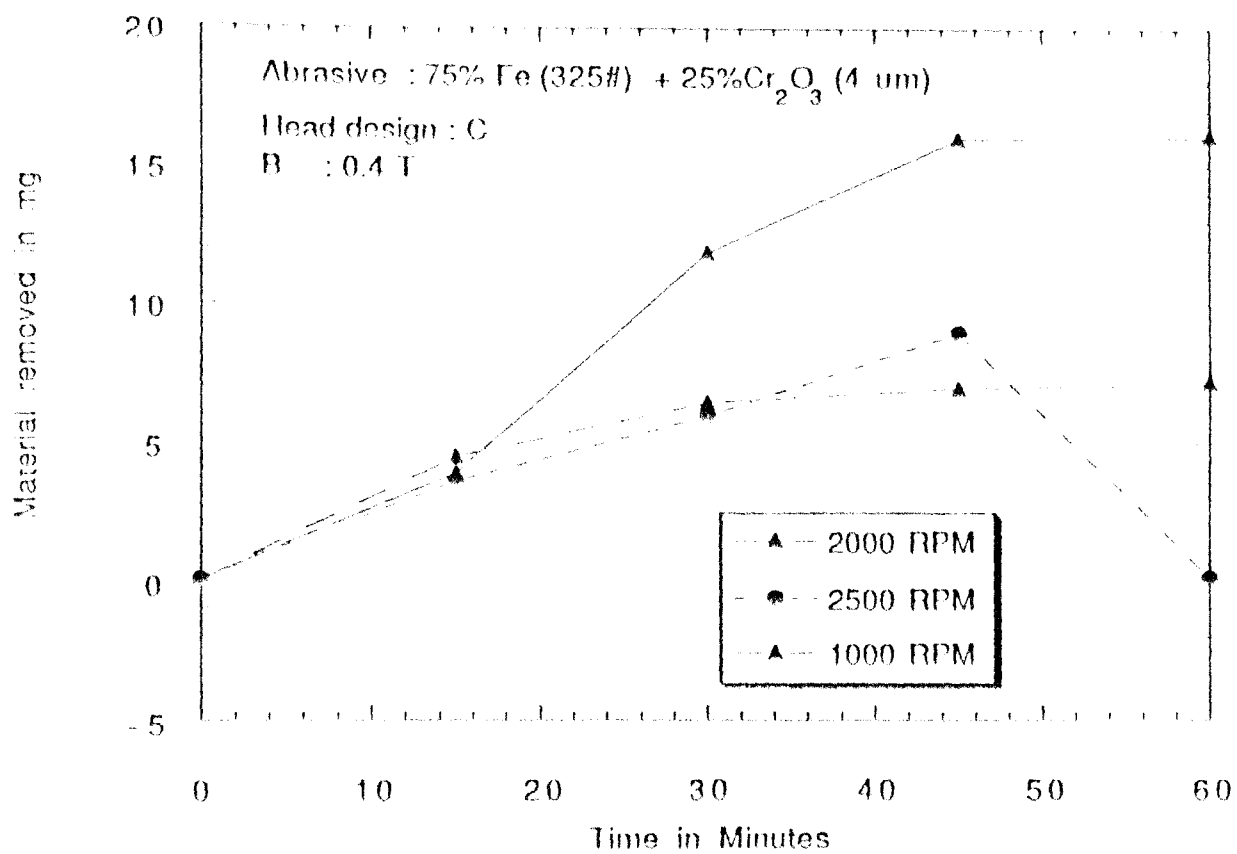


Figure 4.15 Effect of revolution speed of the workpiece on the material removal rate for head design C with included angle of 90°.

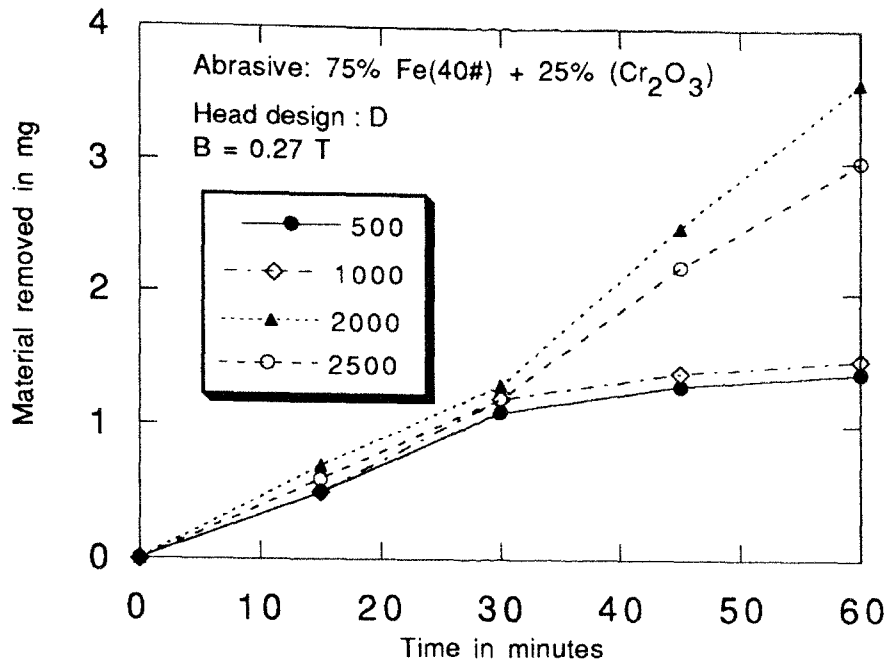


Figure 4.16 Effect of revolution speed of the workpiece on the material removal rate for head design D with included angle of 30° .

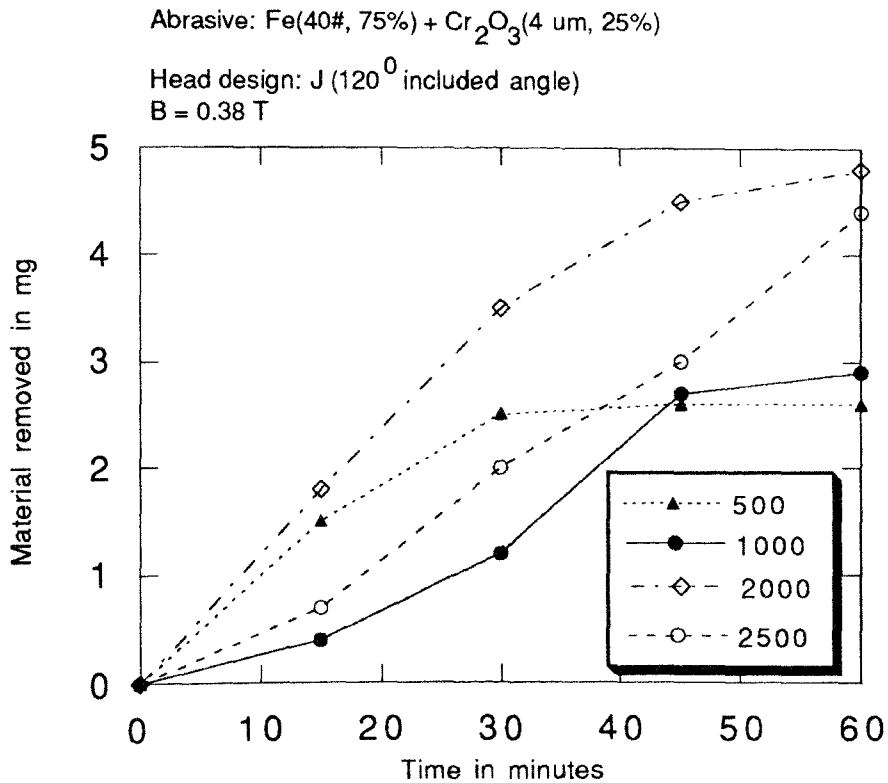


Figure 4.17 Effect of revolution speed of the workpiece on the material removal rate for head design J with included angle of 120° .

Figure 4.18 shows the variation of surface roughness R_a obtained after polishing for 30 minutes in the case of different head designs at different rotational speeds of the workpiece. It appears that surface roughness is lowest at 2000 rpm of the workpiece and deteriorates on either side of it. Figure 4.19 shows the variation of surface roughness and material removal obtained for different head designs after polishing for 30 minutes. The surface roughness appeared to decrease with the increase of the included angle of the magnetic head. The material removal rate appears to increase upto 120° included angle of the magnetic head and then decrease thereafter.

Figure 4.20 shows the micrographs of the Si_3N_4 roller before and after polishing. The surface of unpolished Si_3N_4 shows pits. The surface of polished roller showed uniform finished surface (Figure 4.21a). At high magnification uniform abrasive grooves were observed on the surface of the roller in the direction of finishing (Figure 4.21b).

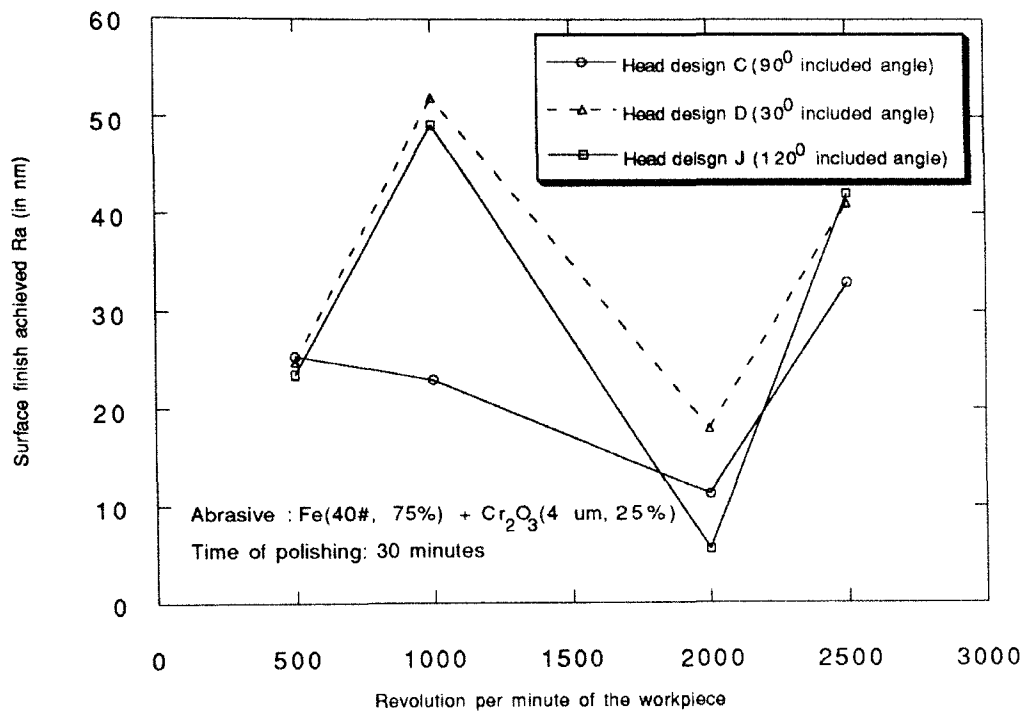


Figure 4.18: Effect of revolution speed of the workpiece on the surface roughness achieved for different head designs

Abrasive: Fe(40#, 75%), + Cr_2O_3 (4 μm , 25%)

Time of polishing: 30 minutes

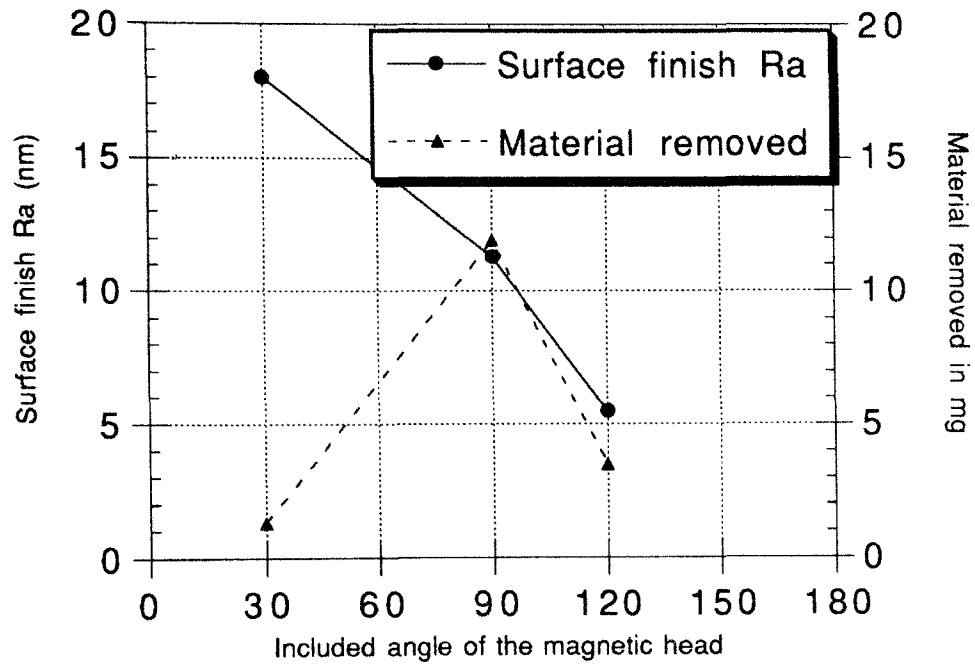
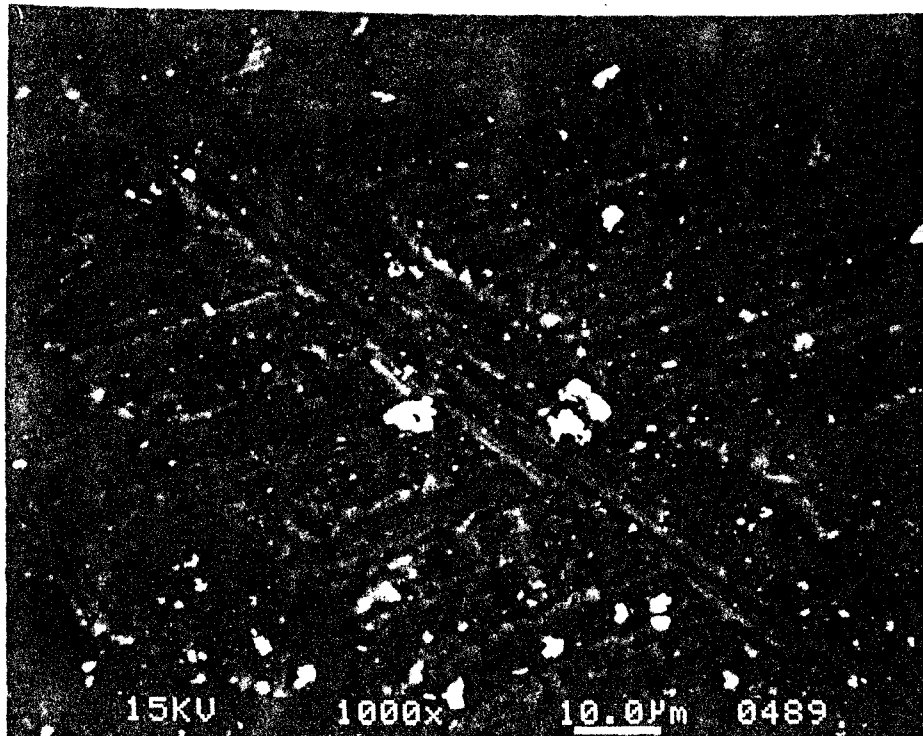
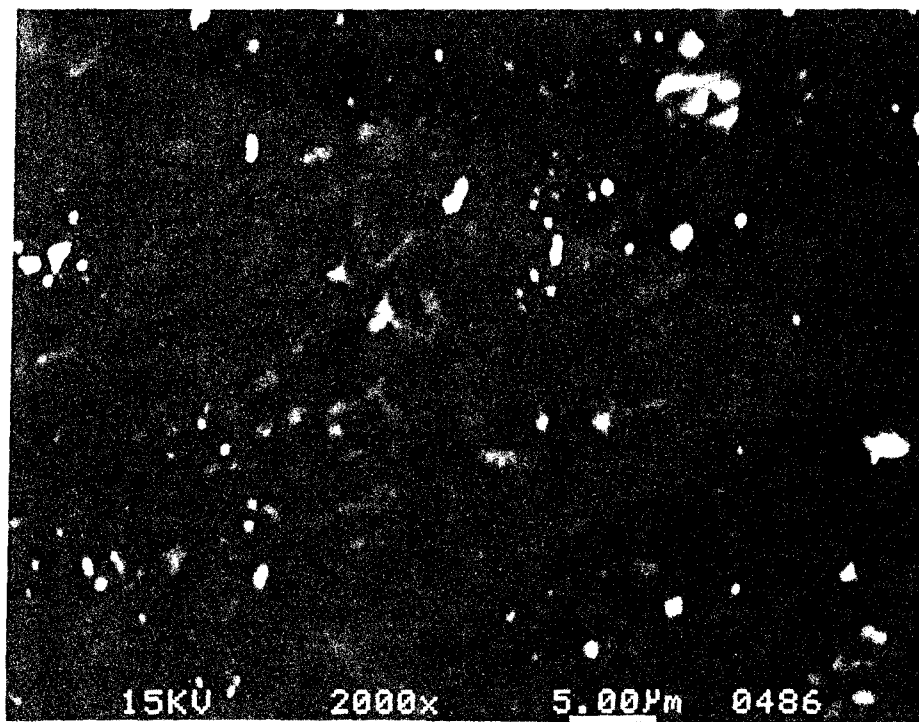


Figure 4.19 Effect of different head designs for different included angles on surface roughness achieved for Si_3N_4 rollers.

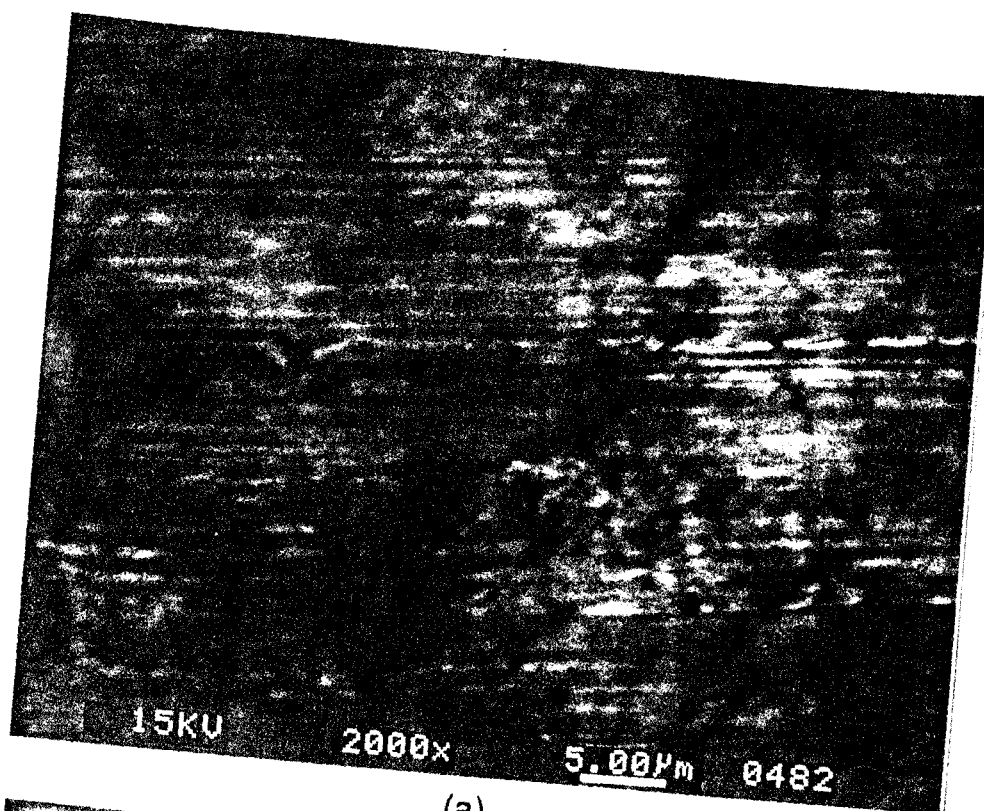


(a)

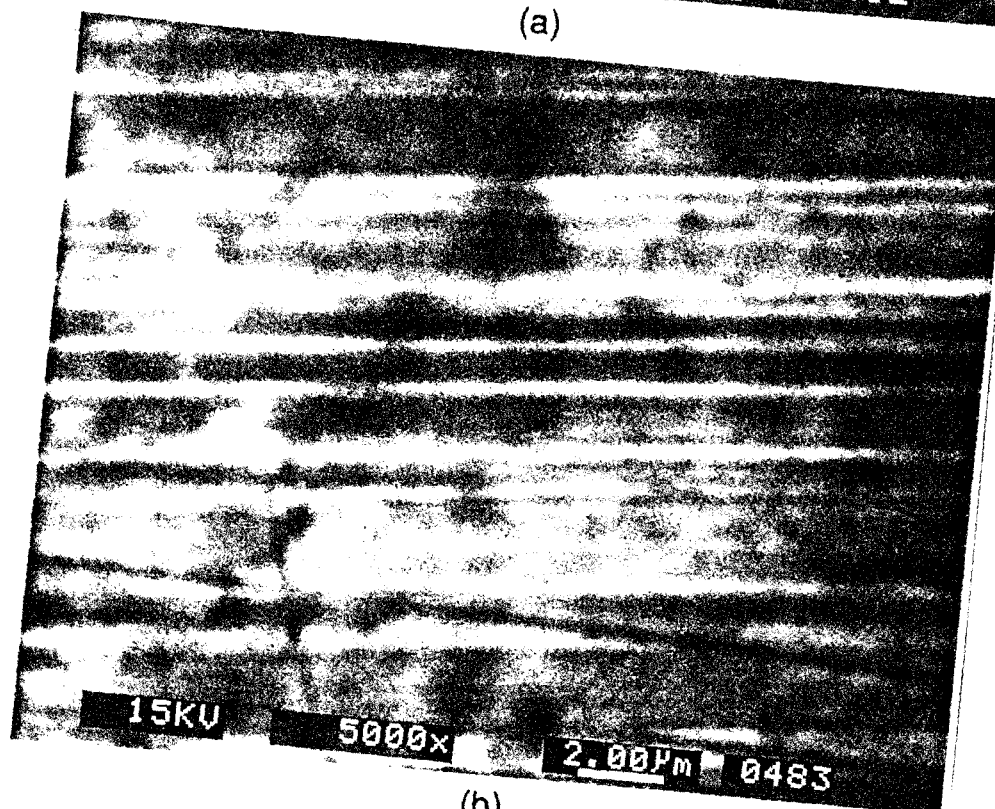


(b)

Figure 4.20 SEM micrograph of unpolished Si₃N₄ roller at 100X, and 2000X magnifications



(a)



(b)

Figure 4.21 SEM micrograph of polished Si_3N_4 roller at 2000X, and 5000X magnifications

CHAPTER 5

DISCUSSION

Magnetic Abrasive Finishing (MAF) process evolved out of necessity in polishing irregular shaped articles. The process could be applied to the finishing of ceramics because of its ability to produce surface with minimal or no surface defects such as microcracks, pits etc. This is accomplished by applying a low level of force ($\sim 1\text{N}$) which can be controlled.

MAF can be used for polishing both nonmagnetic and magnetic materials. In the case of magnetic workpiece, the workpiece is also magnetized. The abrasives are concentrated in the region near the magnetic head at the curved part (Figure 1.5). This lowers the magnetic flux drop in the gap between the magnetic head thus giving very high field density ($\sim 1\text{T}$) and high polishing pressure. This pressure is adequate to polish the surface of a magnetic roller. However, in the case of polishing nonmagnetic materials, such as hard brittle ceramics, the magnetic abrasives are concentrated in the region between the two magnetic heads (Figure 1.6). The permeability of the magnetic abrasive nearly equals to that of air. As the magnetic flux passes through the magnetic abrasive region, considerable drop in the magnetomotive force takes place in this region. This lowers the magnetic pressure exerted by the abrasives on the surface of the roller. Hence, it is difficult to achieve high magnetic field density in the abrasive region. Also, one normally requires higher polishing pressure in polishing of ceramics. The magnetic heads need to be carefully designed so as to achieve high magnetic field intensity and magnetic pressure. FEM analysis can be used for this purpose to simulate the performance of different magnetic head geometries and the more promising ones can be built. This will eliminate building various magnetic heads and test their performance by experimentation. Consequently considerable time and the cost of building these designs is saved.

Based on the FEM analysis, it is found that the field density is stronger in the abrasive region away from either magnetic head (Figure 3.17). Therefore, the main finishing action takes place in the region away from the magnetic heads. It is also found that the magnetic pressure varies parabolically with the magnetic field density in the abrasive region (Figure 3.12). Higher tangential magnetic flux density in the magnetic head results in stiffer magnetic brush. B-H curves of iron core and magnetic abrasives show that these do not attain saturation at the operating condition of magnetic field density (0.4 T) (Figure 3.3 and 3.4). This provides the possibility for further increase in the magnetic field density. The magnetic head designs should be capable of giving high magnetic field density over considerable length of the magnetic abrasives so as to generate high magnetic pressures over the length which can aid in the material removal process and enhance finishing action.

With increasing weight of the abrasives, the action force F also increases (Figure 3.16b). This could be again due to increase in the packing density of the abrasives in the air gap between the N and the S poles. The axial vibration in the magnetic head enhances interlinking among the abrasives between the N and the S poles thus increasing the packing density. This results in substantial increase of the action force F exerted by the abrasives on the surface of the roller (Figure 3.16b). Also, axial vibration of the magnetic head prevents the formation of circumferential grooves on the surface of the roller during finishing. Hence, higher removal rates and best finish is obtained with an increase in the axial vibration of the magnetic head (Figure 4.12).

Introduction of a notch in the magnetic head, bifurcates the magnetic flux through the two halves of the magnetic head, resulting in better normal flux density concentration in the abrasive region at the curved part (Figure 3.25). In magnetic materials, as the abrasives are concentrated at the curved part of the magnetic head, the introduction of notch results in higher polishing pressure. However, in the case of nonmagnetic materials, the magnetic abrasives are concentrated in the region away from the magnetic head. Introducing a notch consequently, does not result in an appreciable increase in the magnetic pressure. Thus magnetic head designs can be simplified for finishing nonmagnetic materials.

In the case of polishing nonmagnetic materials, the magnetic field density in the abrasive region can be effectively controlled by controlling the magnetic conducting path of the abrasives. The lower magnetic conducting path results in lowering the magnetic pressure. Hence, higher magnetic field density and higher magnetic pressure results. However, the length of the abrasives in contact with the surface of the roller should be long enough to obtain sufficient magnetic strength and polishing pressure. A compromise between the magnetic conducting path and magnetic pressure desirable will result in an optimized magnetic head design capable of providing desired finishing action. It was found from the characterization of the magnetic heads that the magnetic head design with an included angle of 120° resulted in an optimum action force F (Figure 3.12). Experiments conducted with head designs of different lengths of the magnetic abrasive path showed that the magnetic poles with an included angle of 120° resulted in the best surface finish (~ 5.5 nm) and the magnetic poles with an included angle of 90° resulted in optimal surface finish and material removal rate (Figure 4.19).

In conclusion, in this investigation, magnetic abrasive finishing process was studied by varying different parameters involved in the process. Design principles for the magnetic poles used in this process were developed. The process was modelled using FEM analysis which can further aid in the understanding of the process.

CHAPTER 6

CONCLUSIONS

Analytical Modelling:

From the FEM analysis of the MAF process, the following conclusions can be drawn for the magnetic head design.

- i) FEM analysis can be effectively used to model the MAF process to understand the nature of distribution of the magnetic field density and magnetic force generation in the finishing apparatus.
- ii) Complicated magnetic head designs can be effectively simulated using FEM analysis, which overcomes the need to actually build the head designs. Hence it is less time consuming and economical.
- iii) In the case of finishing of nonmagnetic rollers, the main finishing action occurs in the region away from either magnetic poles.
- iv) The magnetic force is found to vary parabolically with the magnetic field density. Hence, a high magnetic field density should be achieved in the abrasive region to achieve high magnetic pressure exerted on the surface of the roller. This becomes an important factor in the case of finishing of ceramic rollers which are hard and brittle.
- v) A Magnetic head with a converging geometry and sharper corner results in a better magnetic flux density concentration in the magnetic abrasive region.
- vi) Air gap slot in the magnetic head bifurcates the magnetic flux through the two halves of the magnetic head, resulting in better normal flux density concentration in the abrasive region next to the magnetic head.

vii) As the abrasives are present in the region away from the two magnetic heads and in the middle, the finishing zone is between the two magnetic poles and away from the poles.

viii) The shorter magnetically conducting path in the abrasive region results in better field density concentration in this region. However, this decreases the length of the magnetic abrasives in contact with the surface of the roller.

ix) Wedging action of the abrasives, though not considered in ANSYS analysis, is an important factor in the material removal process and should be given due consideration while designing the magnetic heads.

Experimental work:

i) Nonmagnetic rollers (austenitic stainless steel and ceramic - Si_3N_4) can be finished using magnetic abrasive finishing apparatus mounted on a conventional lathe. Hence, the cost of the equipment is minimal and existing machine can be modified for this purpose.

ii) A surface finish of $10 \approx \text{nm}$ (Ra) can be achieved on rollers in ≈ 10 minutes in the case of austenitic stainless steel rollers and 30 minutes in case of Si_3N_4 rollers.

iii) Increasing the weight percentage of zinc stearate in the magnetic field abrasive was found to yield a better surface finish upto a 5 w% of zinc stearate.

iv) Increasing the magnetic field density was found to increase the rate of finishing, as well as the finish attainable.

v) Axial vibration of the magnetic heads was found to be critical for finishing by magnetic field assisted polishing. High removal rates and best finish can be obtained with an increase in the axial vibration (frequency as well as amplitude). Both axial vibration and rotational speed of the workpiece have to be taken into consideration for obtaining the best cross pattern that would give best finish as well as high removal rates. Half included angles between 15 and 35 deg. are found to be optimum for best finish and high removal rates.

vi) As the polishing zone for nonmagnetic rollers exists in the region away from the magnetic poles, the length of the magnetic abrasive path is found to be an important parameter in the design of the magnetic heads.

vii) It is found that in the case of polishing of nonmagnetic rollers, the magnetic pole with the included angle of 120° results in the best surface finish and the magnetic pole with the included angle of 90° results in the optimal surface finish and material removal rate.

REFERENCES

Baron, J., "Technology of Abrasive Machining in a Magnetic Field [in Russian]," masino-strojniye, Leningrad, (1975).

Baron, J., "Magnetic abrasive finishing parts and cutting tools," [in Russian], Mashinostroyeniye, Leningrad, (1986).

Bodine, A., "Method and apparatus for sonic polishing and grinding," U. S. Patent No. 2,796,702, dated June 25, 1957.

Bradvorov, A., "Magnetic abrasive materials based on Iron Corundum with improved service properties," [in Bulgarian], Proceedings of the third scientific - technical seminar on technology of finishing, Tsentralen Mashinostroitelen Institut, Sofia, Bulgaria, (1987).

Coats, H., "Method of and apparatus for polishing containers," U. S. Patent No. 2,196,058, dated April 2, 1940.

Dehoff, A., Krull, R., Mattke, W., and P., Lochschmidt., "Magnetabrasives Engraten der Zahnstirnkanten von Zahnradern," Werkstatt und Betrieb, 117, 2, (1984) 77-79.

Dehoff, A., "Engraten und Polieren von Werkstücken mit Elektromagnetischen Feldern," Metallverarbeitung, 41, 6, (1993) 56.

Dyad'ko, Y., Krymsky, M., "Influence of macrostructure of magnetic abrasive powder on their service properties," Soviet Powder Metallurgy and Metal Ceramics, 355, 7, (1992), 67-71.

Fox, M., Agrawal, K., Shinmura, T., Komanduri, R., "Magnetic abrasive finishing of rollers," Annals of the CIRP, 43, 1 (1994) 181-184

Hershler, A., U. S. Patent No. 3,423,880, dated January 28, 1969,

- Hori, S., Watanbe, N., U. S. Patent No., 4,685,937, dated August 11, 1987,
- Kargalov, N., Inventor's certificate No. 55507, Otkrytiya Izobreteniya, USSR, 8, (1939).
- Kiparisov, S., Levinsky, Y., "Internal oxidation and nitriding of alloys," Metallurgiya, Moscow, (1979).
- Konovalov, E., Shulev, G., "Finishing of parts in Magnetic field by ferromagnetic powder," [in Russian], Nauka and Technica, Minsk, (1967).
- Krymsky, M., Dyad'ko, E., Muchnik, S., Kochura, Y., "Powder metallurgical materials, parts, and coatings - Magnetoabrasive material with corundum and titanium carbide," Poroshkovaya Metallurgiya, 263, 11, (1984) 45-49.
- Krymsky, M., "Theory and technology of the component formation process - shaping of a magnetoabrasive powder tool I, Restoration of shape," Poroshkovaya Metallurgiya, 297, 9, (1987a) 8-12.
- Krymsky, M., "Shaping of a magnetoabrasive tool II - Conditions of wedging," Poroshkovaya Metallurgiya, 298, 10, (1987b) 23-28.
- Krymsky, M., "Test methods and properties of powder metallurgical materials - Magnetoabrasive materials produced by an internal nitriding process," Poroshkovaya Metallurgiya, 249, 9, (1991a) 77-82.
- Krymsky, M., "Shaping of a magnetoabrasive powder tool III - Shaping of an annular rotating magnetic-abrasive tool," Poroshkovaya Metallurgiya, 345, 9, (1991b) 47-52.
- Krymsky, M., "Magnetic abrasive finishing," Metal Finishing, 7, (1993) 21-25.
- Kunieda, M., Hiramatsu, H., and T., Nakagawa, "Magnetic attraction system grinding method," U. S. Patent No. 4,603,509, dated August 5, 1986.
- Liaschenko, A., Krymskii, M., Tul'chinskii, L., and B., Kharenko, "Production of composite magnetoabrasive materials under solid-phase combustion conditions," Poroshkovaya Metallurgiya, 249, 9, (1982) 44-48.

Liashchenko, A., "Production of composite magnetoabrasive materials under solid-combustion conditions," Soviet Powder Metallurgy and Metal Ceramics, 15, 2, (1983) 531-536.

Loveness, W., and J., Feldhaus, "Apparatus for treating objects with particles moved by magnetic force," U. S. Patent No. 3,848,363, dated November 19, 1974,

Maiboroda, V., Shlyuko, V., and T., Gridasova, "Features of the powder movement in magnetoabrasive polishing of small parts of complex configuration," Poroshkovaya Metallurgia, 271, 7, (1985) 90-95.

Maiboroda, V., Shlyuko, V., Lapin, N., and L., Shvedov, "Magnetoabrasive treatment of components in equipment with magnetic gaps distributed in the form of a ring," Poroshkovaya Metallurgia, 283, 7, (1986) 60-63.

Maiboroda, V., and V., Shlyuko, "Motion of a ferromagnetic powder during magnetoabrasive polishing," Poroshkovaya Metallurgia, 296, 8, (1987) 3-8.

Maiboroda, V., Stepanov, O., Shlyuko, V., Maksimenko, L., and V., "Dzhemelinsky, Rules of formation of ferroabrasive powder in a magnetoabrasive tool under circular deposition of the magnetic gaps," Poroshkovaya Metallurgia, 317, 5, (1989) 72-76.

Makedonski, B., and A., Kotschemidov, "Schleifen im Magnetfeld," Fertigungstechnik und Betrieb, 24, H.4, (1974) 230-235.

Makedonsky, B., "Experimental investigation of magnetic abrasive finishing in rotating magnetic field," Technologiya na Machinostroyeneto, Tsentralen Machinostroitelen Institut, Sofia, Bulgaria, 5, (1977) 29-33.

Nalivka, G., "Powder materials for ferromagnetic abrasive finishing," Soviet Powder Metallurgy and Metal Ceramics, 30, 9, (1991)

Oliker, Y., "Forming structure of magnetic abrasive materials made of high carbon steels alloyed by carbide elements," Soviet Powder Metallurgy and Metal Ceramics, 22, 2, (1983) 411-417.

Oliker, V., Gridasova, T., Shlyuko, V., and A., Zhornyak, "Theory of the magnetic reactions occurring in abrasive machining with a ferromagnetic powder," *Poroshkovaya Metallurgia*, 263, 11, (1984) 62-67.

Oliker, V., Zhornyak, A., Gridasova, T., and K., Chebotareva, "Functional role of the structural constituents of the particles of magnetic abrasive powder," *Poroshkovaya Metallurgiya*, 273, 9, (1986) 71-75.

Radomysel'sky, I., Yaglo, G., Efremova, N., and O., Panasyuk, "Effect of particle size on the magnetic properties powders and finished pieces," *Poroshkovaya Metallurgiya*, 253, 1, (1984) 73-76.

Ruben, H., *Magnetoabrasive Finishing: "A method for the machining of complicated shaped workpieces,"* Proceedings of the AST world conference advances in surface treatments and surface finishing, Pergamon, Tarrytown, NY, 5, (1986) 239-256.

Sakulevich, F., "Magnetic abrasive finishing of precision parts," [in Russian], *Visheyshaya Shkola*, Minsk, (1977)

Sakulevich, F., and A., Kosobutsky, "Rotary machine for three-dimensional polishing of workpieces shaped as solids of revolution in a magnetic field using ferromagnetic abrasive powders," U. S. Patent No. 4,170,849, dated October 16, 1979.

Sakulevich, F., Minin, L., J., B., Bauble, A., and N., Skvorchevsky, "Method for finishing of nonmagnetic articles by means of ferromagnetic abrasive powder in magnetic field," U. S. Patent No. 4,175,930, dated November 11, 1979,

Sakulevich, F., and E., Kudinova, "Method of finishing ferromagnetic articles by ferromagnetic abrasive powders in magnetic field," U. S. Patent No. 4,306,386, dated December 22, 1981.

Shikhirev, B., Matrosov, E., and I., Deresh, "Device for the treatment of sheet materials," U. S. Patent No. 4,040,209, dated August 9, 1977.

Shikhirev, B., Matrosov, E., and I., Deresh, "Apparatus for the treatment of sheet material with the use of ferromagnetic powder," U. S. Patent No. 4,187,081, dated February 5, 1980.

Shikhirev, B., Matrosov, E., and I., Deresh, "Apparatus for working sheet materials with ferromagnetic powder," U. S. Patent No. 4,204,370, dated May 27, 1980.

Shinmura, T., Takazawa, K., Hatano, E., and T., Aizawa, "Study on magnetic abrasive process - Finishing Characteristics," Bull. Japan Society of Precision Engineering, 18, 4, (1984) 347-348.

Shinmura, T., Takazawa, K., and E., Hatano, "Advanced development of magnetic abrasive finishing and its application," Deburring and Surface Conditioning, Chicago, Illinois, (1985a).

Shinmura, T., Takazawa, K., and E., Hatano, "Study on magnetic abrasive process - Application to edge finishing," Bull. Japan Society of Precision Engineering, 19, 3, (1985b) 218-220.

Shinmura, T., Takazawa, K., and E., Hatano, "Study on magnetic abrasive process - Application to plane finishing," Bull. Japan Society of Precision Engineering, 19, 4, (1985c) 89-291.

Shinmura, T., Takazawa, K., Hatano, E., and T., Aizawa, "Study on magnetic abrasive process - Process principles and finishing possibility," Bull. Japan Society of Precision Engineering, 19, 1, (1985d) 54-55.

Shinmura, T., Hatano, E., and K., Takazawa, "The development of magnetic abrasive finishing and its equipment by applying a rotating magnetic field," Bull. Japan Society of Mechanical Engineering, 29, 258, (1986a) 4437-4443.

Shinmura, T., Takazawa, K., and E., Hatano, "Development of Spindle type finishing apparatus and its finishing performance using a magnetic abrasive machining process," Bull. Japan Society of Precision Engineering, 20, 2, (1986b) 79-84.

Shinmura, T., Takazawa, K., Hatano, E., and T., Aizawa, "Study on magnetic abrasive process - Effects of machining fluid on finishing characteristics," Bull. Japan Society of Precision Engineering, 20, 1, (1986c) 52-54.

Shinmura, T., Takazawa, K., and E., Hatano, "Study on magnetic abrasive finishing - Effects of various types of magnetic abrasives on finishing characteristics," Bull. Japan Society of Precision Engineering, 21, 2, (1987a) 139-141.

Shinmura, T., "A study on polishing mechanism of magnetic abrasive polishing and development of the apparatus," PhD thesis, Utsunomiya Univeristy, (1987b).

Shinmura, T., "Development of a unit system magnetic abrasive finishing apparatus using permanent magnets," Bull. Japan Society of Precision Engineering, 23, 4, (1989a) 313-315.

Shinmura, T., and T., Aizawa, "Study on magnetic abrasive finishing process - Development of plane finishing apparatus using a stationary type electromagnet," Bull. Japan Society of Precision Engineering, 23, 3, (1989b) 236-239.

Shinmura, T., and T., Aizawa, "Study on internal finishing of a nonferromagnetic tubing by magnetic abrasive machining process," Bull. Japan Society of Precision Engineering, 23, 1, (1989c) 37-41.

Shinmura, T., Takazawa, K., and E., Hatano, E., "Study of magnetic abrasive finishing," Annals of CIRP, 39, 1, (1990) 325-328.

Shinmura, T., Yamaguchi, H., and T., Aizawa, "A new internal finishing process of nonferromagnetic tubing by the application of a magnetic field - the development of a unit type finishing apparatus using permanent magnets," International Journal of Japan Society of Precision Engineering, 27, 2, [1993] 132-137.

Shinmura, T., Iizuka, T., and Shinbo, Y., "A new process for internal finishing of non-ferromagnetic tubing using rotating magnetic field", Transactions of NAMRI/SME, XXI (1993).

Shinmura, T., and H., Yamaguchi, "Study on a new internal finishing process of a nonferromagnetic tube by the application of a linearly travelling magnetic field - on the process principle and the behaviors of magnetic finishing tool," International Journal of Japan Society of Precision Engineering, 28, 1, (1994) 29-34.

Shinmura, T., Wang, F., and T. Aizawa, "Study on a new finishing process of fine ceramics by magnetic abrasive machining - on the improving effects of finishing efficiency by mixing diamond magnetic abrasives with ferromagnetic particles", (1994).

Shlyuko, V., Maiboroda, V., Gridasova, T., and N., Lapin, "Magnetoabrasive polishing of blade type parts," Technol. Organiz. Porizv., 3, (1985) 35-36.

Simijian, L., "Sharpening or polishing device," U. S. Patent No. 2,735,231, dated February 21, 1956,

Simijian, L., "Polishing device," U. S. Patent No. 2,735,232, dated February 21, 1956.

Simijian, L., "Method of treating an object," U. S. Patent No. 2,787,854, dated April 9, 1957.

Simijian, L., "Treating or polishing apparatus," U. S. Patent No. 2,880,554, dated April 7, 1959.

Sugawara, S., Kaji, H., and M., Shimda, "Abrasing apparatus using magnetic abrasive powder," U. S. Patent No. 4,730,418, dated March 15, 1988.

Suzuki, K., Uematsu, T., and H. Ohashi, "Magnetic polishing of moulds using short-fiber polishing materials," Die and Mould Technology International, 6, (1991) 58-63.

Takazawa, K., Hatano, E., Aizawa, T., and T., Shinmura, "Development of magnetic abrasive finishing and its equipment," 12 Deburring and Surface Conditioning'83, Orlando, Florida, (1983) 1-13.

Tipnis, V., "Cutting tool wear," Wear Control Handbook, An ASME centennial research project, (1980), 38.

Watanbe, Y., Takahashi, T., and K., Haga, "Travelling magnetic field type crusher," U. S. Patent No., 4,601,431, dated July 22, 1986.

Yascheritsyn, P., Sakulevich, F., Olender, L., and A., Kosobutsky, "Machine for treating spherical surfaces of parts with magneto-abrasive powder," U. S. Patent No. 4,186,528, dated February 5, 1980.

Zgdanovich, V., "Research of magnetic abrasive finishing external cylindrical surfaces," Docoral dissertation, Physical Technical Institute, Minsk, Byelorussia, (1974).

APPENDIX

Surface Characterization equipments

Form Talysurf and Talyrond 250 were used for the surface characterization of the nonmagnetic rollers polished using MAF technique.

The Form Talysurf series of instruments for surface analysis, comprises a range of compatible, interchangeable modules and accessories which can be combined to form the system most suited to a particular application. Talyrond 250 is a computer controlled software instrument, for the precision measurement of errors of geometric form as departures from roundness or straightness. The instrument is a stylus type with rotating worktable and has two motorized axes for measurement (the worktable and the vertical straightness unit) and one motorized axis for gage contact. The operation and data processing are computer controlled, the results being output to the visual display unit and/or printer, as required.

The data obtained from the Talysurf measurement is used for the characterization of the surface texture of the polished surface by the various parameters such as average roughness, rms roughness, maximum height and depth of the surface profile, and maximum peak to valley height. Figure A1 shows a typical Talysurf trace of the stainless steel roller and the various parameters measured by the Talysurf series. Some of the important surface roughness parameters are discussed below.

Ra: Ra is the universally recognized and most commonly used, international parameter of roughness. It is the arithmetic mean of the departures of the profile from the mean line.

$$Ra = 1/L \int_0^L |z(x)| dx$$

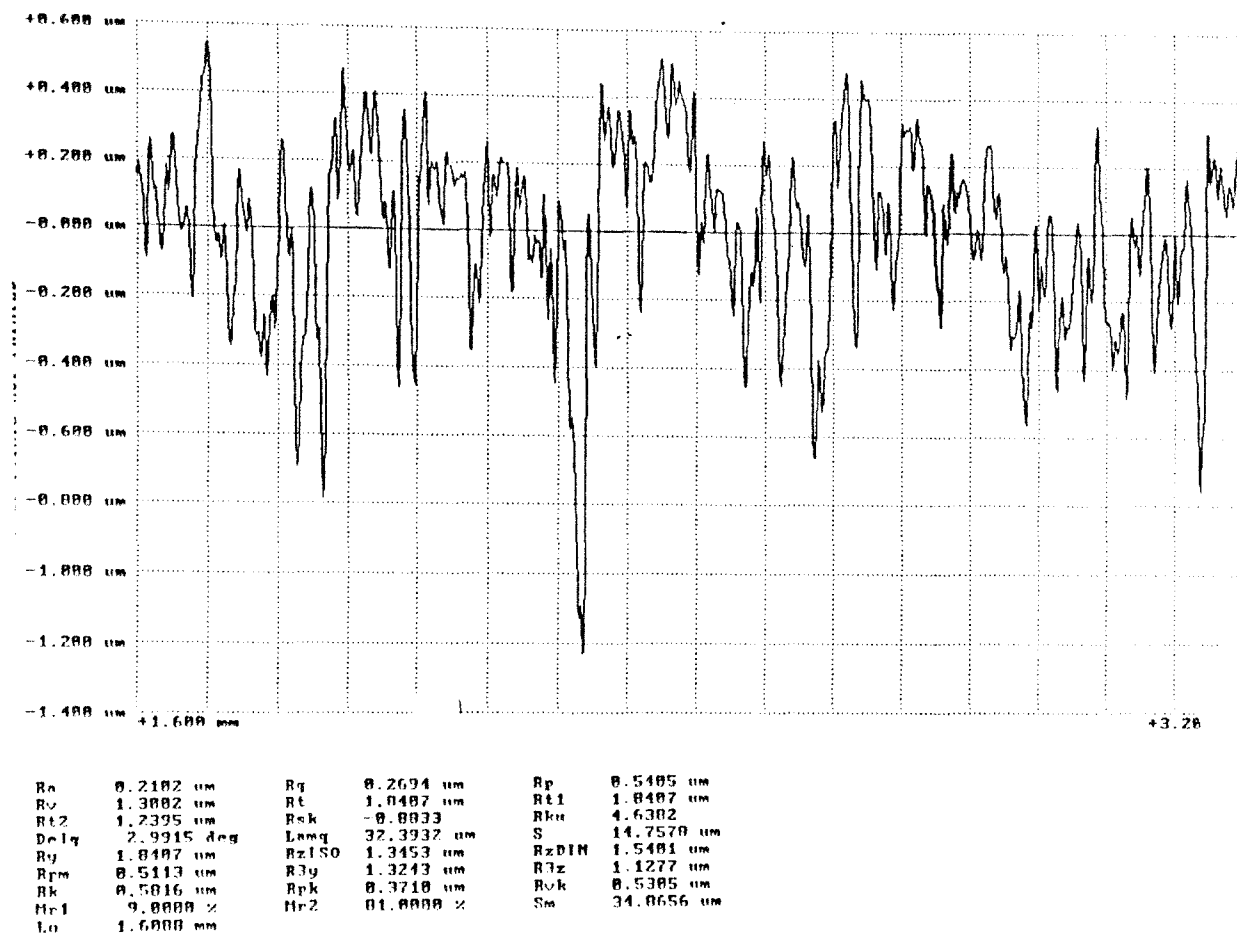


Figure A1 Figure showing a typical Talysurf trace of the stainless steel roller and the various parameters measured by the Talysurf series

where, $z(x)$ is the departure of the profile from the mean line at distance x from the origin along the X-axis.

Rq: Rq is the rms parameter corresponding to Ra.

$$Rq = \sqrt{\frac{1}{L} \int_0^L |Z^2(x)| dx}$$

Rt: Rt is the maximum peak to valley height of the profile in the assessment length.

Rv: Rv is the maximum depth of the profile below the mean line within the assessment length.

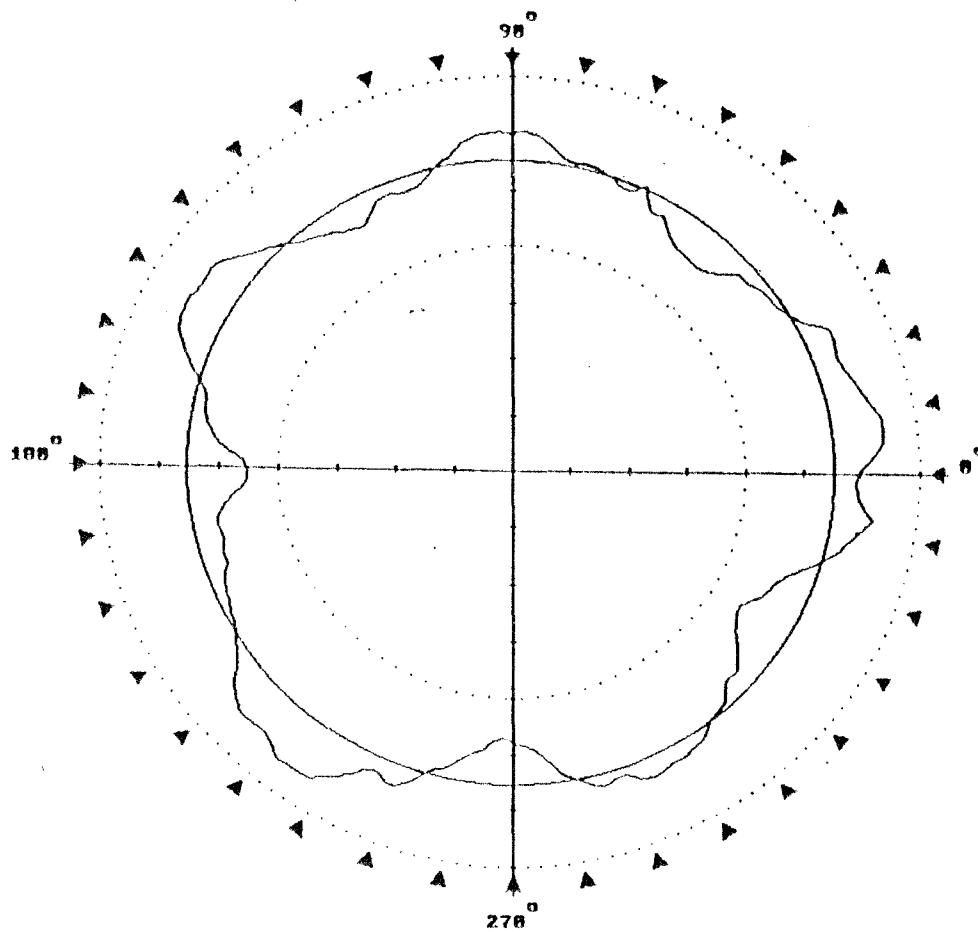
Rp: Rp is the maximum height of the profile above the mean line within the assessment length.

The data obtained from the Talyrond measurement is used for the evaluation of the polished surface by the various parameters such as roundness, vertical straightness, cylindricity. Figure A2 shows a typical Talyrond trace of the stainless steel roller and the various parameters measured by the Talyrond series. Some of the important parameters are discussed below.

Peak to valley (O): The radial separation between two concentric circles, which are themselves concentric to the reference figure, and totally enclose the centered, measure profile.

Eccentricity (E): The radial distances from the selected datum axis (or point) to the center of the selected reference circle.

Angle (<): The angle between 0 degrees position of the spindle and the line joining the center of the references circle to the datum axis as shown in Figure A3(a).

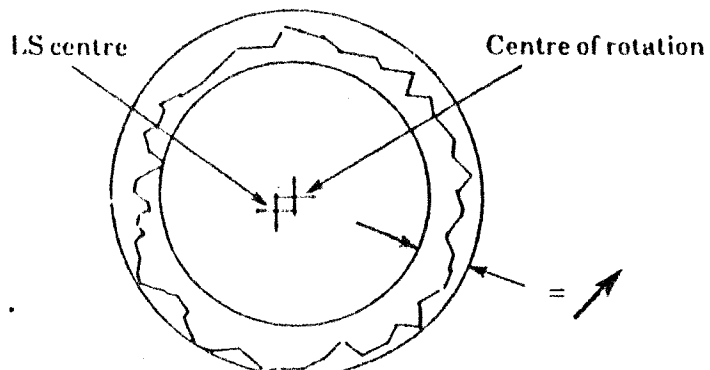


LS ROUNDNESS RESULTS

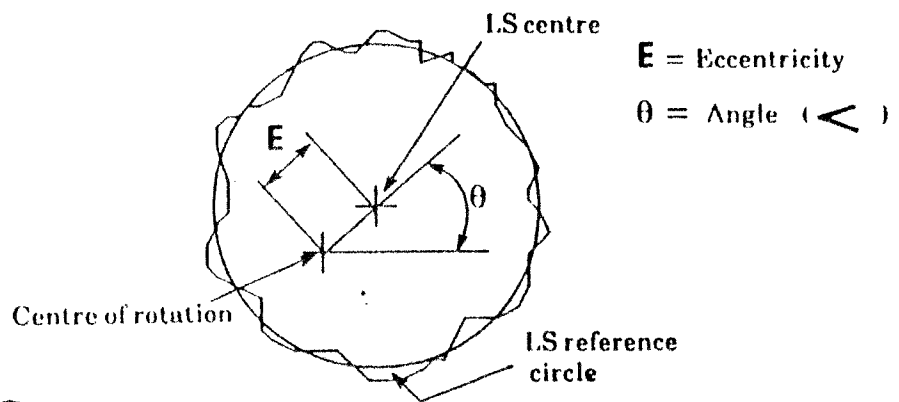
○	1.95 um	Meas. mode	External
E	4.98 um	Z Height	278.5 mm
∠	267.6 deg	Filter	15 upr 2CR
↗	9.95 um	Profile	100.0 %

Datum : SPINDLE

Figure A2 Figure showing a typical Talyrond trace of the stainless steel roller and the various parameters measured by the Talyrond series



(a) Measurement of angle (<)



(b) Measurement of Runout (->)

Figure A3 Figure explaining the different parameters evaluated by the Talyrond series

Concentricity (o): Twice the eccentricity.

Runout (->): The radial separation of two concentric circles, which themselves are concentric to the datum axis (or point), and totally enclose the measured profile, i.e. total indicator reading as shown in Figure A3(b).

VITA²

Kishor Agrawal

Candidate for the Degree of

Master of Science

Thesis: MAGNETIC ABRASIVE FINISHING OF NONMAGNETIC ROLLERS

Major Field: Mechanical Engineering

Biographical:

Personal Data: Born in Bombay, India, On May 22, 1970,
the son of Satyanarayan and Sushila Agrawal.

Education: Graduated from D. G. Ruparel College, Bombay,
India, in June 1987; received Bachelor of
Technology degree in Metallurgical Engineering
from Indian Institute of Technology, Bombay, India
in July 1992. Completed the requirements for the
Master of Science degree with a major in
Mechanical Engineering at Oklahoma State
University in December 1994.

Experience: Graduate research assistant, Oklahoma State
University, 1992 to 1994.